

**SHAPE MEMORY RESPONSE AND MICROSTRUCTURAL EVOLUTION OF A
SEVERE PLASTICALLY DEFORMED HIGH TEMPERATURE SHAPE
MEMORY ALLOY (NiTiHf)**

A Thesis

by

ANISH ABRAHAM SIMON

Submitted to the Office of Graduate Studies of
Texas A&M University
in partial fulfillment of the requirements for the degree of

MASTER OF SCIENCE

December 2004

Major Subject: Mechanical Engineering

**SHAPE MEMORY RESPONSE AND MICROSTRUCTURAL EVOLUTION OF A
SEVERE PLASTICALLY DEFORMED HIGH TEMPERATURE SHAPE
MEMORY ALLOY (NiTiHf)**

A Thesis

by

ANISH ABRAHAM SIMON

Submitted to Texas A&M University
in partial fulfillment of the requirements
for the degree of

MASTER OF SCIENCE

Approved as to style and content by:

Ibrahim Karaman
(Chair of Committee)

Richard Griffin
(Member)

Aydin I. Karsilayan
(Member)

Dennis L. O'Neal
(Head of Department)

December 2004

Major Subject: Mechanical Engineering

ABSTRACT

Shape Memory Response and Microstructural Evolution of a Severe Plastically
Deformed High Temperature Shape Memory Alloy (NiTiHf).

(December 2004)

Anish Abraham Simon, B.S., Mahatma Gandhi University, India

Chair of Advisory Committee: Dr. Ibrahim Karaman

NiTiHf alloys have attracted considerable attention as potential high temperature Shape Memory Alloy (SMA) but the instability in transformation temperatures and significant irrecoverable strain during thermal cycling under constant stress remains a major concern. The main reason for irrecoverable strain and change in transformation temperatures as a function of thermal cycling can be attributed to dislocation formation due to relatively large volume change during transformation from austenite to martensite. The formation of dislocations decreases the elastic stored energy, and during back transformation a reduced amount of strain is recovered. All these observations can be attributed to relatively soft lattice that cannot accommodate volume change by other means. We have used Equal Channel Angular Extrusion (ECAE), hot rolling and marforming to strengthen the 49.8Ni-42.2Ti-8Hf (in at. %) material and to introduce desired texture to overcome these problems in NiTiHf alloys. ECAE offers the advantage of preserving billet cross-section and the application of various routes, which give us the possibility to introduce various texture components and grain morphologies. ECAE was performed using a die of 90° tool angle and was performed at high temperatures from 500°C up to 650°C. All extrusions went well at these temperatures. Minor surface cracks were observed only in the material extruded at 500 °C, possibly due to the non-isothermal nature of the extrusion. It is believed that these surface cracks can be eliminated during isothermal extrusion at this temperature. This result of improved formability of NiTiHf alloy using ECAE is significant because an earlier review of the formability of NiTiHf using 50% rolling reduction concluded that the minimum temperature for rolling NiTi12%Hf alloy without cracks is 700°C. The strain level imposed during one 90° ECAE pass is equivalent to 69% rolling reduction. Subsequent to ECAE processing, a

reduction in irrecoverable strain from 0.6% to 0.21% and an increase in transformation strain from 1.25% to 2.18% were observed at a load of 100 MPa as compared to the homogenized material. The present results show that the ECAE process permits the strengthening of the material by work hardening, grain size reduction, homogeneous distribution of fine precipitates, and the introduction of texture in the material. These four factors contribute in the increase of stability of the material. In this thesis I will be discussing the improvement of mechanical behavior and stability of the material achieved after various passes of ECAE.

To My Parents
&
The community at St. Mary's Catholic Church

ACKNOWLEDGEMENTS

I am thankful for the many people in both professional as well as personal circles at the completion of this thesis. Without these people I may have never been able to complete this work.

First of all I would like to thank God for the opportunity He granted me to experience this challenge. I would especially like to express my gratitude to the following people and organizations.

I would like to thank my advisor Prof. Ibrahim Karaman for his constant encouragement and trust in me. I believe that his commitment and passion towards his work has inspired me to set high standards and goals in life.

I would like to express my gratitude to Prof. Yuriy Chumlyakov for his invaluable suggestions and guidelines in my research and also for sharing with me his deep knowledge in shape memory alloys. Discussions with him have always been a pleasure for me.

It is with sincere gratitude that I look upon Prof. Richard Griffin and Prof. Aydin I Karsilayan for their willingness to honor me with their presence in my advisory panel.

I would like to thank my parents Mr. Simon Abraham and Prof. Annie Simon, for their unconditional love and prayerful encouragement. Thank you for being the most amazing parents.

It is with a humble and thankful heart that I look upon the community of St. Mary's Catholic Church, which has impacted my life unlike anything in the past 2 years. People who have been there like pillars of support, who became shoulders for me to weep on and ears to share my agony; thanks for the wonderful hugs and the hours y'all have spent with me. Is with great pleasure I remember the daily mass and especially the 11 am mass on Sundays that was the life giving routine in my life. The homilies by Fr. Mike Sis and Fr. Keith Koehl were always inspirational, calls to look back, straighten life, and to be more sharp and dedicated in professional life.

It is with thankful a heart that I stand before God when I think about the wonderful friends that he allowed in my life in the past 2 years - friends who gave so much love and life to me. I would like to extend my sincere gratitude to Jeremy Poole,

Jorja Duffin, Ann Marie Yeley, Richele Rainosek, Tracey Book, Alli Duffel, Cassie Mechler, Gracie Arenas, Chuck Kiereleber, Rachel Stensrude, Andrew Robinson and Cheryl Dale – who were always there with love and constant support. I would also like to extend my thanks to the Book family, the Rainosek family and Helping Hands for being there in my life at the most needful time. I am thankful for God's intervention in my life through these wonderful people without whom none of this would have become a reality.

Special thanks to my officemates: Ajay Kulkarni, Haluk Karaca, Joesph Mather, Bryan Bagley, Guney Yapici, Mohammed Haouaoui, Benat Kockar, Burak Basaran and Yang Cao for being helpful and providing a good environment for research. It is with gratitude that I look upon the friendship that I have built with Mohammed for he was a brother for me in the lab, a person who always pumped positive thoughts into my mind.

TABLE OF CONTENTS

	Page
ABSTRACT.....	iii
DEDICATION.....	v
ACKNOWLEDGMENTS	vi
TABLE OF CONTENTS.....	viii
LIST OF FIGURES	ix
LIST OF TABLES.....	xiii
 CHAPTER	
I INTRODUCTION	1
1.1 Background.....	1
II MOTIVATION: DEMAND FOR HIGH TEMPERATURE SHAPE	
MEMORY ALLOYS.....	5
III EXPERIMENTAL PROCEDURE	9
3.1 Initial Material	9
3.2 Processing by Rolling and ECAE.....	9
3.2.1 Rolling.....	9
3.2.2 ECAE	10
3.3 Differential Scanning Calorimetry.....	13
3.4 Thermo-mechanical Testing	14
3.5 Microstructural Evolution.....	16
IV RESULTS AND DISCUSSION	17
4.1 Calorimetric Analysis	17
4.2 Microstructural Evolution after Processing	22
4.3 Thermo-mechanical Experiments.....	32
V CONCLUSIONS.....	64
REFERENCES	66
VITA	68

LIST OF FIGURES

	Page
Figure 1.1 Macroscopic and microscopic views of the two phases of SMA's	2
Figure 2.1 Schematic of the response of an SMA during differential scanning calorimetry (DSC).	6
Figure 2.2 Schematic of the temperature-strain response of an SMA having irrecoverable strains per thermal cycling.	6
Figure 3.1 Schematic of the ECAE routes	11
Figure 3.2 Images of the ECAE processed homogenized 49.8%Ni-42.2%Ti-8%Hf (at. %) alloy after extracting from Ni cans. (a) one pass at 500°C, (b) one pass at 600°C, (c) two Route B passes at 650°C, and two Route C passes at 650°C.....	12
Figure 3.3 Relative workability of NiTi and NiTiHf alloys. The previous studies were done for attaining a 50% reduction by rolling	13
Figure 3.3 Schematic of finding transformation temperatures from a DSC curve.....	14
Figure 3.4 Schematic of the analysis of temperature-strain curve	15
Figure 4.1 Identification of 49.8Ni-42.2Ti-8Hf transformation temperatures by differential scanning calorimetry (DSC). (a) homogenized sample at 1000 °C for 24 hours, (b) hot rolled at 1000°C to 40% reduction after homogenization. The transition characteristics are much more stable after hot rolling.....	17
Figure 4.2 Identification of 49.8Ni-42.2Ti-8Hf transformation temperatures after (a) homogenized flowserve material - HIPed 49.8Ni-42.2Ti-8Hf (2hrs @ 900°C) (b) one ECAE pass at 500°C, (c) one ECAE pass at 600°C, (d) two ECAE passes at 650°C using Route B and (e) two ECAE passes at 650°C using Route C.	19

Figure 4.3	Optical micrographs of (a) homogenized (24hrs @1000°C) 49.8Ni-42.2Ti-8Hf Ames material, (b) as received HIPed 49.8Ni-42.2Ti-8Hf (2hrs @ 900°C) flowserve material and (c) homogenized 49.8Ni-42.2Ti-8Hf (2hrs @ 1000°C) flowserve material.....	22
Figure 4.4	Optical micrographs of the Ames material, 49.8Ni-42.2Ti-8Hf, hot rolled at 1000°C to 40% reduction after homogenization.....	23
Figure 4.5	Optical micrographs of the flowserve material 49.8Ni-42.2Ti-8Hf, after one ECAE pass at 500°C.....	24
Figure 4.6	Optical micrographs of the flowserve material 49.8Ni-42.2Ti-8Hf, after one ECAE pass at 600 °C.....	25
Figure 4.7	Optical micrographs of the flowserve material 49.8Ni-42.2Ti-8Hf, after two ECAE passes using Route C at 650 °C.	26
Figure 4.8	Optical micrographs of the flowserve material 49.8Ni-42.2Ti-8Hf, marformed to 5% reduction.	27
Figure 4.9	Optical micrographs of the flowserve material 49.8Ni-42.2Ti-8Hf, marformed to 10% reduction.	28
Figure 4.10	Optical micrographs of the flowserve material 49.8Ni-42.2Ti-8Hf, marformed to 15% reduction.	29
Figure 4.11	Bright field TEM images of hot-rolled material (starting material from Ames: 49.8Ni-42.2Ti-8.0Hf). The images are at approximately 17,000 X, 10,000 X and 60,000 X, respectively. In the lower magnification image, three families of martensite variants and internal twins are apparent, while the higher magnification image shows a high density of dislocations between martensite variants. (c) is the higher magnification image of the region enclosed with the white box in (b).....	31

Figure 4.12	Bright field TEM image of the sample ECAE processed at 500°C using Route A, only one pass. Martensite variants with straight boundaries and internal twins are evident.....	32
Figure 4.13	Thermal cycling at 0 (a), 100 (b) and 200 (c) MPa tensile loads for cast, HIP'ed and homogenized 49.8Ni-42.2Ti-8.0Hf from flowserve.....	33
Figure 4.14	Transformation strain vs. temperature response of the ECAE 1A 500°C sample during 4 thermal cycles under (a) 0 MPa, 10 thermal cycles under (b) 100 MPa, and (c) 200 MPa.	35
Figure 4.15	Transformation strain vs. temperature response of the ECAE 1A 600°C sample during 4 thermal cycles under (a) 0 MPa, 10 thermal cycles under (b) 100 MPa, and (c) 200 MPa.	37
Figure 4.16	Transformation strain vs. temperature response of the ECAE 2B 650°C sample during 4 thermal cycles under (a) 0 MPa, 10 thermal cycles under (b) 100 MPa, and (c) 200 MPa.	39
Figure 4.17	Transformation strain vs. temperature response of the ECAE 2C 650°C sample during 4 thermal cycles under (a) 0 MPa, 10 thermal cycles under (b) 100 MPa, and (c) 200 MPa.	41
Figure 4.18	Transformation strain vs. number of thermal cycles of the homogenized and ECAE processed 49.8Ni-42.2Ti-8Hf flowserve material under (a) 100 MPa and (b) 200 MPa constant stress.	43
Figure 4.19	Creep strain (irrecoverable transformation strain) vs. number of thermal cycles of the homogenized and ECAE 49.8Ni-42.2Ti-8Hf flowserve material under (a) 100 MPa and (b) 200 MPa constant stress.....	45
Figure 4.20	Hysteresis ($A_f - M_s$) vs. number of thermal cycles of the homogenized and ECAE processed 49.8Ni-42.2Ti-8Hf flowserve material under (a) 100 MPa and (b) 200 MPa constant stress.	48

Figure 4.21	Change in M_s temperature vs. number of thermal cycles in the homogenized and ECAE 49.8Ni-42.2Ti-8Hf flowserve material under (a) 100 MPa and (b) 200 MPa constant stress.	51
Figure 4.22	Transformation strain vs. temperature response of the ECAE 2C 650°C sample annealed at 400°C for 15mins, during 4 thermal cycles under (a) 0 MPa, 10 thermal cycles under (b) 100 MPa, and (c) 200 MPa.	53
Figure 4.23	Transformation strain vs. temperature response of the hot-rolled sample during 4 thermal cycles under (a) 0 MPa, 10 thermal cycles under (b) 100 MPa, and (c) 200 MPa.	55
Figure 4.24	Transformation strain vs. temperature response of the 10% marformed sample during 4 thermal cycles under (a) 0 MPa, 10 thermal cycles under (b) 100 MPa, and (c) 200 MPa.	57
Figure 4.25	Two-way Shape memory response of the samples after training under constant external stress of 100 MPa and 200 MPa. (a) homogenized flowserve material, 49.8Ni-42.2Ti-8Hf, (b) homogenized flowserve material, 49.8Ni-42.2Ti-8Hf after one ECAE passes at 500°C, (c) homogenized flowserve material, 49.8Ni-42.2Ti-8Hf after one ECAE passes at 600°C, (d) homogenized flowserve material, 49.8Ni-42.2Ti-8Hf after two ECAE passes using Route B at 650°C, (e) homogenized flowserve material, 49.8Ni-42.2Ti-8Hf after two ECAE passes using Route C at 650°C.	59

LIST OF TABLES

	Page
Table 3.1 Summary of the thermo-mechanical processing conducted	16
Table 4.1 Summary of the results from thermal cycling conducted under constant load.	63

CHAPTER I

INTRODUCTION

The objective of this study is to analyze the effects of thermo-mechanical treatments on the shape memory behavior of the high temperature shape memory alloy NiTiHf. Both ausforming and marforming was conducted on the material. Ausforming is the deformation in austenitic state and marforming is deformation in martensitic state. Ausforming was conducted using the technique of Equal Channel Angular Extrusion, a severe plastic deformation technique at high temperatures of the range of 650°C and also by hot rolling at 1000°C. Marforming was conducted by rolling the sample to various reductions such as 5%, 10% and 15% at room temperature. First an introduction to basic concepts of shape memory alloys (SMAs) is presented followed by experimental procedure including a brief summary of extrusions followed by results and discussion i.e. calorimetric analysis, microstructural evolution, and thermo-mechanical testing and finally we draw conclusions based on the results and discussion and give some recommendations for future work.

1.1 Background

Shape memory alloys (SMA's) are special kind of intermetallics, which exhibit unique properties such as high recoverable strains as a result of reversible, diffusionless martensitic transformation (MT), pseudoelasticity, and the shape memory effect. Even though Arne Olander first observed these unusual properties in 1938, not until the 1960's were any serious research advances made in the field. The most effective and widely used alloys include NiTi (Nickel - Titanium), CuZnAl, and CuAlNi.

The two unique properties- shape memory effect and pseudo elasticity, described above are made possible through a solid state phase change. A solid state phase change is similar in that a molecular rearrangement is occurring, but the molecules remain closely packed so that the substance remains a solid. The two phases, which occur in shape memory alloys, are Martensite, and Austenite.

This thesis follows the style of *Acta Materialia*.

SMA's are able to convert its shape to a preprogrammed structure with change in temperature. The much studied NiTi is soft and easily deformable in its lower temperature form (martensite), it resumes its original shape and rigidity when heated to its higher temperature form (austenite). This is called the one-way shape memory effect. Figure 1.1 shows transformation from the austenite to the martensite phase and shape memory effect. The high-temperature austenitic structure undergoes twinning as the temperature is lowered. This twinned structure is called martensite. The martensitic structure is easily deformed by outer stress into a particular shape, and the crystal structure undergoes parallel registry. When heated, the deformed martensite resumes its austenitic form, and the macroscopic shape memory phenomenon is seen.

Martensite, is the relatively soft and easily deformed phase of shape memory alloys, which exists at lower temperatures. The microstructure in this phase is twinned. Austenite, the stronger phase occurs at higher temperatures. The austenite has a cubic structure in the most well known SMA, i.e. NiTi.

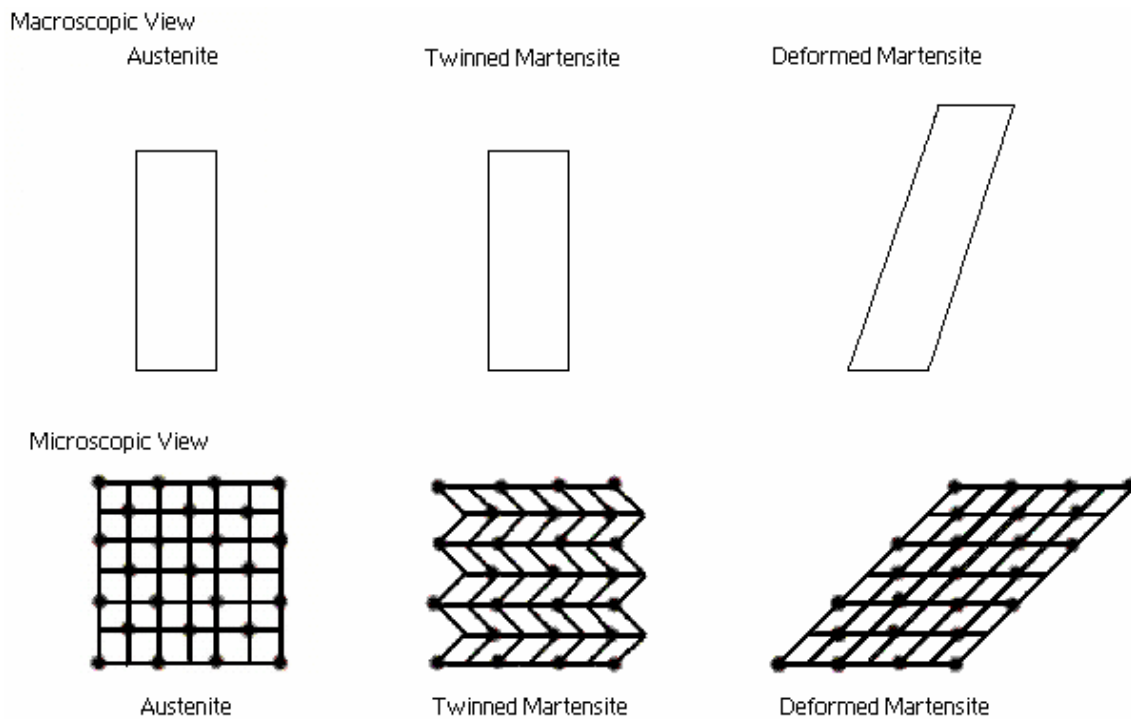


Figure 1.1. Macroscopic and Microscopic views of the two phases of SMA's [1].

The temperatures at which each of these phases begin and finish forming are represented by the following variables: M_s , M_f , A_s , A_f . The transformation start and finish temperatures from austenite to martensite are called M_s and M_f respectively and transformation start and finish temperatures from martensite to austenite are called A_s and A_f where the former transformation is called as forward transformation and the latter one as back or reverse transformation.

The stress level on shape memory alloys increases the values of these four variables. The initial values of these four variables are also affected by the composition of alloys.

The shape memory effect is observed when the SMAs are cooled down below M_f . At this stage the alloy is completely composed of Martensite. After deforming the SMA when it is at fully martensitic stage, if we heat it up above A_f the alloy will recover its original shape. The deformed Martensite is now transformed to the cubic Austenite phase, which is configured in the original shape of the alloy

The driving force for phase transformation in shape memory alloys is the chemical free energy between the phases. When the difference in chemical free energies is enough to overcome the energy to nucleate the other phase, transformation will start and continue as the energy for growth is supplied by further increase in chemical energy difference.

When the MT (Martensitic transformation) starts during cooling, in order to minimize the volume change, the self accommodation of martensite variants takes place. Martensite variants mutually reduce the transformation strain accompanying the formation of the individual variants. Thus the specimen as a whole will not experience significant shape change.

There are two deformation types in shape memory alloys which lead to recoverable strains: reorientation of martensite and stress induced martensite. When NiTi alloys cooled down under zero stress, parent phase transforms to martensite and 24 possible internally twinned martensite variants form self-accommodating structures to minimize the macroscopic volume change [2]. The applied stress biases the self-accommodating structure and favors the growth of selected martensite variants at the expense of others. When this biased structure is heated above A_f temperature, it recovers

back to its original shape which is called shape memory effect (SME) and there will be no net transformation strain with following forward transformation under zero applied stress. But if these variants are permanently biased due to the formation of dislocations or internal stress a large amount of macroscopic strain will be experienced under zero load with forward and reverse transformation which is called Two Way Shape Memory Effect (TWSME) [3,4]. TWSME can be obtained by “training”. The common methods of two-way shape memory training include shape memory training, pseudoelastic training, and thermal cycling training under a constant stress which is the approach that we had followed in this research.

CHAPTER II

MOTIVATION: DEMAND FOR HIGH TEMPERATURE SHAPE MEMORY ALLOYS

High temperature SMA's are needed in applications that require reliable means to actuate valves and other system components at temperatures above 100°C. Near equiatomic TiNi SMA's are technologically important because of their superior shape memory properties. But the uses of these alloys are restricted to temperatures below 100°C because martensitic transformation in these alloys starts at values lower than 100°C. High-temperature SMA's whose martensitic transformation begins (M_s) at temperatures higher than 100°C has been an interest because of their potential applications. Ternary NiTiX high-temperature SMA's, with X being precious metals such as Pd and Pt have been developed [5, 6]. But these metals are limited in practical applications because of their high cost. So other low cost NiTiX systems have been studied, among them the most significant candidates were TiNiHf alloys with Hf being used to replace Ti. It has been shown that with an increase in the Hf content the transformation temperature increases [7]. However the addition of Hf to the alloy will have reduced ductility and thereby pure workability.

A major problem with these alloys is the lack of stability in the transformation temperatures and recoverable strains if the reverse transformation strains are not equal to the corresponding forward transformation strains. This is explained in Figures 2.1 and 2.2. In Figure 2.1, M_{s1} and M_{s2} represent the starting temperature for martensitic transformation during first cycle and second cycle respectively. We can see a considerable decrease in M_s temperature with # of cycles. In Figure 2.2, the strain vs. temperature response of an SMA under constant stress is presented. We can see that there is a considerably large irrecoverable strain after each cycle which contributes to the total creep strain. The irrecoverable strain could be because of the formation of localized lattice defects, or by stabilization of martensite [8]. Probable reasons for unstable mechanical and thermal response are introduction of primary defects like dislocations during the austenite to martensite transformation and poor strength of the parent phase [8-14]. A possible solution to minimize and/or avoid the formation of lattice dislocations during cycling is to increase the strength of parent phase [8-11].

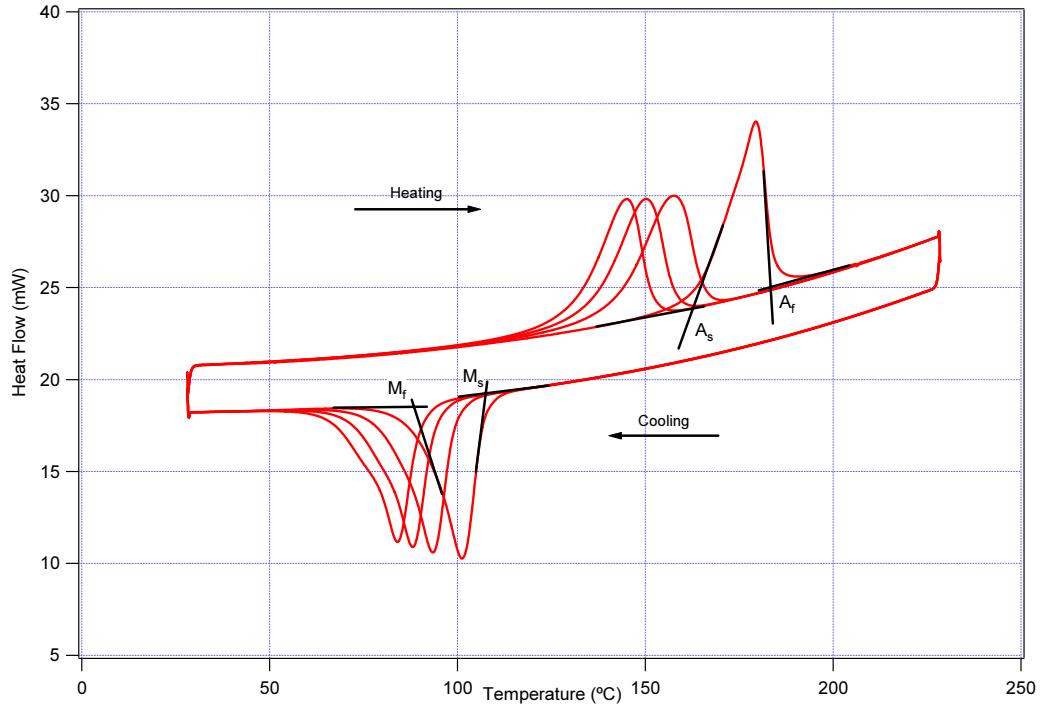


Figure 2.1. Schematic of the response of an SMA during differential scanning calorimetry (DSC).

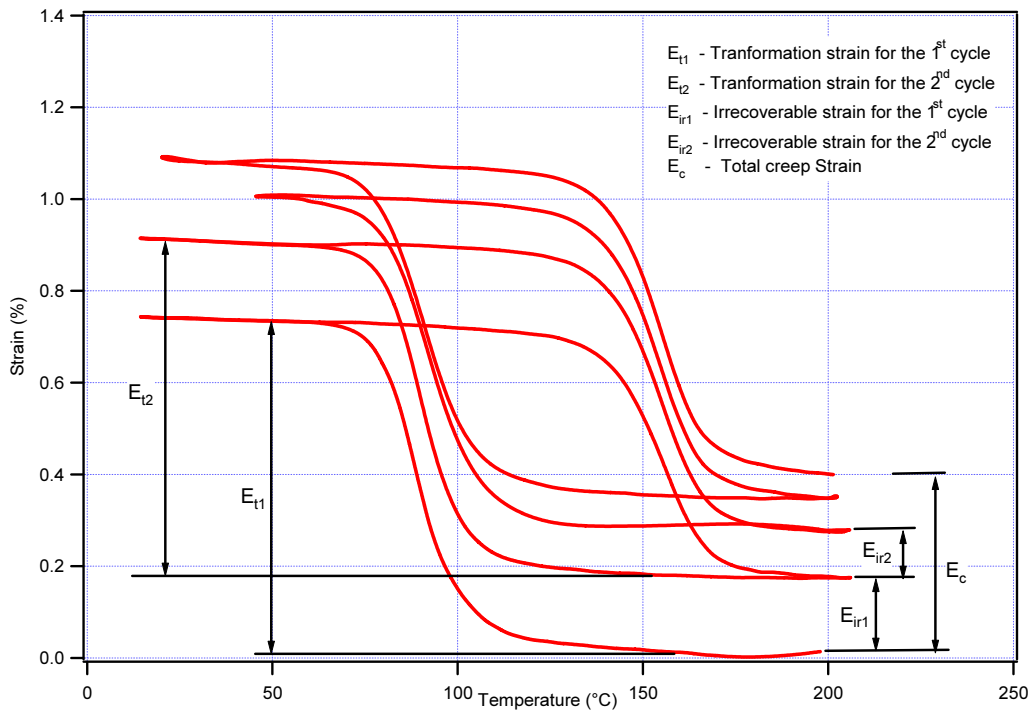


Figure 2.2. Schematic of the temperature-strain response of an SMA having irrecoverable strains per thermal cycling.

As observed in previous studies NiTiHf shape memory alloys shows mechanical peculiarities compared with the NiTi alloy. Dependence of martensitic transformation temperature with cycling is one among them. It is observed that with cycles the transformation temperature increases and there after attains relatively significant stability, in 20 cycles [15, 16]. It was also observed that the increase in transformation attained by the addition of Hf is at the expense of the deterioration of major shape memory properties when compared to NiTi alloys like lower recoverable strains, absence of plateau region in the stress strain curve [15] and the absence of pseudoelasticity [17]. The absence of the stress plateau can be attributed to the deformation mechanism in the NiTiHf system. The stress plateau observed in shape memory alloys during deformation in austenitic state is because of the formation of stress induced martensite. In the case of NiTiHf alloys instead of the formation of pure stress induced martensite, work hardening due to dislocation slip takes place. This is because in NiTiHf alloys, the critical stress required for dislocation slip of parent phase is almost equal to that for stress induced martensitic transformation [17, 18]. This points to the softness of the matrix.

These peculiarities can also be attributed to the 1) distortion of habit plane of the ternary alloy and 2) the observed (001) compound twinning which helps to accommodate the plastic deformation in NiTiHf alloy. Instead in NiTi alloys it is the type 1 and type 2 twins. The distortion of habit plane results in the lesser mobility of the interface which results in the deterioration of shape memory properties in NiTiHf when compared to NiTi alloys. The distorted habit plane favors the nucleation of new variants than reorientation during NiTiHf deformation for it is energetically more favorable. It is also reported that during tension testing a supplementary (001) mechanical twinning is more favorable than detwinning in case of NiTiHf [15].

It is observed that dislocation slip is easy to be introduced during the stressed induced martensitic transformation and the dislocation slip leads to strong work hardening. Otsuka et al [19] reported that the high temperature properties of TiPd and TiPdNi alloys can be improved by strengthening the parent phase which can be used in case of NiTiHf too. Thermo-mechanical treatment (TMT) using Equal Channel Angular Extrusion (ECAE) provides a way to achieve this goal. Possible consequences of TMT can include grain refinement, an increase in dislocation density (strain hardening) via ausforming or

marforming, crystallographic texture strengthening and precipitation hardening [7-10]. In the present case, TMT includes a combination of severe plastic deformation and subsequent annealing heat treatment. Annealing heat treatment may or may not be necessary depending on the temperature at which the deformation is carried out or the way deformation is carried out i.e. stress state and strain level. Usually, deformation above austenite finish (A_f) suppresses the transformation to a very low transformation temperature. ECAE followed by annealing causes the formation of coherent precipitates which favors improved shape memory behavior for precipitated form internal stress fields and there by orients the martensite inside the matrix.

ECAE is superior to the other techniques because of the formation of uniform microstructures, control over the development of grain morphology, formation of specific texture and ease of process [20]. Load is applied from the top of the vertical channel, and the billet is deformed in the shear zone and extruded from the horizontal channel. The angle between the two channels is 90° in the die that we used. The passage of a billet through such a tool produces simple shear in the billet at plane in the channel intersection. SPD of NiTiHf using ECAE is challenging, as for NiTiHf the workability is very limited. ECAE tool design should be able handle high strength levels by limiting friction possibly through a sliding walls concept [21].

In the present study, effects of SPD using ECAE are investigated on the microstructure, transformation behavior and thermo-mechanical cyclic stability for the NiTiHf alloy 49.8Ni-42.2Ti-8Hf (in at. %). The objective is to establish a processing-microstructure-property relationship. Observed unique microstructural features in ECAE processed material show that ausforming with ECAE followed by a small annealing treatment is a powerful tool for improving the cyclic thermal stability of NiTiHf alloys and opens new opportunities for grain boundary engineering in SMAs. ECAE processed samples shows promising results and an outstanding improvement in the thermal stability by stabilizing the M_s Temperature by the 2nd cycle.

CHAPTER III

EXPERIMENTAL PROCEDURE

3.1 Initial Material

We acquired two batches of NiTiHf, one from Department of Energy, AMES Laboratory and the other from flowserve Corporation. The AMES material, 49.8Ni-42.2Ti-8Hf (in at.%) was in plate form, 50 x 50 x 12 mm³ arc melted several times to provide homogeneity, and the flowserve material was in cast form of the same composition with a diameter of 32 mm and a length of ~635 mm. The bar was fabricated by vacuum induction skull melting, casting into cold copper crucibles and hot isostatic pressed (HIP, 2 hours at 900°C). HIPing was performed in order to remove porosity that occurs during casting, but some porosity remained even after HIP. Both the alloy samples were homogenized at 1000°C for 24hrs. For homogenizing, the specimens were inserted into quartz capsules which were evacuated. Then they were placed into an electric furnace after the temperature in the furnace became stable. The specimens were held in the furnace for 24hrs and then quenched into ice water by crushing the quartz capsules. Small samples were cut from the homogenized material using low speed diamond saw for conducting differential scanning calorimetry (DSC) analysis in order to obtain the phase transformation temperatures.

3.2 Processing by Rolling and ECAE

3.2.1 Rolling

We hot-rolled a piece of the plate from Ames Lab to increase the strength of the material and to introduce desired texture. The hot rolling was done non-isothermally at 1000°C and the material thickness was reduced by 40% from the starting thickness of 12 mm.

Three slabs of 3 mm thickness and 50 mm length were cut from the homogenized flowserve sample. Marforming of reductions 5%, 10% and 15% were performed on these samples by multiple passes.

3.2.2 ECAE

The tool for ECAE with 90° corner angle is capable of processing parts with a 25 mm x 25 mm square cross section and a length up to 203 mm. The tool can operate isothermally only up to 300°C, and so we have pre-heated the SMA billets to perform extrusions with the sample at temperatures above 300°C. Since the strength and strain-hardening response of NiTiHf at different temperatures and strain rates under very high strain levels are not well-known, we have canned the materials in Ni. The reason for this was to minimize possible damage to the tool and to minimize the significant temperature drop during non-isothermal extrusions above 300°C. Because of the non-isothermal nature of the extrusions, the extrusion rates used were quite fast (12.5 mm/sec and 25 mm/sec).

The canned SMA samples had a 12 mm diameter and a length of 50 mm. We have performed the ECAE at temperatures ranging from 500 to 650°C as summarized in Table 3.1. We have used three different ECAE routes (A, B and C). The ECAE routes are described in Figure 3.1. Each route results in a different deformation morphology and texture depending on crystallographic structure. For example, Routes A and B result in elongated grain morphology while Route C led to equiaxed structure.

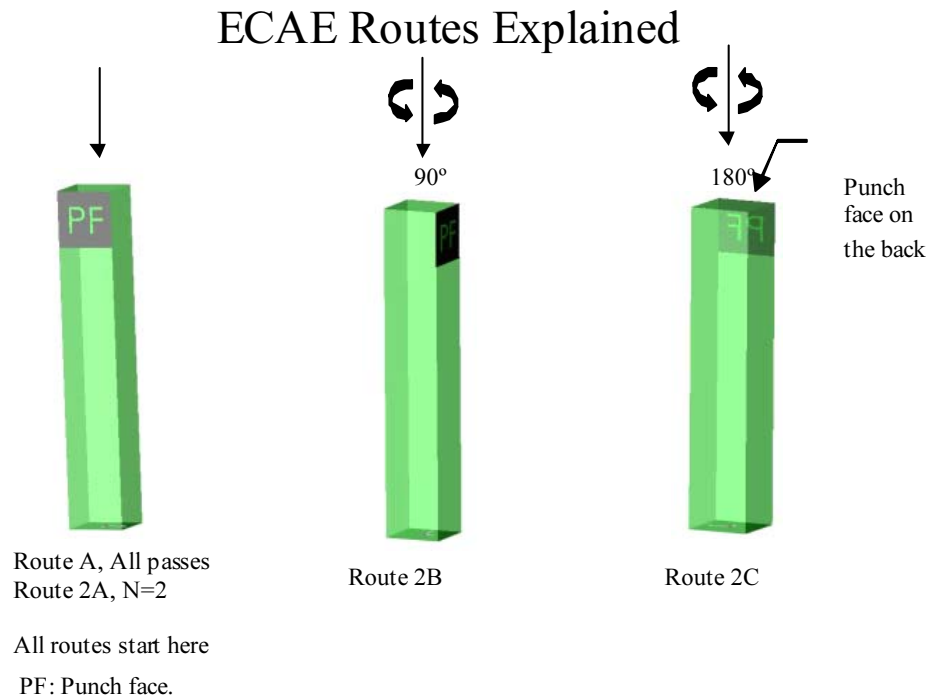


Figure 3.1. Schematic of the ECAE routes.

Digital images of the extracted ECAE billets are shown in Figure 3.2. All extrusions were completed without any problem or sample failure. Minor surface cracks were observed only in the material extruded at 500°C, possibly due to the non-isothermal nature of the extrusion and die chilling effect. The digital images of the extruded samples can be seen in Figure 3.2. It is believed that these surface cracks can be eliminated during isothermal extrusion at this temperature. This improved formability of the NiTiHf alloy using ECAE is significant because an earlier review [22] of the formability of NiTiHf alloys using 50% rolling reduction concluded that the minimum temperature for rolling NiTi12%Hf alloy without cracks or shear localization is 700°C. The strain level imposed during one ECAE pass is equivalent to 69% rolling reduction. Figure 3.3 depicts the improved workability attained through ECAE when compared with the conventional ausforming process of hot rolling.



Figure 3.2. Images of the ECAE processed homogenized 49.8%Ni-42.2%Ti-8%Hf (at.%) alloy after extracting from Ni cans. (a) one pass at 500°C, (b) one pass at 600°C, (c) two Route B passes at 650°C, and two Route C passes at 650°C.

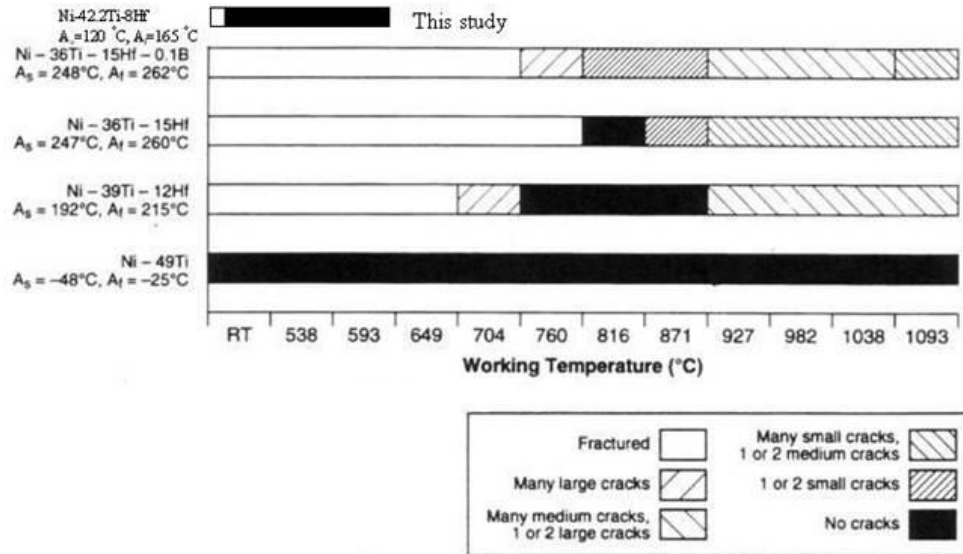


Figure 3.3. Relative workability of NiTi and NiTiHf alloys. The previous studies were done for attaining a 50% reduction by rolling.[22]

3.3 Differential Scanning Calorimetry

Small samples from the processed materials were used to conduct DSC analysis to obtain the phase transformation temperatures. DSC was conducted on samples weighing an average of 30 mg at a constant rate of $10^\circ\text{C}/\text{min}$. Figure 3.4 depicts the schematic a typical DSC curve. Transformation Temperatures M_s , M_f , A_s and A_f are calculated by tangent method. They are obtained by drawing tangents on the curve where the phase transformation occurs.

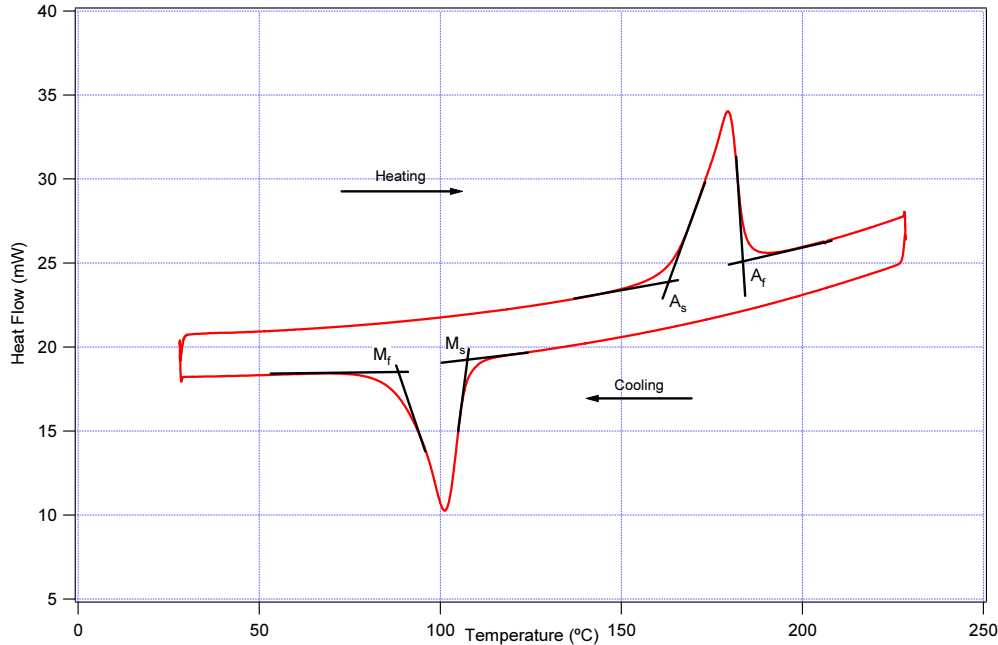


Figure 3.4. Schematic of finding transformation temperatures from DSC curve.

3.4 Thermo-mechanical Testing

Dog bone shape tension specimens were EDM machined from the homogenized, extruded as well as hot rolled and marformed samples to have an 8 mm(Height) * 3 mm(Width) * 2 mm(Thickness) gauge section. Thermal cycling was conducted on the specimens using a servo hydraulic MTS machine. The test equipment is a MTS 810 servo-hydraulic test frame with in-house built heating and cooling capabilities. The specimens were heated and cooled at an approximately constant rate of 15°C/ min. The heating and cooling is achieved through thermal conduction from heated/cooled grips. The grips are cooled by liquid nitrogen flow inside the grips and heating elements are used for heating. Temperature was measured in the middle of the sample, and monitored at three different locations. The strain is measured on the sample gage section using an MTS miniature extensometer with 3-mm gage length that is mounted on the sample. The thermal cycling was conducted between 30°C and 200°C. The external stress applied on the specimen was increased from 0 MPa to 100 MPa and thereafter to 200 MPa as the specimens show stabilization of transformation strain or a significant level of unrecoverable transformation strain. After cycling the specimen at 200 MPa load, the

sample is unloaded at fully austenitic stage and are tested for two way shape memory effect by thermally cycling under 0 MPa stress.

Once the strain temperature curve is obtained, it is analyzed to obtain the important factors that determine the shape memory effect for comparison between various routes. The main factors considered are transformation strain, irrecoverable or creep strain Martensitic transformation start temperature (M_s) and hysteresis. A schematic describing the method adopted is shown in Figure 3.5. Transformation strain is obtained by measuring the strain recorded during the martensitic transformation (during cooling). Creep strain is measured by calculating the difference between the forward transformation and reverse transformation in one cycle. M_s is obtained by using the tangent method and hysteresis is calculated by measuring the distance at the mid-point of the curve.

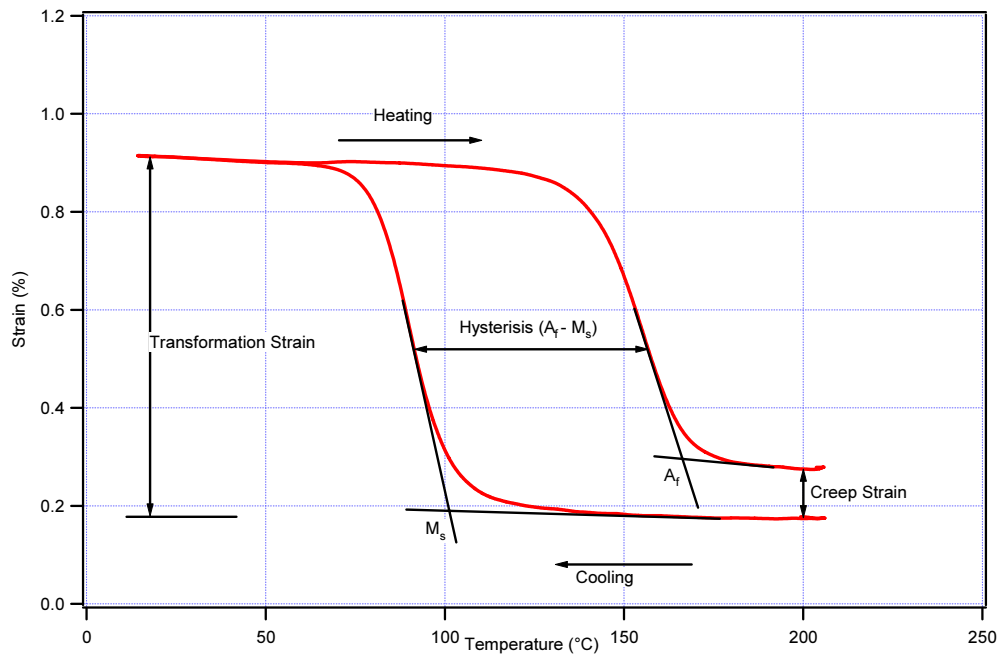


Figure 3.5. Schematic of the analysis of temperature-strain curve.

3.5 Microstructural Evolution

For optical microscopy small samples were cut from the ECAE processed, hot rolled as well as homogenized and marformed samples and were polished using silicon carbide papers followed by colloidal silica or alumina. The polished samples are etched in a solution of 50-ml glycerol , 12 ml concentrated nitric acid, 2-ml concentrated hydro fluoric acid for 5 minutes.

The microstructure of the materials was investigated using transmission electron microscopy (TEM). TEM foils perpendicular to the extrusion direction were prepared from the samples by mechanical thinning down to 100 μm , followed by twin-jet electro polishing with a solution of 20 volume % H_2SO_4 in a methanol solution at 25°C. A JEOL 2010 microscope operated at a nominal accelerating voltage of 200 kV was utilized. The main idea was to investigate the microstructural evolution after ECAE.

Table 3.1. Summary of the thermo-mechanical processing conducted

Process	Material	Extrusion Route	Rolling Reduction (%)	Temperature	Can Material	Extr. Rate(mm/sec)
ECAE	FS	1A	NA	500°C	Ni	12.5
ECAE	FS	1A	NA	600°C	Ni	12.5
ECAE	FS	2B	NA	650°C	Ni	25.0
ECAE	FS	2C	NA	650°C	Ni	12.5
Rolling	AMES	NA	40%	1000°C	SS	NA
Rolling	FS	NA	5%	RT	NA	NA
Rolling	FS	NA	10%	RT	NA	NA
Rolling	FS	NA	15%	RT	NA	NA

FS : Flowserve

CHAPTER IV

RESULTS AND DISCUSSION

4.1 Calorimetric Analysis

For the as-received Ames material and the as-received flowserve material, we find that the transformation temperatures are not stable. Each cycle of DSC leads to lower transition temperatures, at least for the first 5 cycles. The amount of the shift lessens as the number of cycles increases, suggesting asymptotic behavior. It has been reported [15] that the transition temperatures of unprocessed NiTiHf alloys stabilize usually after 20-30 thermal cycles.

For the hot-rolled Ames material we find that the transformations are comparatively much more stable. The difference between homogenized and hot-rolled NiTiHf is illustrated in Figure 4.1.

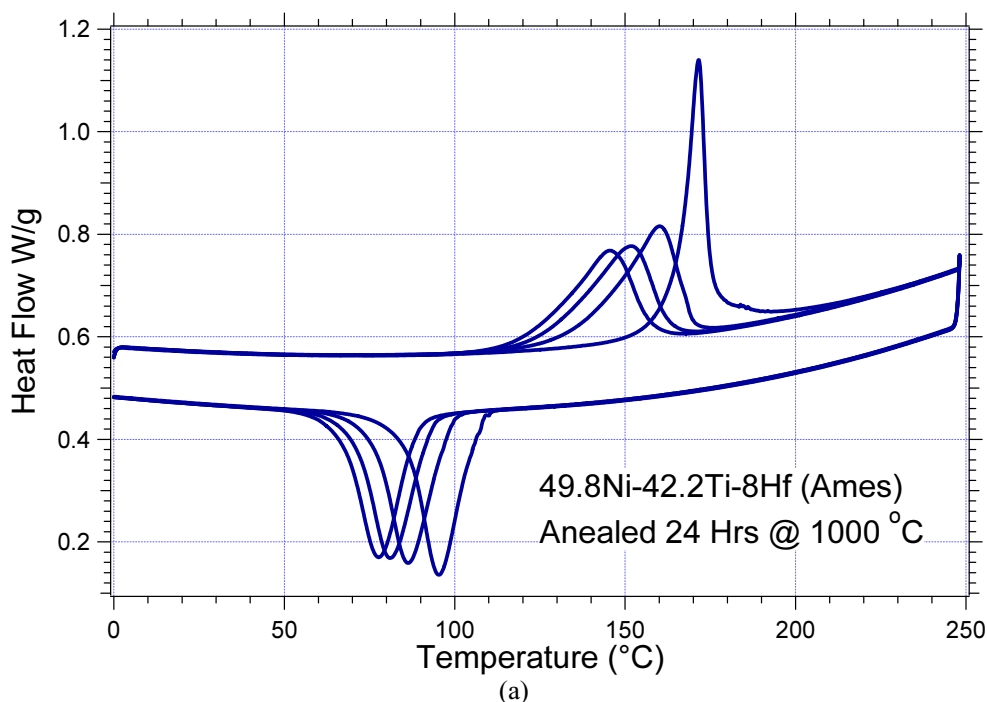


Figure 4.1. Identification of 49.8Ni-42.2Ti-8Hf transformation temperatures by differential scanning calorimetry (DSC). (a) Homogenized sample at 1000 °C for 24 hours,

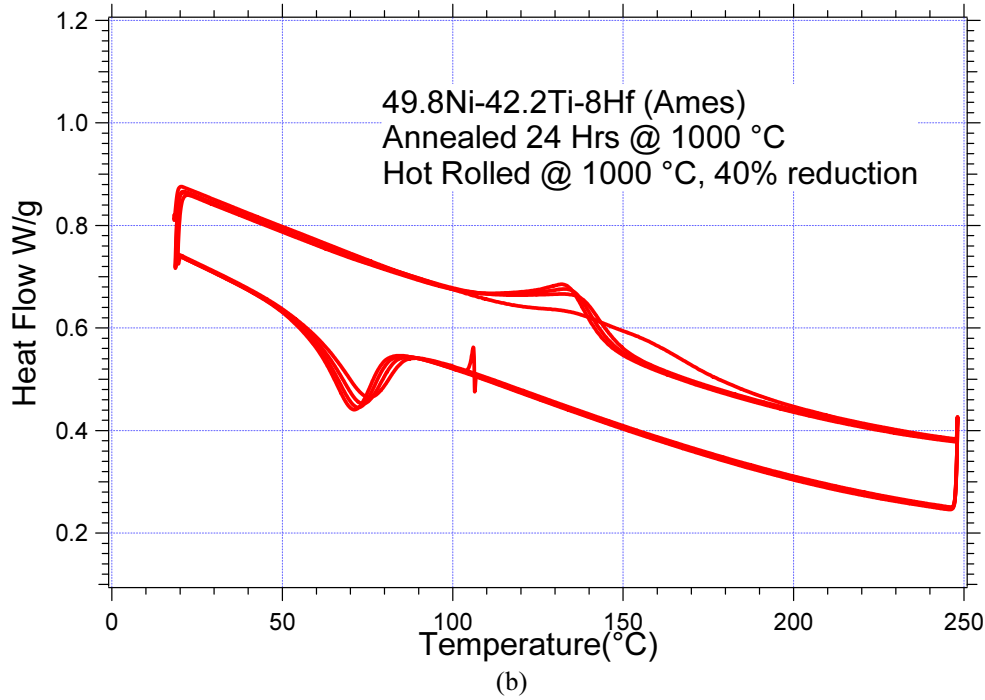


Figure 4.1. Continued. (b) hot rolled at 1000 °C to 40% reduction after homogenization.

The quantity $A_f - M_s$ is a useful measure of hysteresis in shape memory alloys. For the hot-rolled Ames material we have $A_f - M_s \cong 60^\circ\text{C}$ after 5 cycles. It may be desirable to decrease the hysteresis for more rapid thermal control in an application. We expect smaller hysteresis will happen as a byproduct of thermo-mechanical treatments to tailor the microstructure for improved creep behavior, i.e. stable transformation behavior.

DSC experiments have also been conducted on the ECAE processed materials. The results are shown in Figure 4.2. As can be seen in these figures, the transformation temperatures of the ECAE processed materials are significantly more stable as compared to the homogenized materials. The decrease in M_s temperature due to DSC cycling is 1-4°C/cycle in the ECAE 1A 500°C sample, 2-3°C/cycle in the ECAE 1A 600°C sample, 1-4°C/cycle in the ECAE 2B 650°C sample, and 1-2°C/cycle in the ECAE 2C 650°C sample where as it is 6-7°C in the case of homogenized sample. The ECAE 2C 650°C sample demonstrates the best stability among all ECAE samples without any annealing. However, annealing the samples in DSC up to 400°C and holding the sample at this temperature for one minute significantly improves the transformation stability, making

the decrease in $M_s \sim 0-1^\circ\text{C}/\text{cycle}$, similar to conventional NiTi. This can be observed in Figures 4.2 (c) and (d). The hysteresis ($A_f - M_s$) is decreased about 10°C as compared to the homogenized material. The best hysteresis was obtained in the ECAE 2C 650°C sample which was 54°C as compared to 65°C of the homogenized sample.

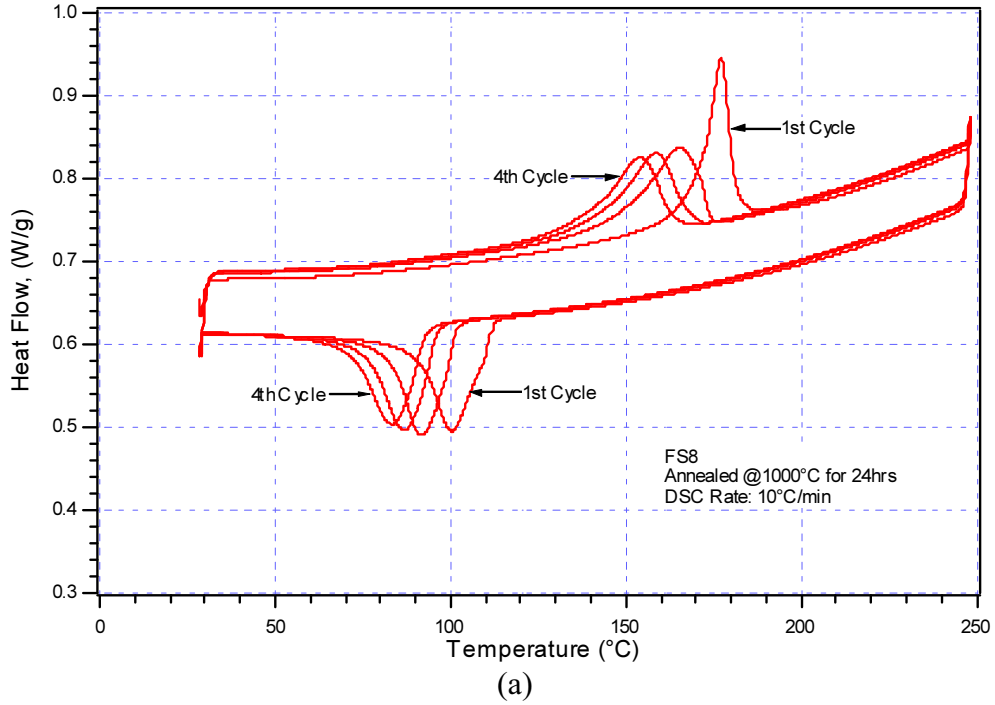


Figure 4.2. Identification of 49.8Ni-42.2Ti-8Hf transformation temperatures after (a) homogenized flowserve material - HIPed 49.8Ni-42.2Ti-8Hf (2hrs @ 900°C)

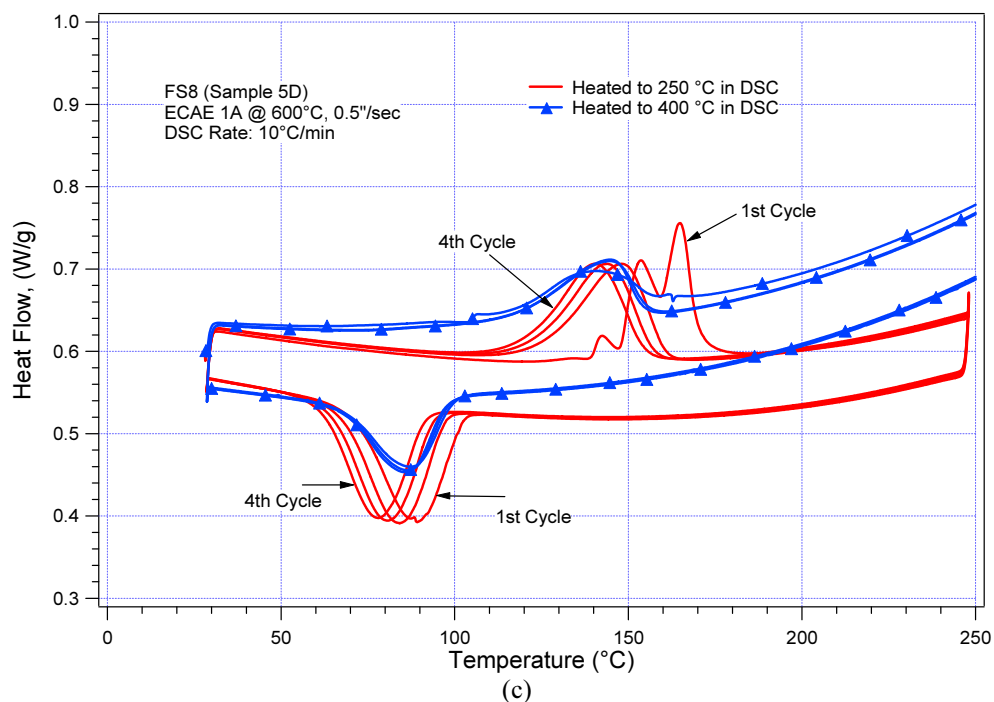
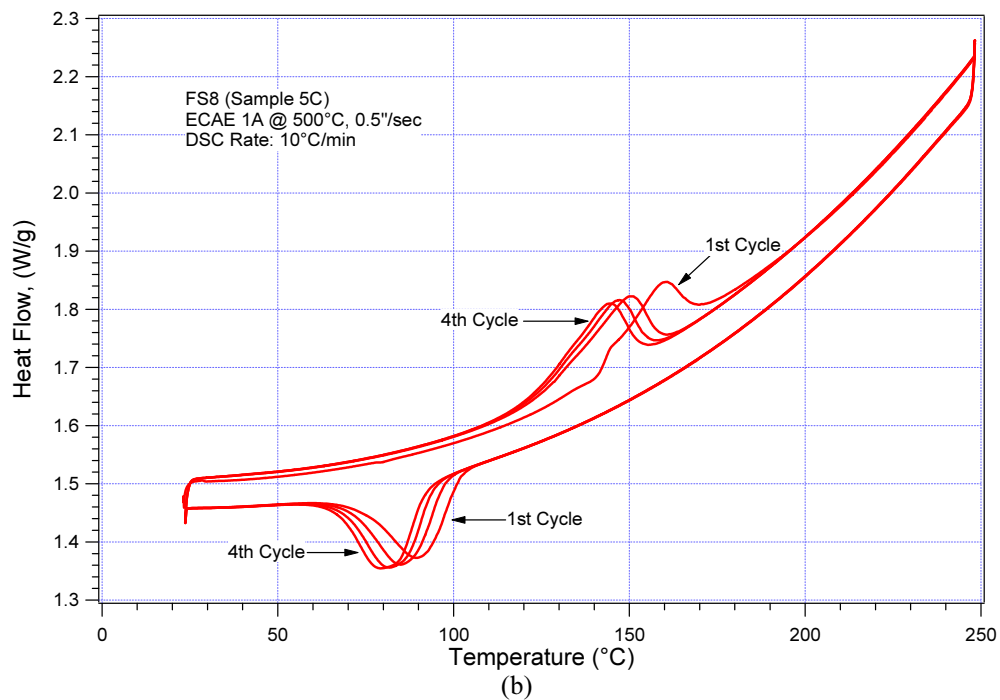


Figure 4.2. Continued. (b) one ECAE pass at 500 °C, (c) one ECAE pass at 600°C

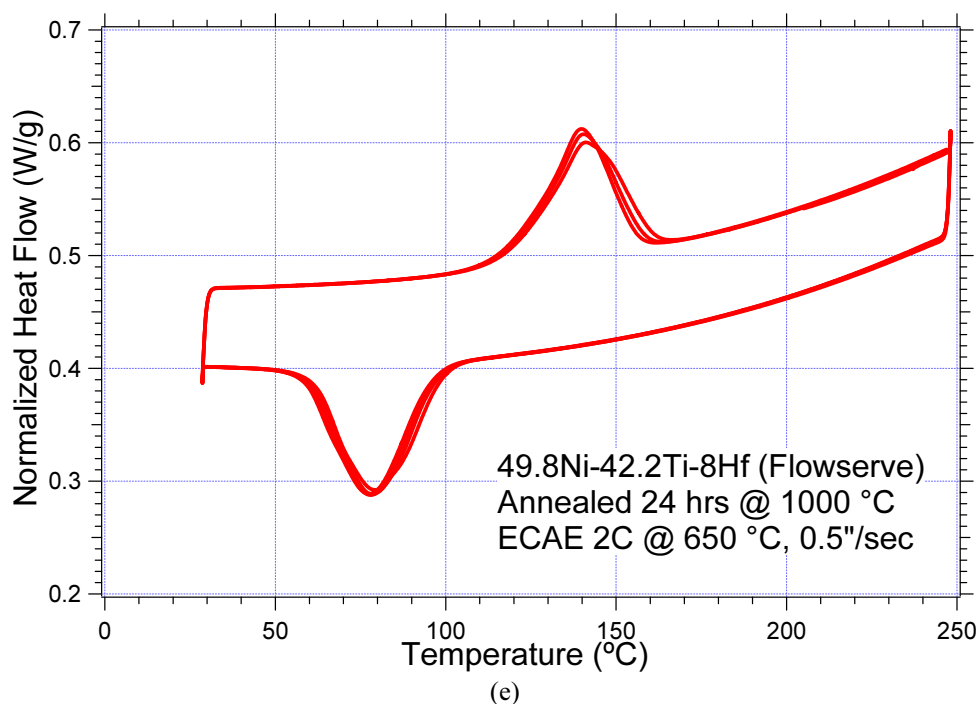
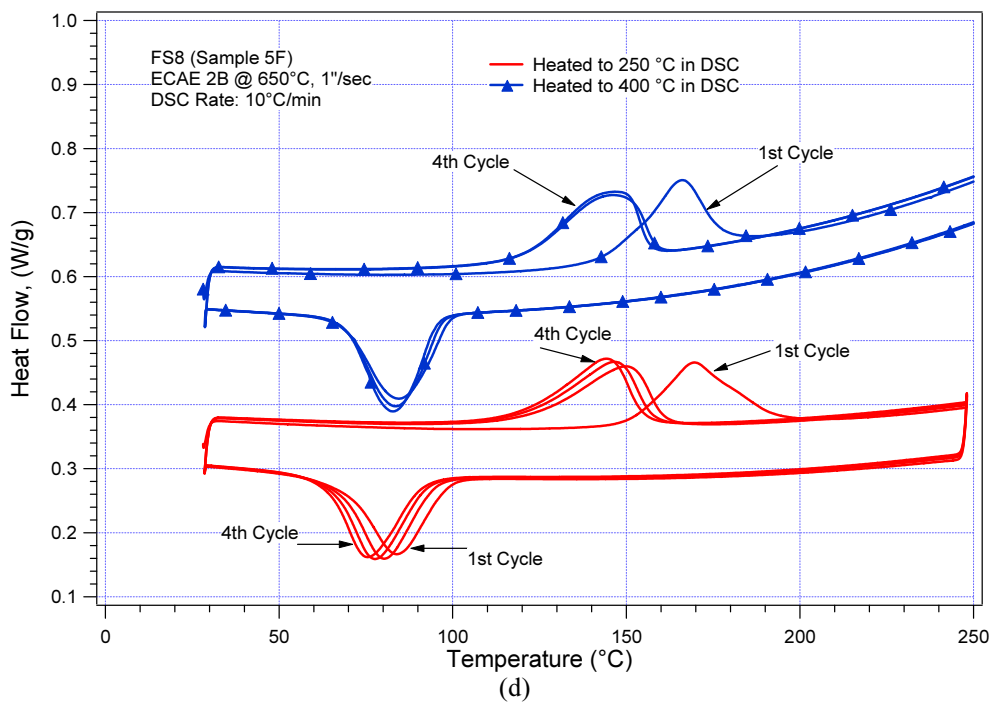


Figure 4.2. Continued. (d) two ECAE passes at 650°C using Route B, (e) two ECAE passes at 650°C using Route C.

In the previous studies it is already established that this drop in transformation temperatures during thermal cycling is due to the defect generation and possibly internal stress induced during fabrication and subsequent thermo-mechanical treatments. After sufficient cycling, when the defects are stabilized, the transformation temperatures are stabilized and this is also observed in afore mentioned samples. We can see a significant decrease in the rate at which the M_s Temperature drops with cycling in case of the ECAE processed material. This can be attributed to the strengthening of the matrix and introduction of precipitates in the matrix.

4.2 Microstructural Evolution after Processing

After etching, the microstructure of the sample is clearly observed and they are presented in Figures 4.3 to 4.10.

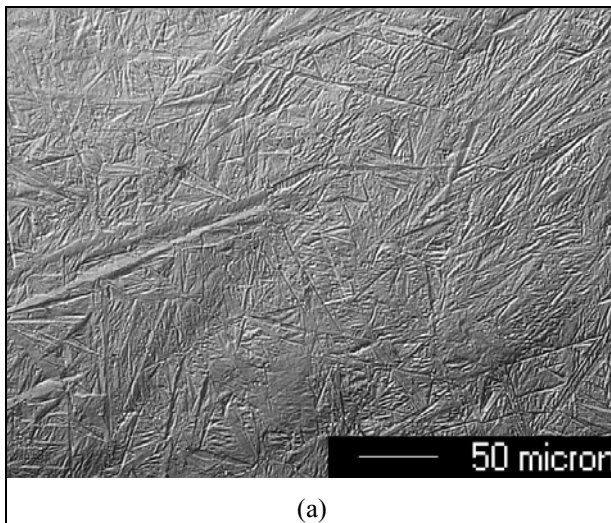


Figure 4.3. Optical micrographs of (a) homogenized (24hrs @1000°C) 49.8Ni-42.2Ti-8Hf Ames material.

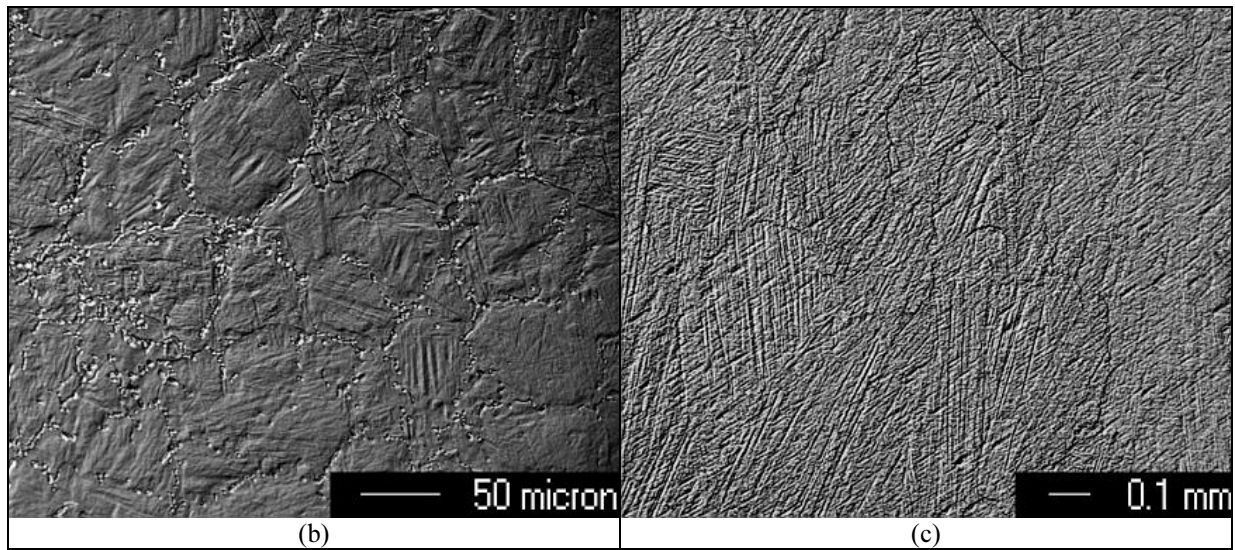


Figure 4.3. Continued. (b) as received HIPed 49.8Ni-42.2Ti-8Hf (2hrs @ 900°C) flowserve material, (c) homogenized 49.8Ni-42.2Ti-8Hf (2hrs @ 1000°C) flowserve material.

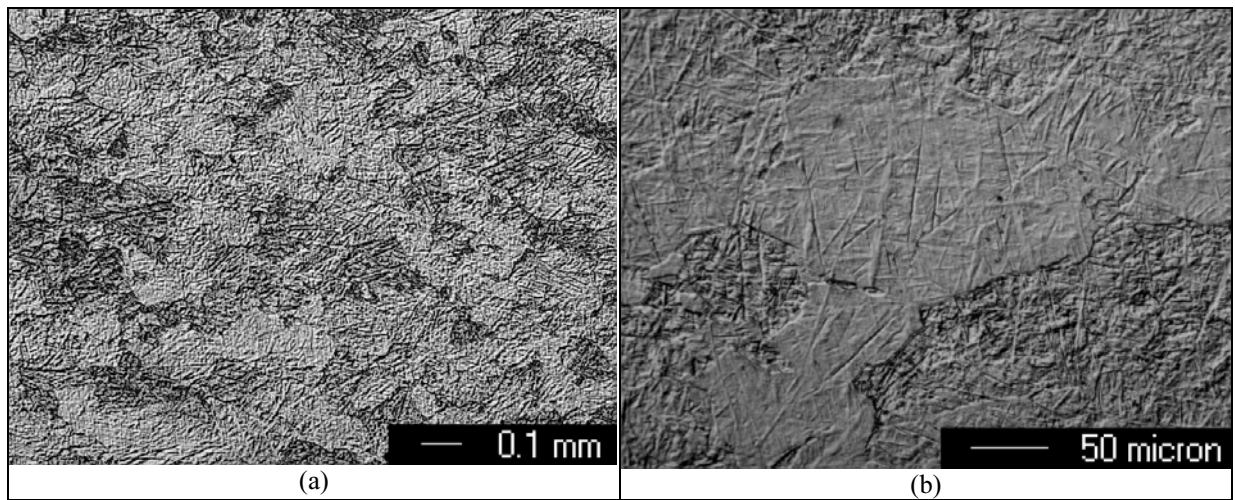


Figure 4.4. Optical micrographs of the Ames material, 49.8Ni-42.2Ti-8Hf, hot rolled at 1000 °C to 40% reduction after homogenization.

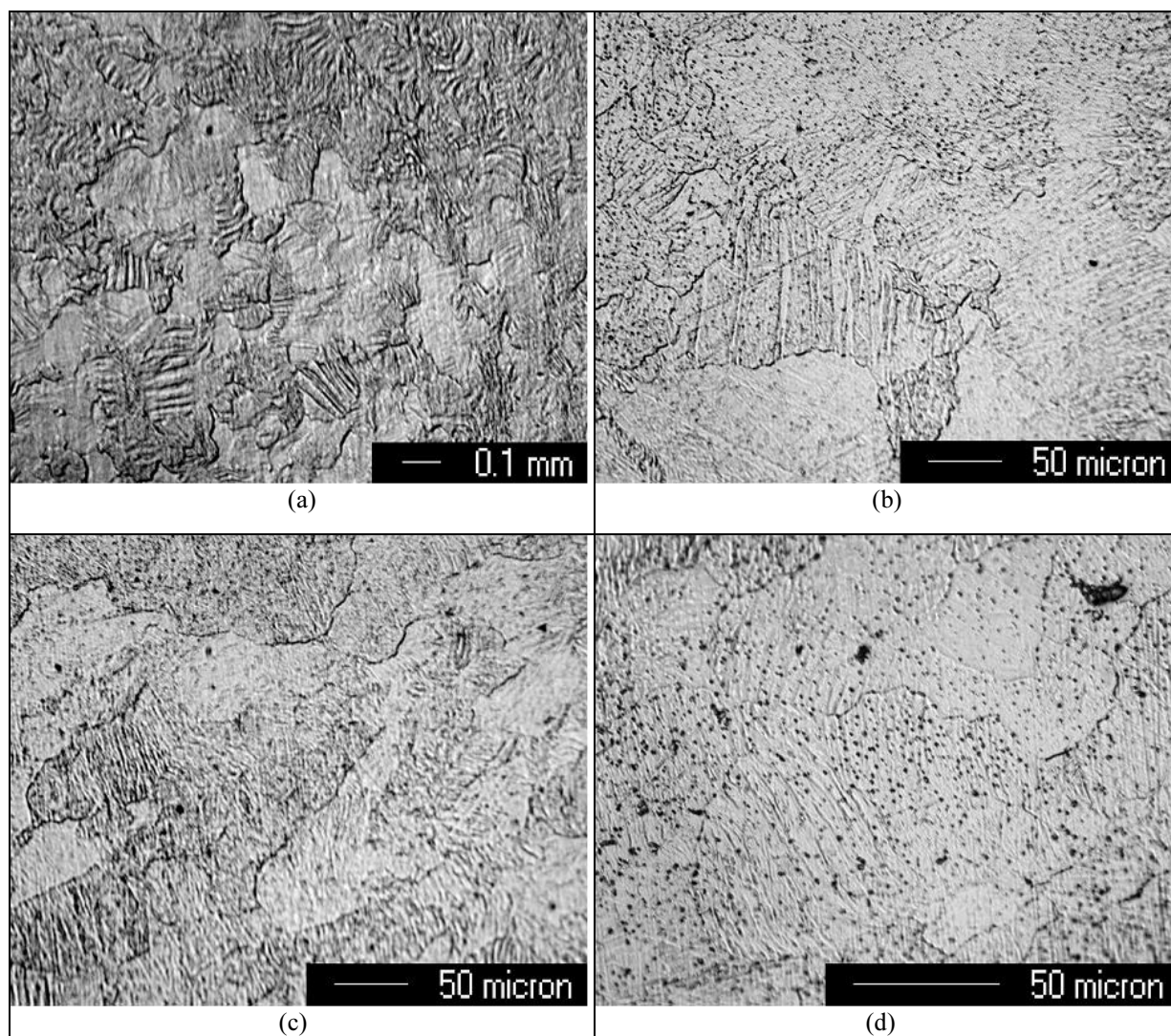


Figure 4.5. Optical micrographs of the flowserve material 49.8Ni-42.2Ti-8Hf, after one ECAE pass at 500°C.

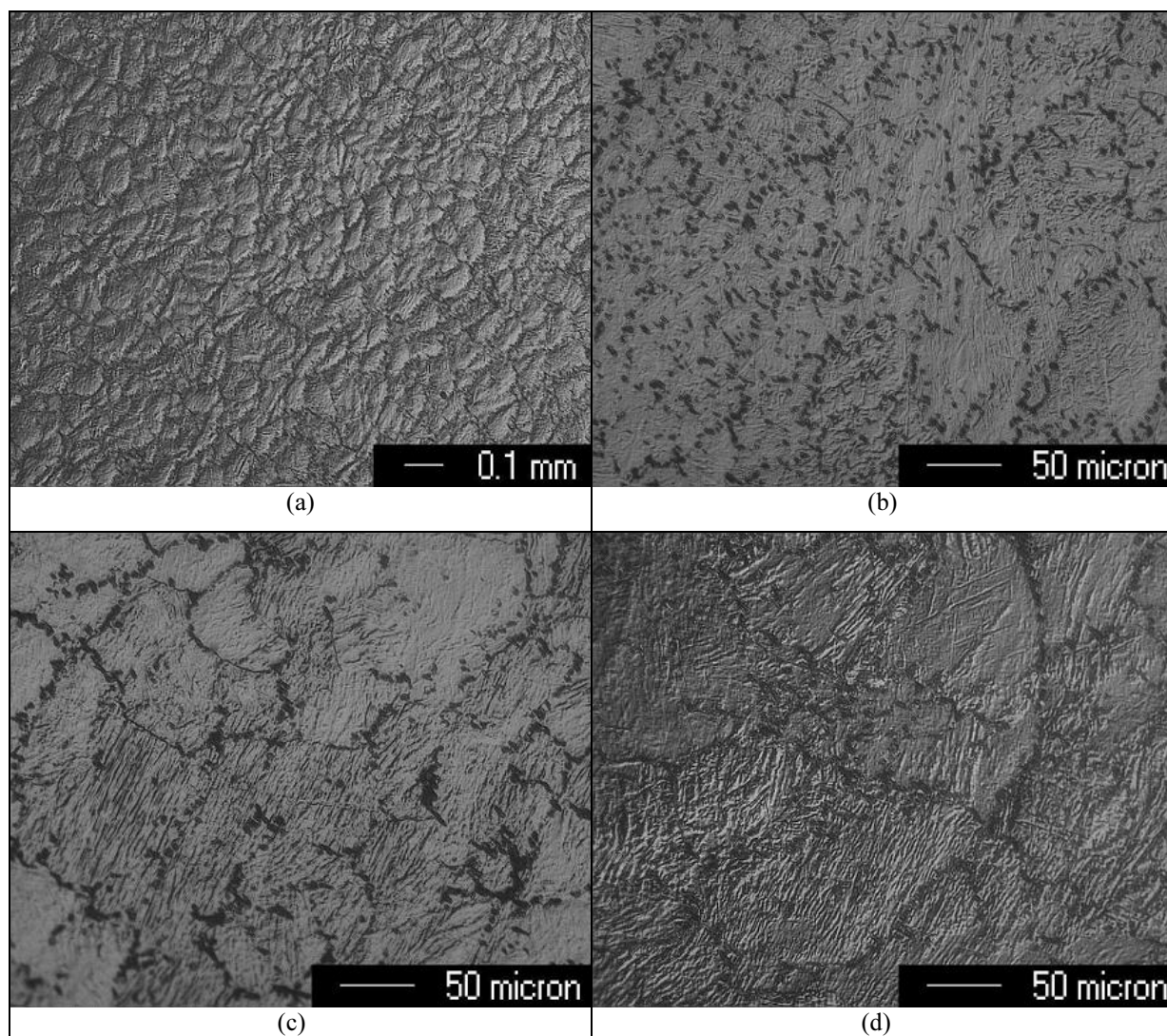


Figure 4.6. Optical micrographs of the flowserve material 49.8Ni-42.2Ti-8Hf, after one ECAE pass at 600°C.

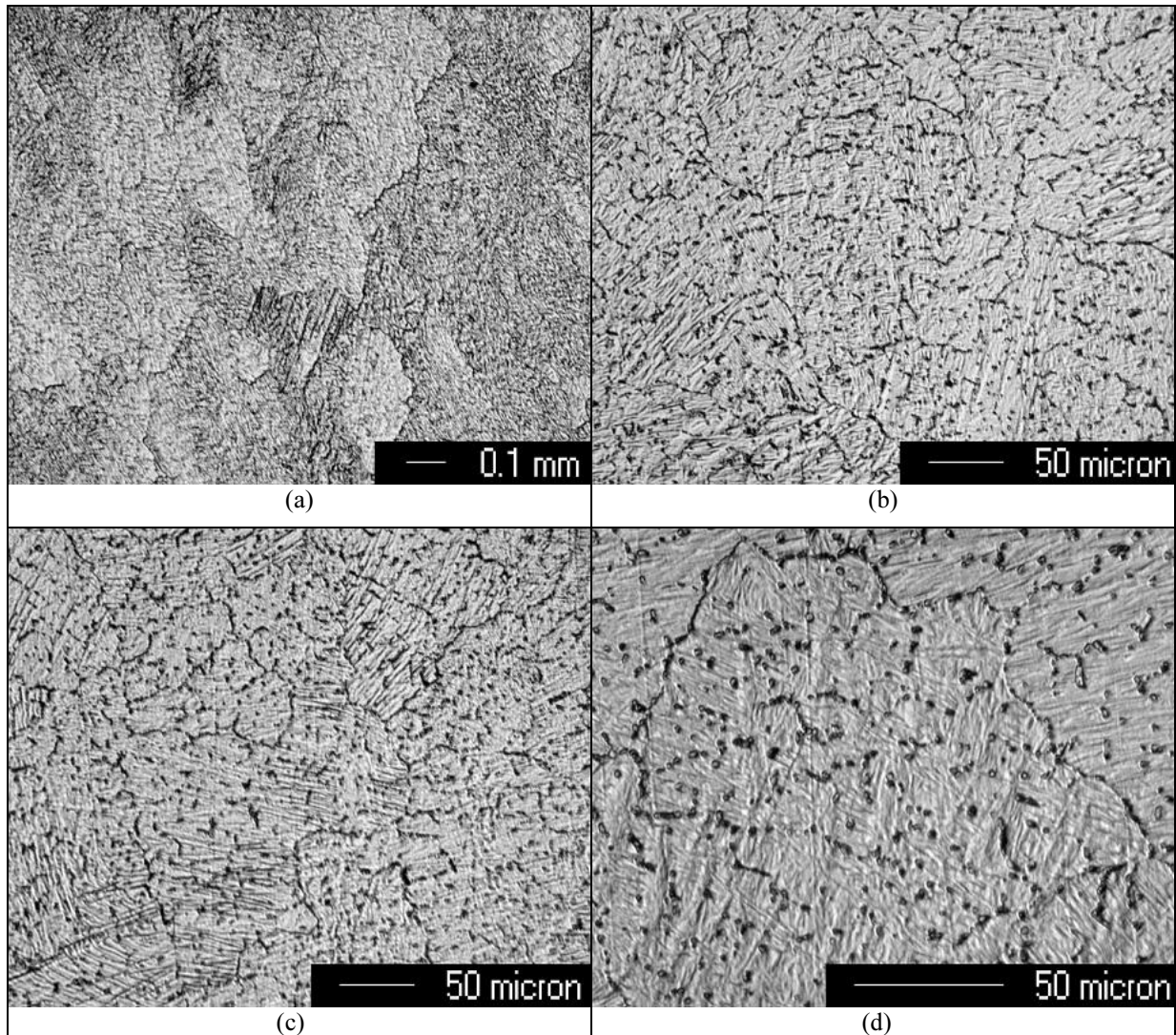


Figure 4.7. Optical micrographs of the flowserve material 49.8Ni-42.2Ti-8Hf, after two ECAE passes using Route C at 650°C.

It is clearly observed that the grain size decreased after processing with ECAE. The presence of precipitates in the flowserve samples is to be noted (Figure 4.3 (b)). In the ECAE 1A 600°C sample there are precipitates along the grain boundaries, which in case of ECAE 2C 650°C sample, the precipitates are more distributed and are mainly present inside the grains. It should be noted that in the hot rolled samples, the precipitates are not observed probably because of the high purity of the AMES material which can be observed in Figure 4.3 (a). Although we have not experimentally determined the

composition and the structure, the precipitates are expected to be oxides because of their size and because of the previous results.

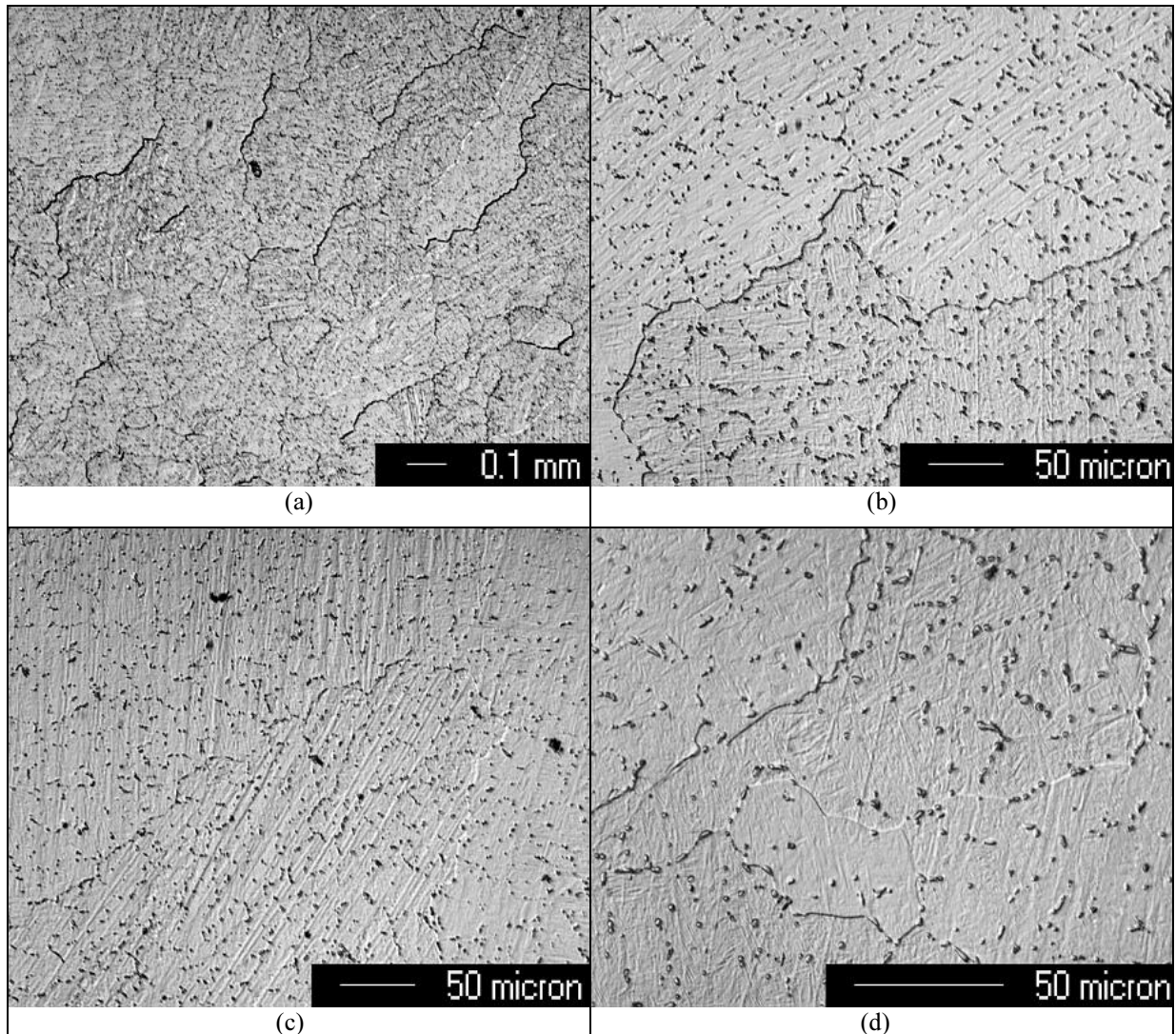


Figure 4.8. Optical micrographs of the flowserve material 49.8Ni-42.2Ti-8Hf, marformed to 5% reduction.

In the ECAE 2C 600°C sample (Figure 4.7) we can see that the precipitates are homogeneously distributed throughout the matrix and the size is smaller when compared to the one pass samples. The formation of finer precipitates evenly distributed along the matrix improves the strength of the material. It is also observed that the grain size is lesser ~40 microns when compared to the one pass sample.

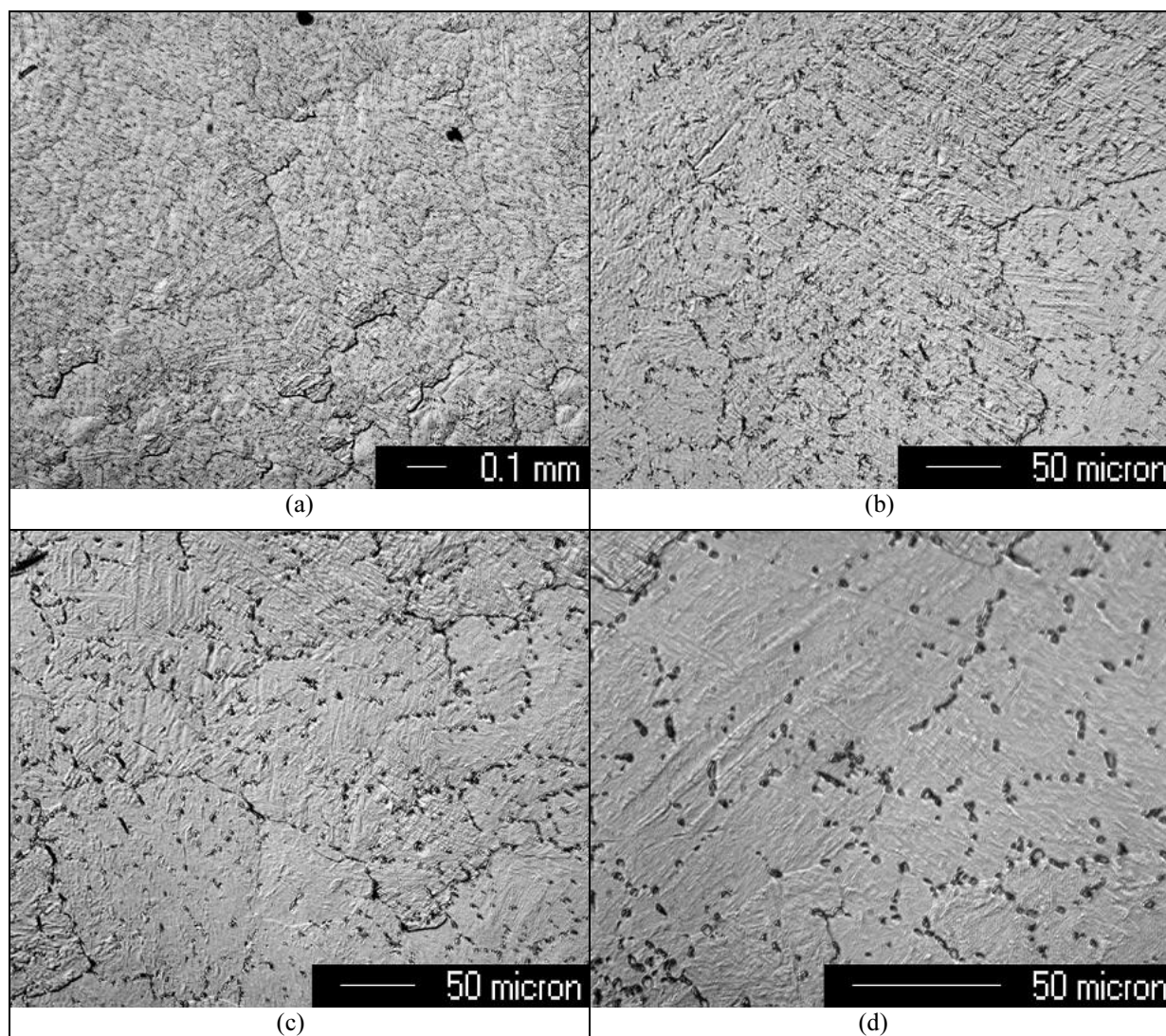


Figure 4.9. Optical micrographs of the flowserve material 49.8Ni-42.2Ti-8Hf, marformed to 10% reduction.

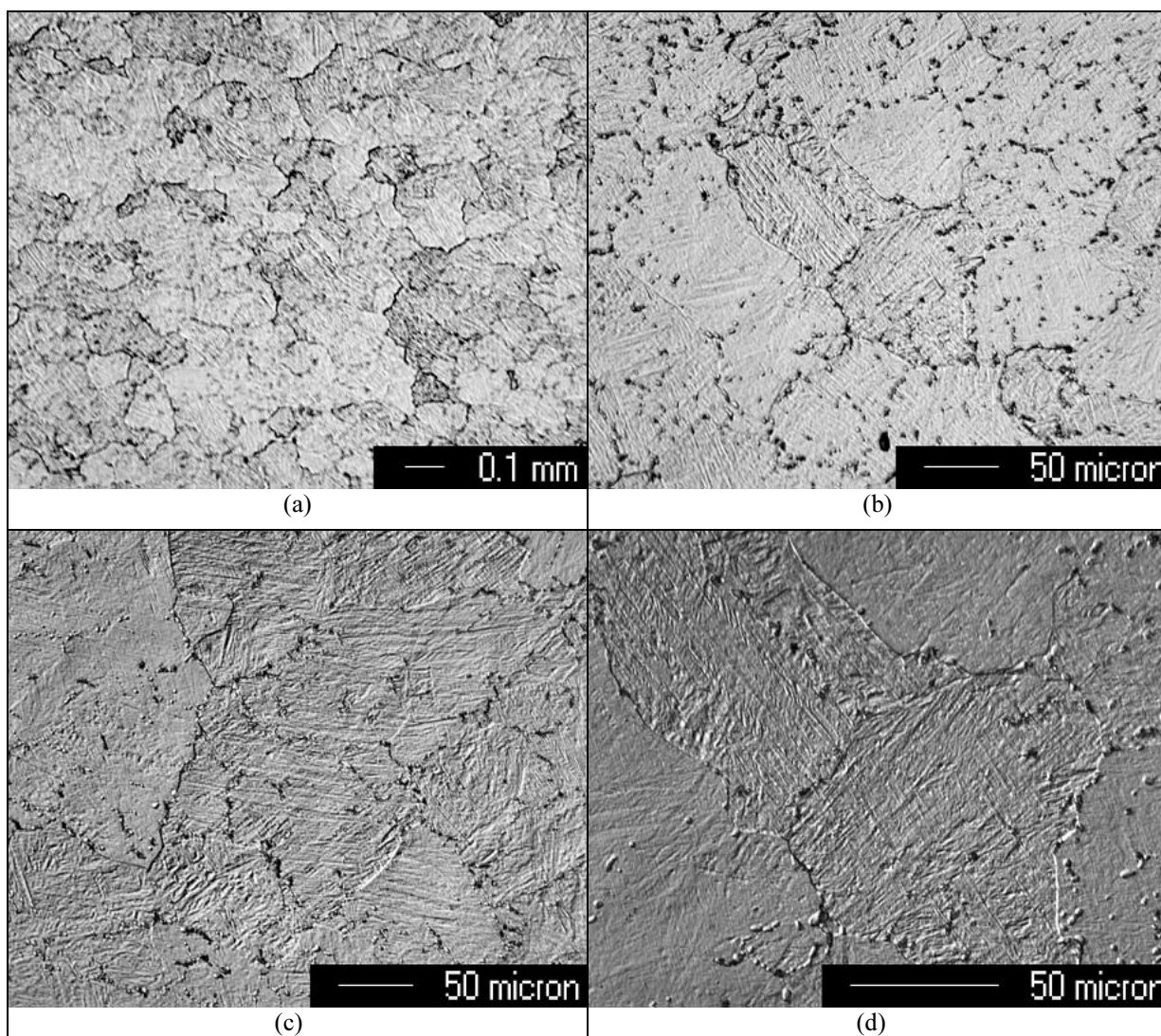


Figure 4.10. Optical micrographs of the flowserve material 49.8Ni-42.2Ti-8Hf, marformed to 15% reduction.

Figure 4.11 shows TEM images from the hot rolled Ames material. No precipitates were observed in these TEM samples, at least at the magnifications used. There are three different martensite morphologies obvious in these images: 1) martensite with thin internal twins, i.e. internal twin boundaries are relatively straight (Region A), 2) martensite with internal twins but some of the internal twin boundaries are not straight (Region B), and 3) martensite with very thick internal twins (Region C). The intervariant boundaries and some of the internal twin boundaries are wavy as opposed to what is typically observed in NiTi and Cu based SMA's. The reason for the waviness of these boundaries is the relatively high volume change during martensite to austenite phase transformation. The volume change can be accompanied either by internal twinning or dislocation slip. If the stress required for dislocation slip activation is low, then dislocations and internal twins form together and both intervariant boundaries and twin boundaries become wavy because of dislocations. Thus, lattice invariant shear assumption of martensitic transformation is not valid anymore. To circumvent this problem and to obtain stable shape memory properties, the volume fraction of martensite variants with thin internal twins and straight boundaries (Region A) should be increased.

This can be achieved by increasing the stress level required for dislocation slip, i.e. strengthening the matrix. The hot rolling sample contains some regions with martensite variants having straight internal twin boundaries, but to improve the properties further, these regions should be increased. Preliminary TEM investigation of the ECAE 1A 500°C sample shows (Figure 4.12) that the volume fraction of martensite variants with straight internal twin boundaries and straight intervariant boundaries increases. Precipitates were not observed in this sample either using TEM, perhaps because they are quite large for the TEM magnification.

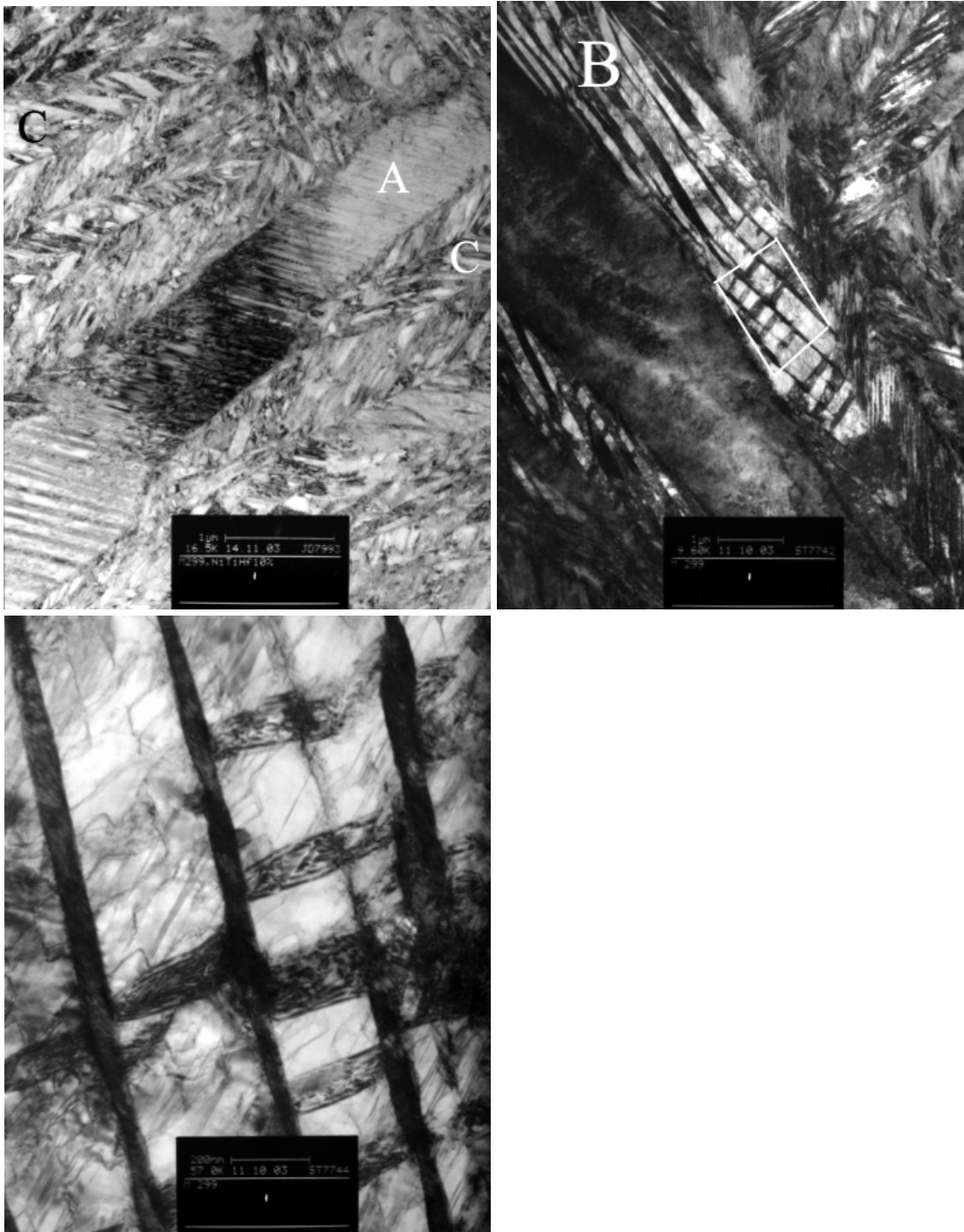


Figure 4.11. Bright field TEM images of hot-rolled material (starting material from Ames: 49.8Ni-42.2Ti-8.0Hf). The images are at approximately 17,000 X, 10,000 X and 60,000 X, respectively. In the lower magnification image, three families of martensite variants and internal twins are apparent, while the higher magnification image shows a high density of dislocations between martensite variants. (c) is the higher magnification image of the region enclosed with the white box in (b).

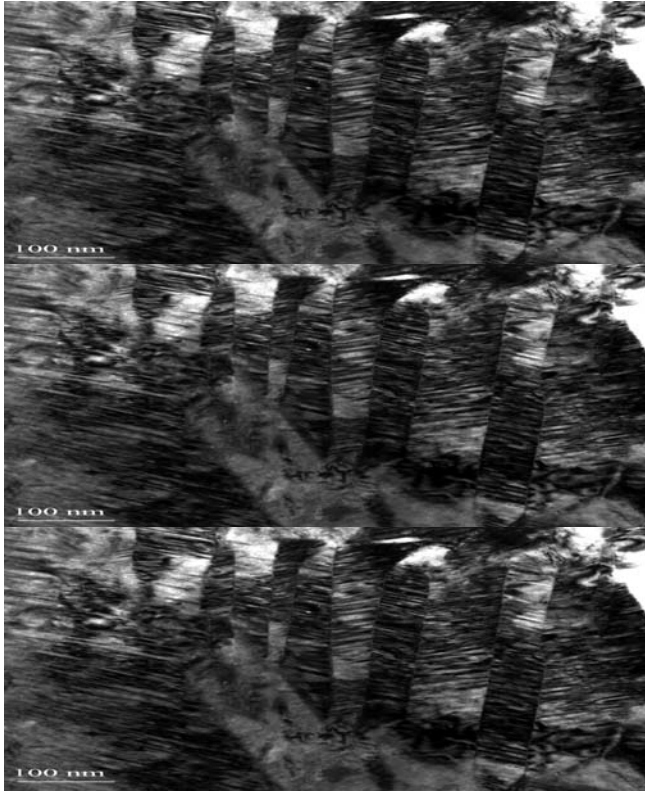


Figure 4.12. Bright field TEM image of the sample ECAE processed at 500 °C using Route A, only one pass. Martensite variants with straight boundaries and internal twins are evident.

The homogeneous distribution of precipitates in the matrix in case of ECAE 2C 650° C samples improves the strength of the matrix and this demands the importance of multiple passes. The increase volume fraction of martensite variants with straight internal twin boundaries and straight intervariant boundaries in the case of ECAE 1A 500°C sample when compared to hot rolled sample proves the advantage of ECAE over conventional ausforming processes.

4.3 Thermo-mechanical Experiments

We have performed thermal cycling under constant stress on ECAE samples, hot-rolled samples as well as homogenized and marformed samples. This was to analyze and study the effect of thermal cycling on the stability of the material.

Figures 4.13 – 4.17 show the thermal cycling results under constant tensile loads (0, 100 and 200 MPa) for homogenized and ECAE samples.

As can be seen in Figure 4.13(a), significant two-way shape memory effect has not been observed for homogenized material. When martensitic transformation occurs, the martensite variants form a self-accommodating structure such that no external shape change is observed. When an external stress is applied, one or more of the martensite variants is biased which leads to external shape change. When the stress level is increased, the magnitude of the external strain also increases as seen in Figure 4.13. An important observation is the significant residual irrecoverable strain in each cycle. This will be called “creep strain” in the rest of the discussion. The creep strain after 10 cycles is 0.6% under 100 MPa stress while it increases to 0.76% under 200 MPa. The main reason for the significant creep strain and the change in transformation temperatures as with thermal cycling is dislocation formation due to relatively large volume change during transformation from austenite to martensite. The formation of dislocations decreases the elastic stored energy, and during back transformation a reduced amount of strain is recovered.

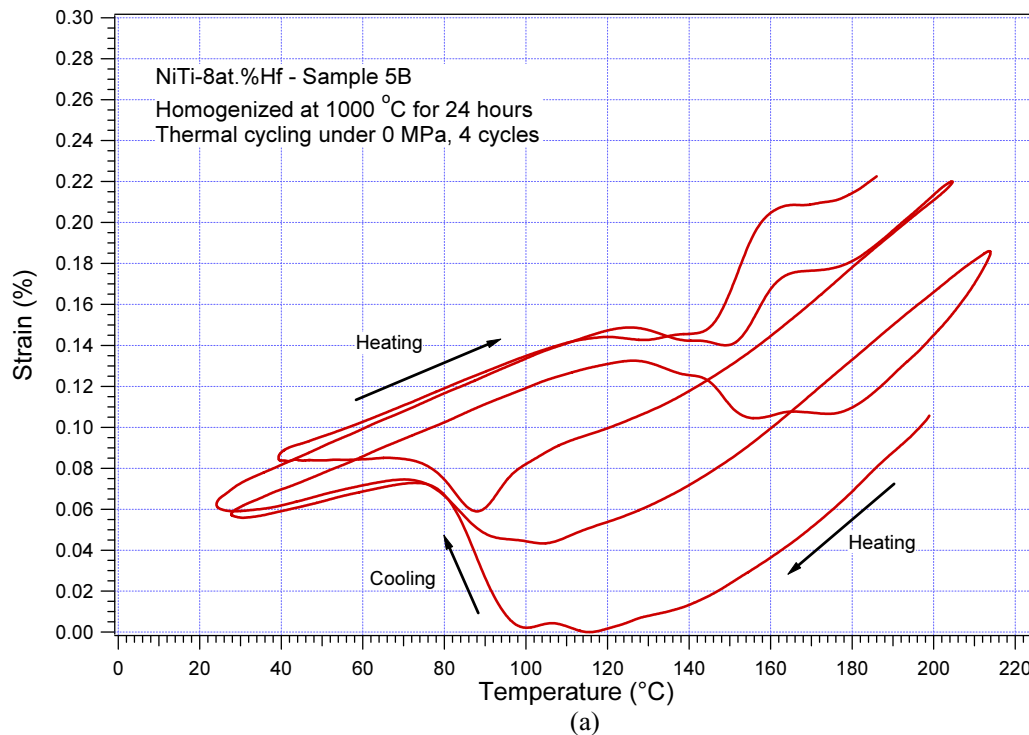


Figure 4.13. Thermal cycling at (a) 0 MPa tensile load for cast, HIP'ed and homogenized 49.8Ni-42.2Ti-8.0Hf from flowservice.

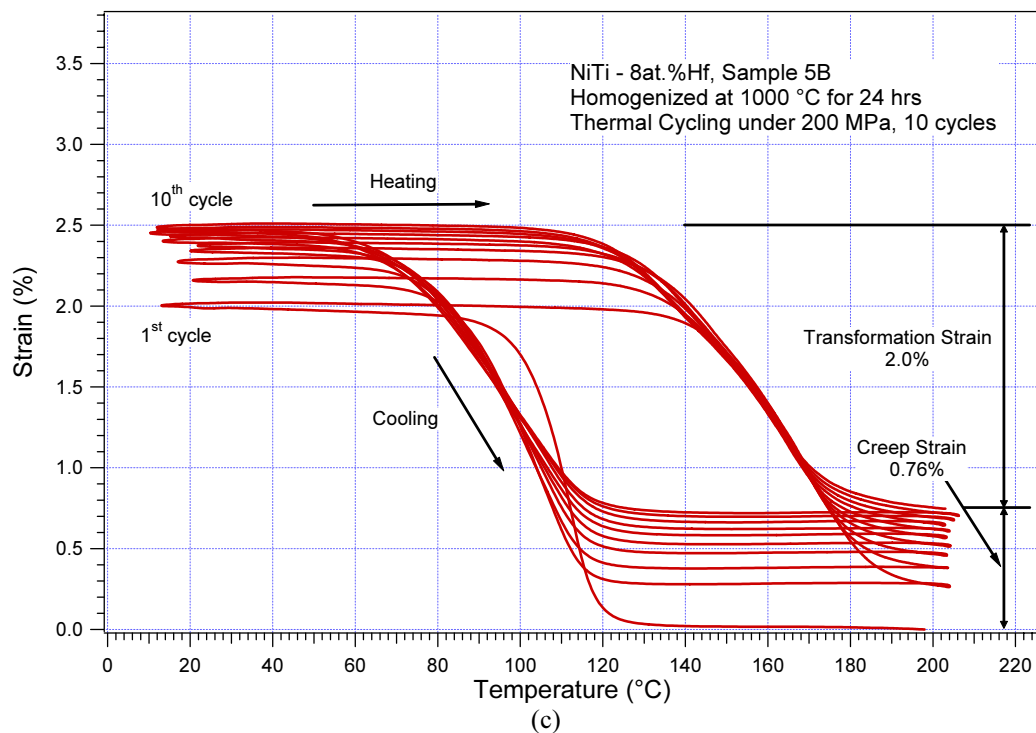
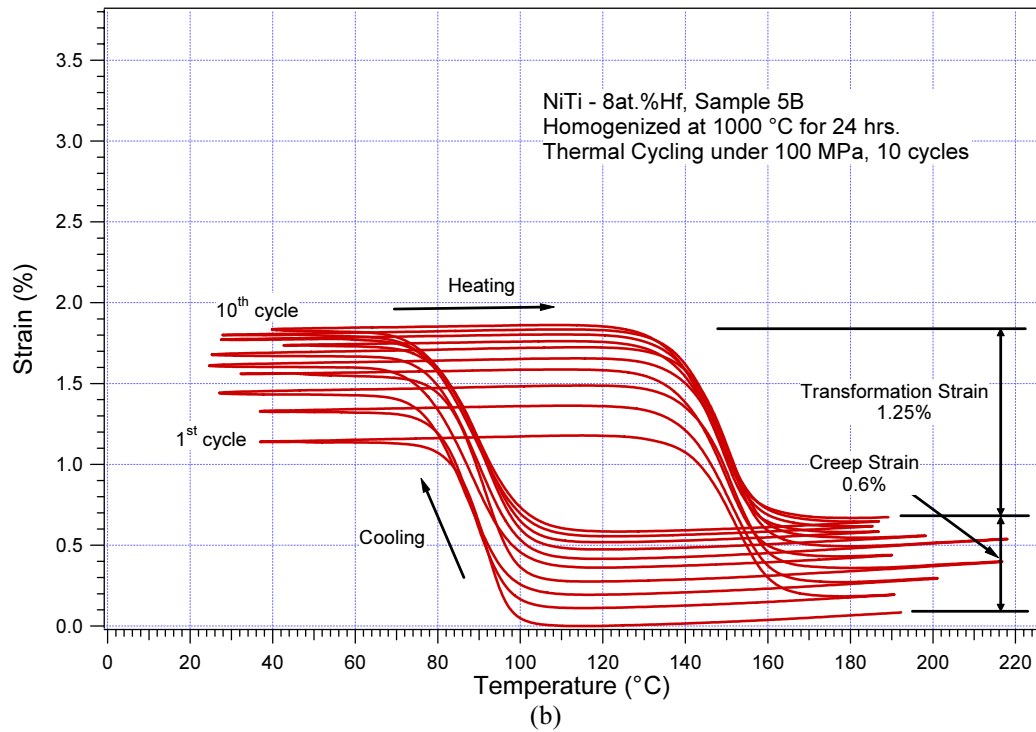


Figure 4.13. Continued. 10 thermal cycles at (b) 100 MPa and (c) 200 MPa.

Under 0 MPa, the homogenized material demonstrates less than 0.05% two-way shape memory (TWSM) strain. The transformation strain increases with cycling but creep strain is large as compared to the TWSM strain. In the ECAE samples, the TWSM strain levels under 0 MPa are about 0.08%, and they are stable under cycling. This demonstrates the existence of tensile internal stress in ECAE samples because the transformation results in positive transformation strains. Internal stress is desirable as it biases which martensite variant will activate and results in TWSM. However, we would expect higher internal stress levels after ECAE, which did not happen probably because of the high extrusion temperatures and deformation heating due to high strain rates accompanied by dynamic recovery.

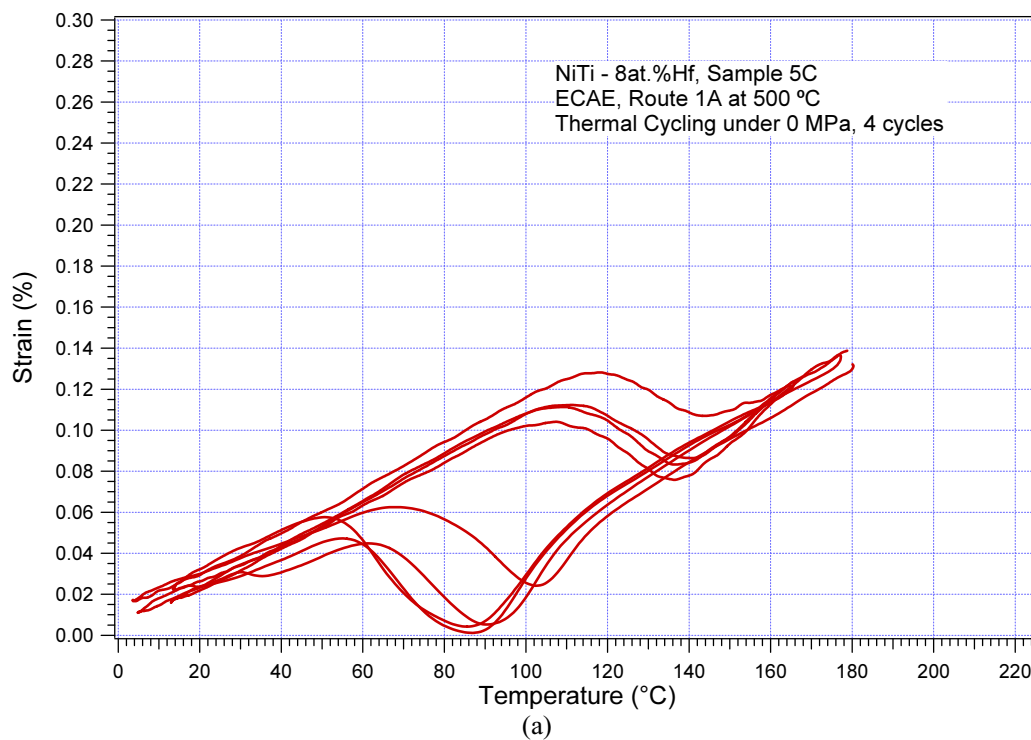


Figure 4.14. Transformation strain vs. temperature response of the ECAE 1A 500 °C sample during 4 thermal cycles under (a) 0 MPa.

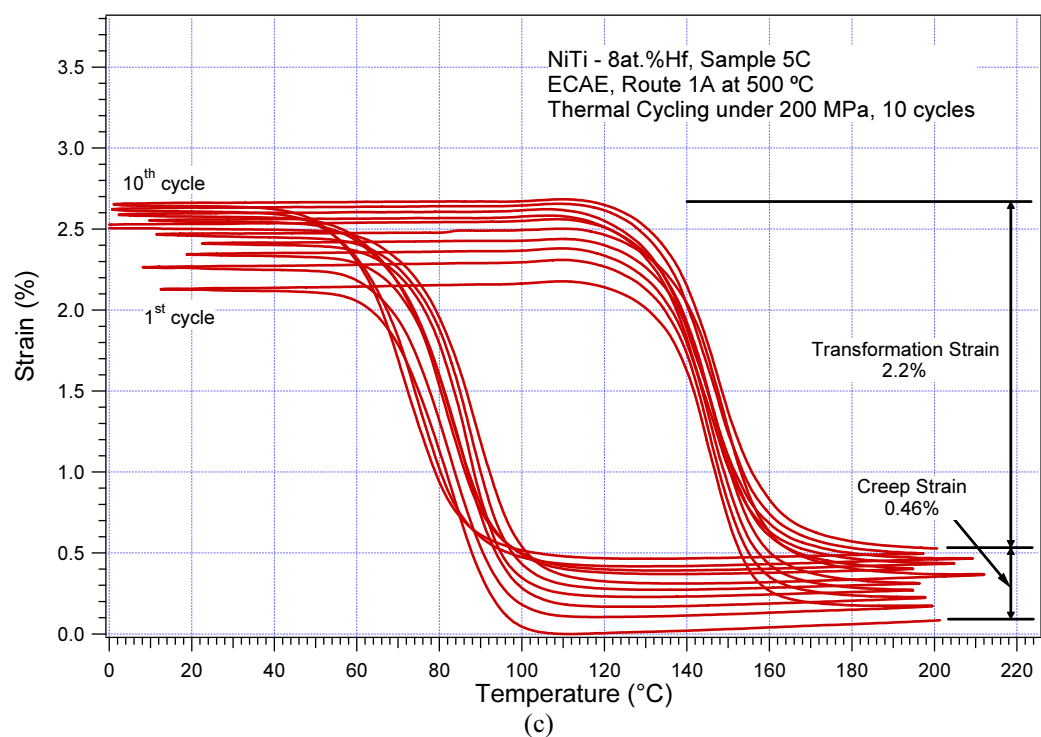
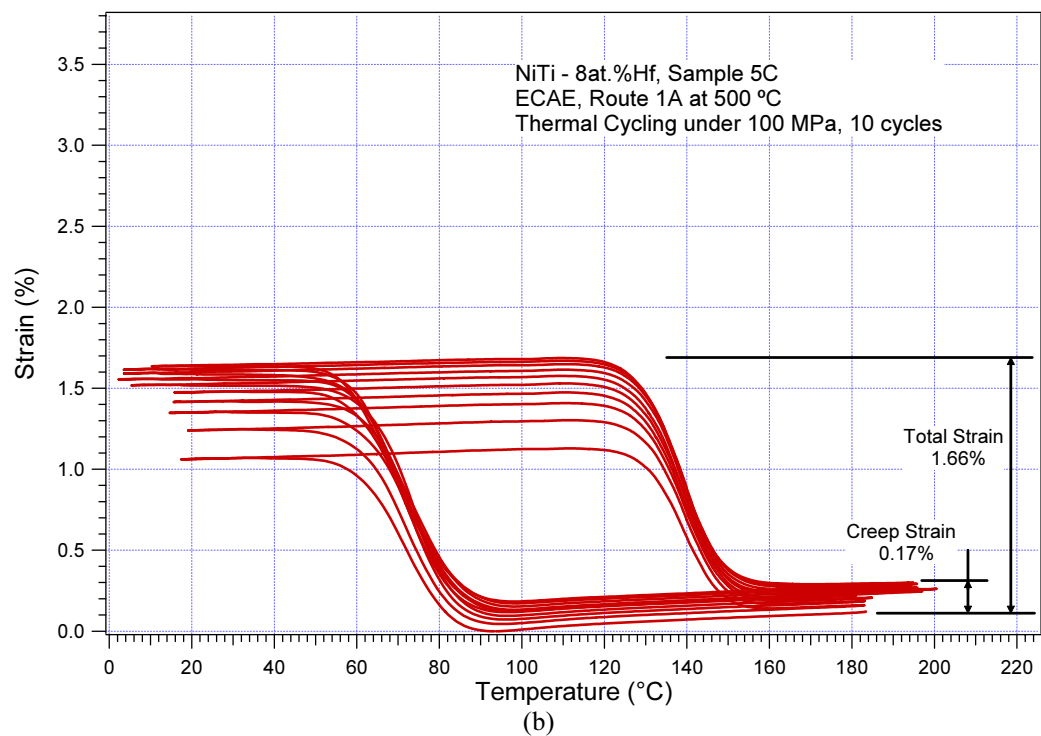


Figure 4.14. Continued. 10 thermal cycles at (b) 100 MPa, and (c) 200 MPa.

Figure 4.14 shows the cyclic response for cast, HIP'ed and homogenized 49.8Ni-42.2Ti-8.0Hf from flowserve after one pass ECAE at 500°C. The sample was cycled at 0 MPa load for 4 cycles and there after 10 cycles each at 100 MPa and 200 MPa respectively. In Figure 4.14(a) we can see that there is no significant two-way shape memory effect. We can see an increase in transformation strain with increase in stress. At 100 MPa the transformation strain is 1.66% and at 200 MPa the transformation strain increased to 2.2%. When compared to the homogenized material we can see a significant drop in the creep strain which is 0.17% for 100 MPa and 0.46% for 200 MPa. This can be attributed to the strengthening of the matrix.

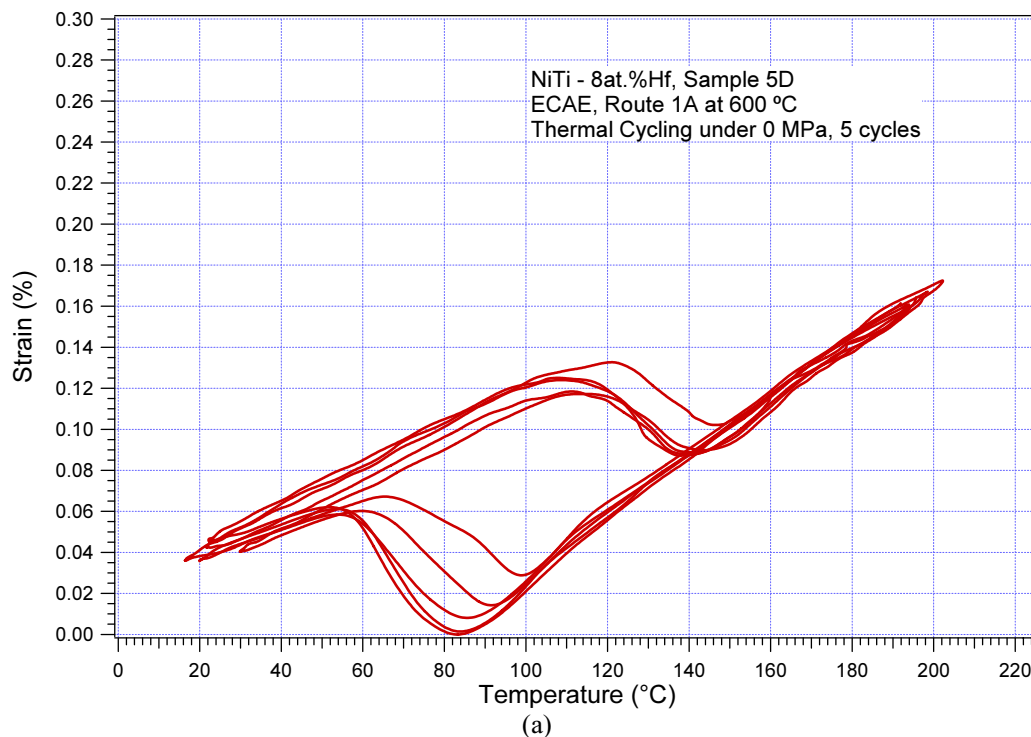


Figure 4.15. Transformation strain vs. temperature response of the ECAE 1A 600 °C sample during 4 thermal cycles under (a) 0 MPa.

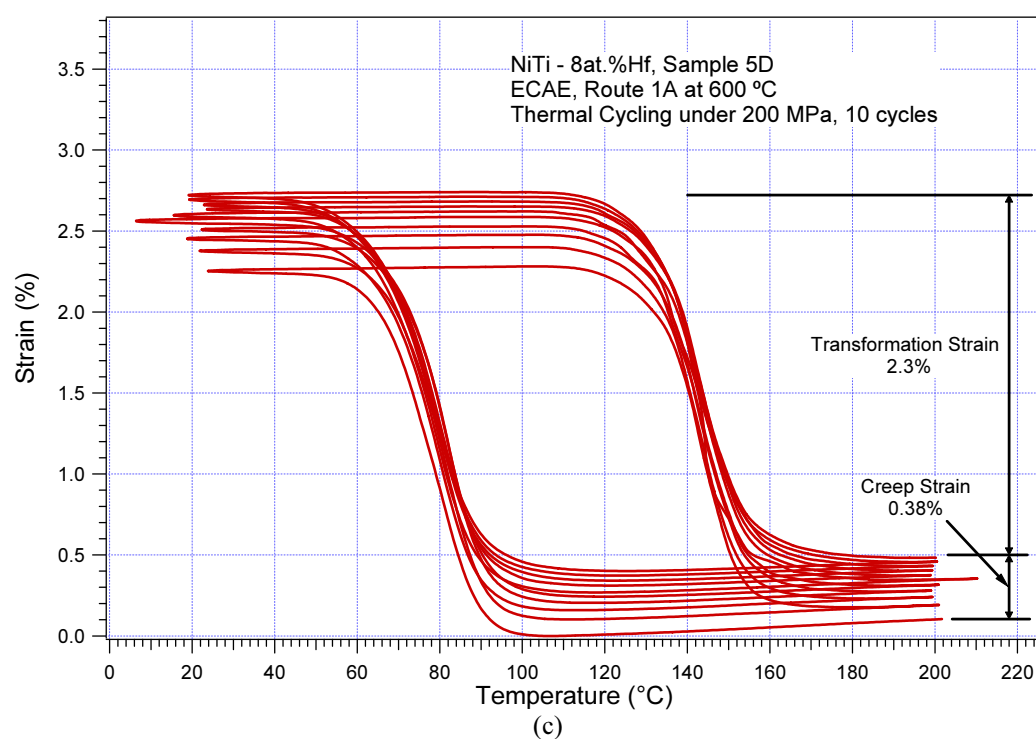
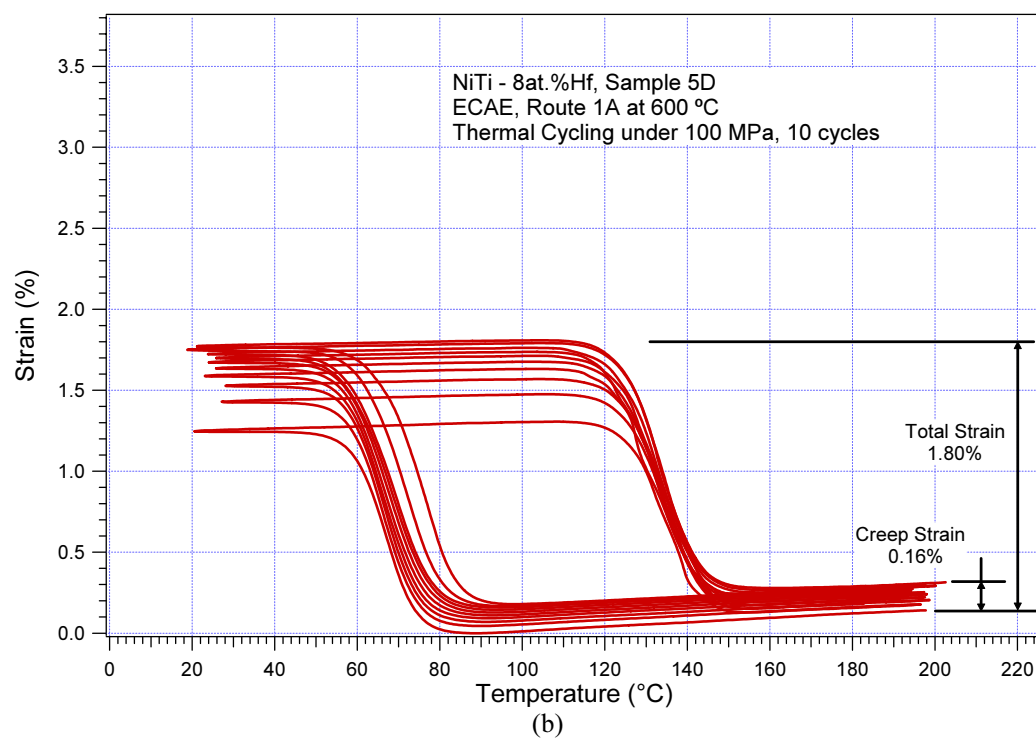


Figure 4.15. Continued. 10 thermal cycles at (b) 100 MPa, and (c) 200 MPa.

Figure 4.15 shows the cyclic response for cast, HIP'ed and homogenized 49.8Ni-42.2Ti-8.0Hf from flowserve after one pass ECAE at 600°C. In Figure 4.15(a) we can see that there is no significant two-way shape memory effect. An increase in transformation strain with increase in stress is observed when the sample is cycled under 100 MPa and there after at 200MPa load. At 100 MPa the transformation strain is 1.80% and at 200 MPa the transformation strain increased to 2.3%. A significant drop in the creep strain which is 0.16% for 100 MPa and 0.38% for 200 MPa is observed when compared to the homogenized sample.

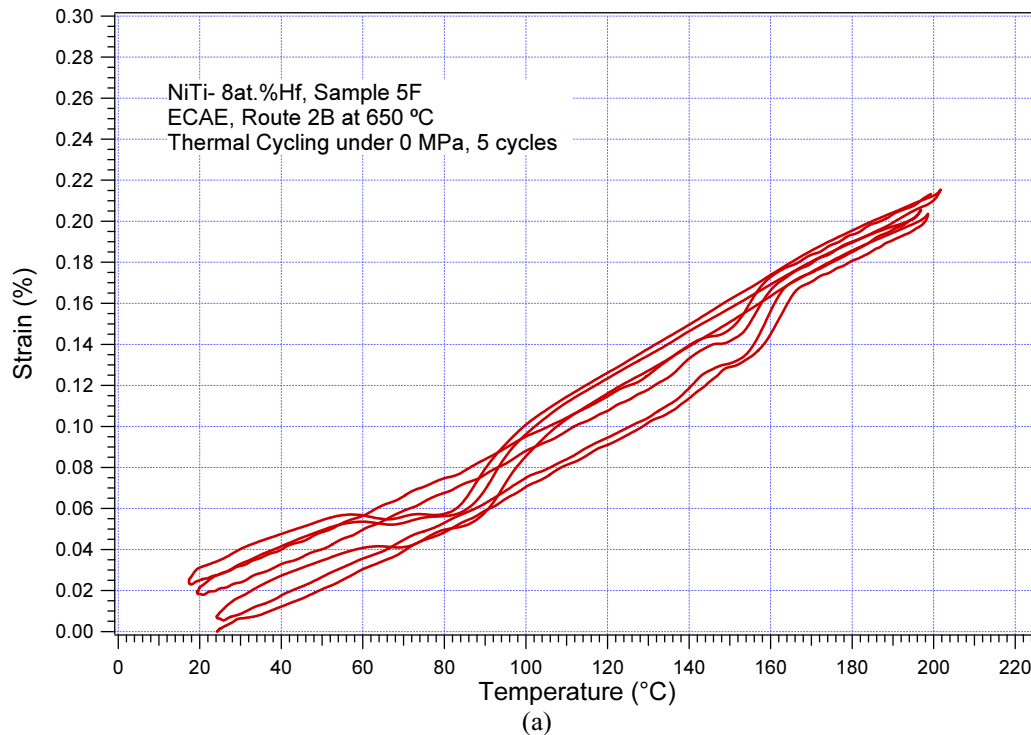


Figure 4.16. Transformation strain vs. temperature response of the ECAE 2B 650°C sample during 4 thermal cycles under (a) 0 MPa.

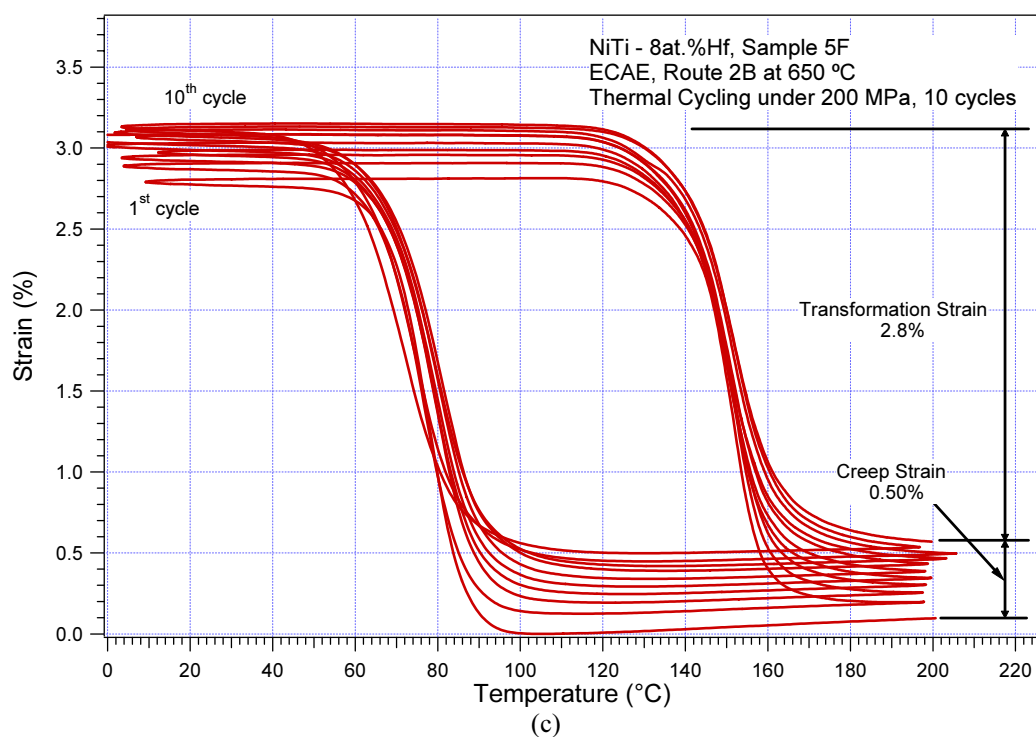
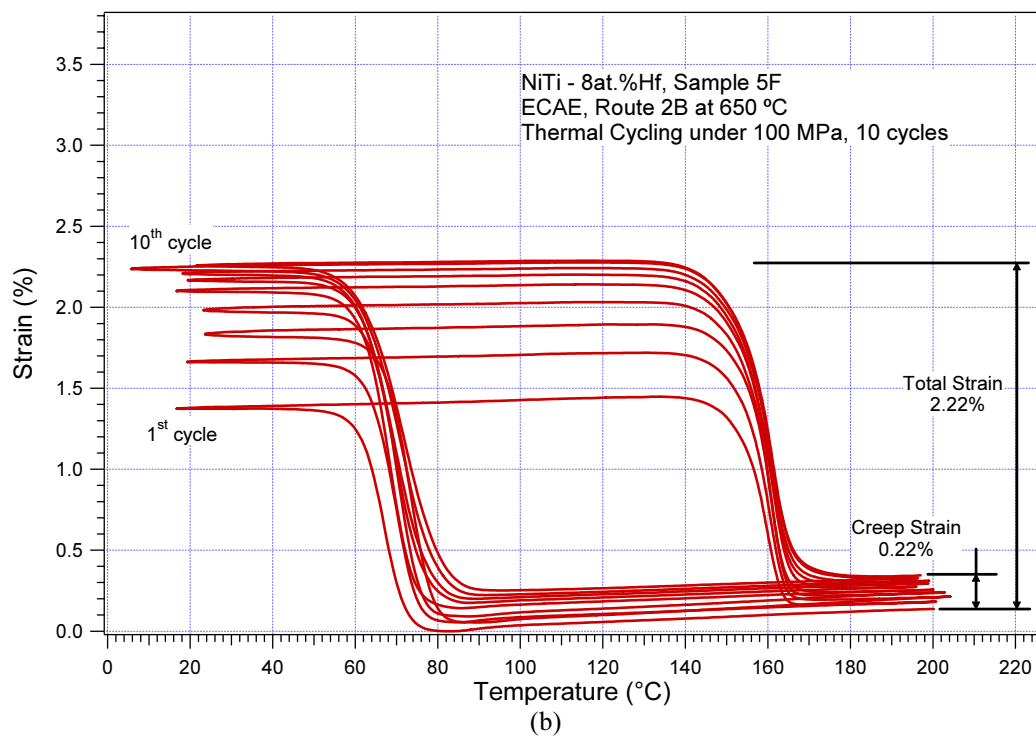


Figure 4.16. Continued. 10 thermal cycles at (b) 100 MPa, and (c) 200 MPa.

Figure 4.16. shows the cyclic response for cast, HIP'ed and homogenized 49.8Ni-42.2Ti-8.0Hf from flowserve after two pass ECAE using Route B at 650°C. When compared to the homogenized material we can see a significant drop in the creep strain which is 0.22% for 100 MPa and 0.50% for 200 MPa.

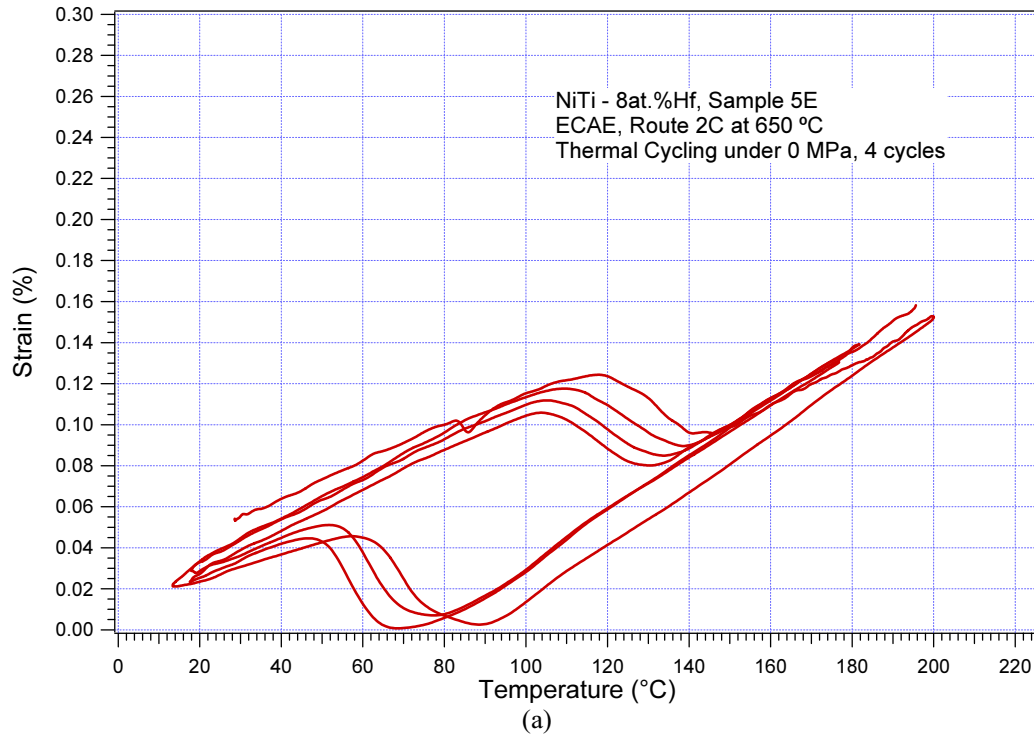


Figure 4.17. Transformation strain vs. temperature response of the ECAE 2C 650 °C sample during 4 thermal cycles under (a) 0 MPa

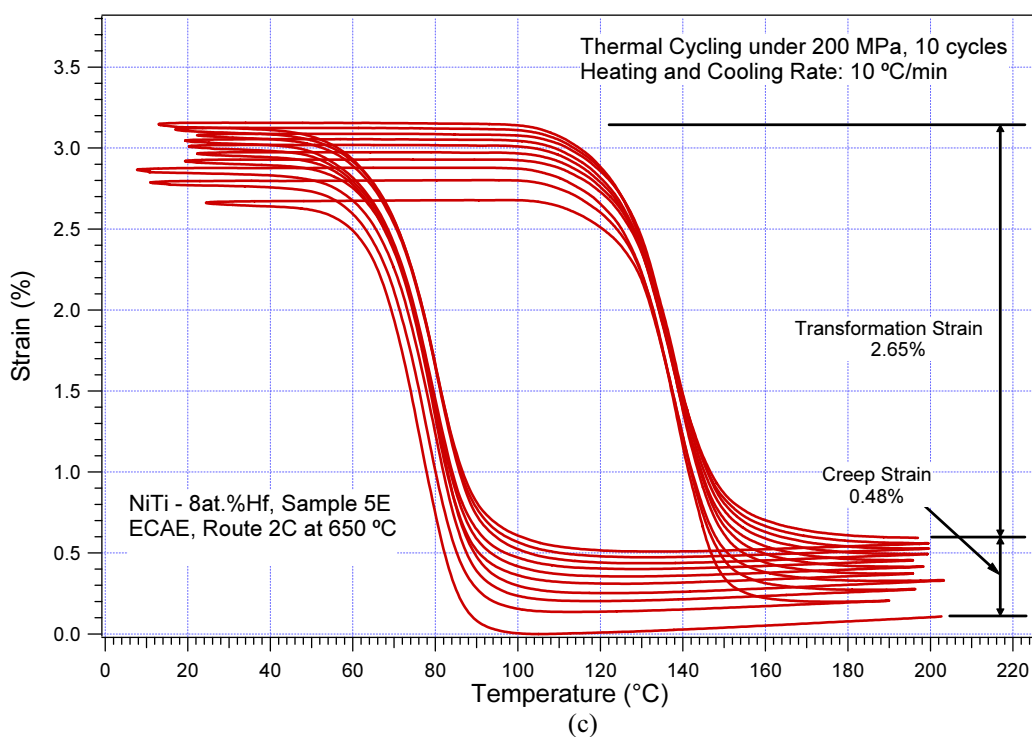
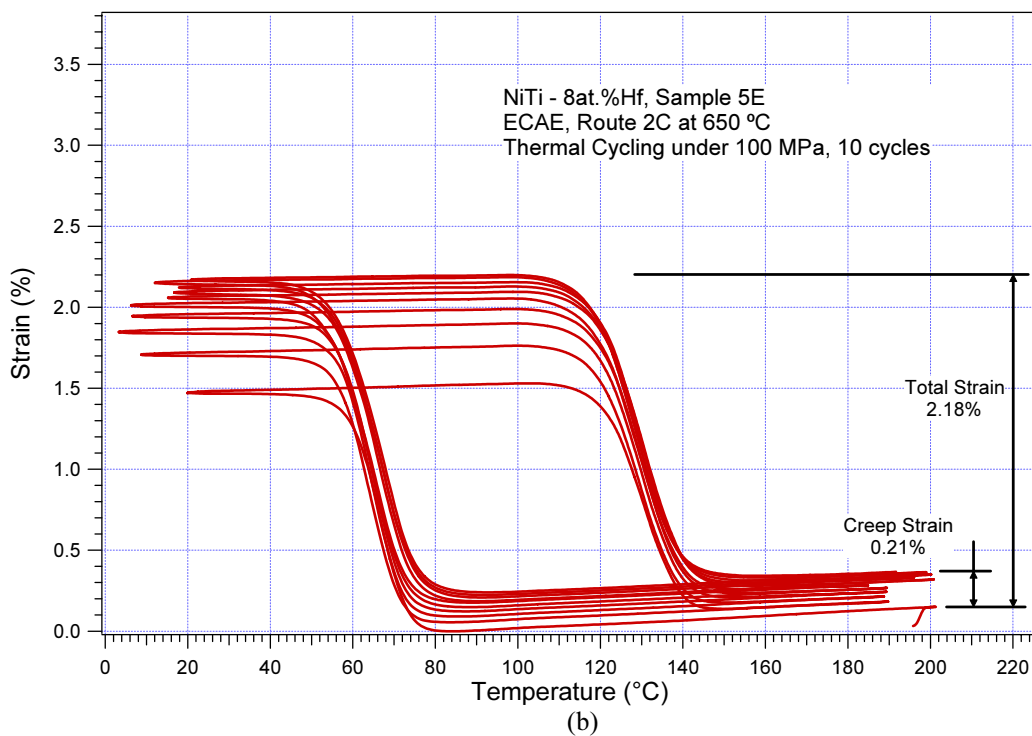


Figure 4.17. Continued. 10 thermal cycles at (b) 100 MPa, and (c) 200 MPa.

The cyclic response for cast, HIP'ed and homogenized 49.8Ni-42.2Ti-8.0Hf from flowserve after two pass ECAE using Route C at 650°C is shown in Figure 4.17. The sample was cycled at 0 MPa load for 4 cycles and there after 10 cycles each at 100 MPa and 200 MPa respectively. There is no significant two-way shape memory effect. We can see an increase in transformation strain with increase in stress. At 100 MPa the transformation strain is 2.18% and at 200 MPa the transformation strain increased to 2.65%. When compared to the homogenized material we can see a significant drop in the creep strain which is 0.21% for 100 MPa and 0.48% for 200 MPa.

To compare the thermal cycling response under 100 and 200 MPa we analyzed the transformation strain levels (Figure 4.18), creep strain levels (Figure 4.19), change in hysteresis ($A_f - M_s$) (Figure 4.20) and change in M_s temperature (Figure 4.21) as a function of number of cycles. These figures were constructed using the data presented in Figures 4.13 - 4.17.

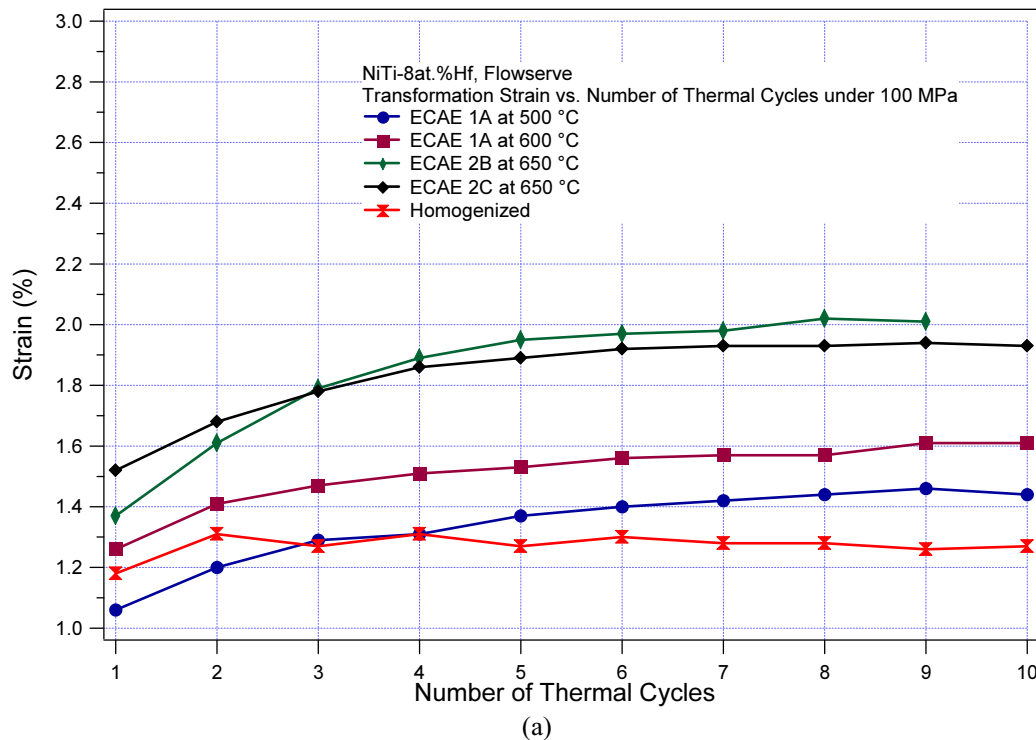


Figure 4.18. Transformation strain vs. number of thermal cycles of the homogenized and ECAEd 49.8Ni-42.2Ti-8Hf flowserve material under (a) 100 MPa.

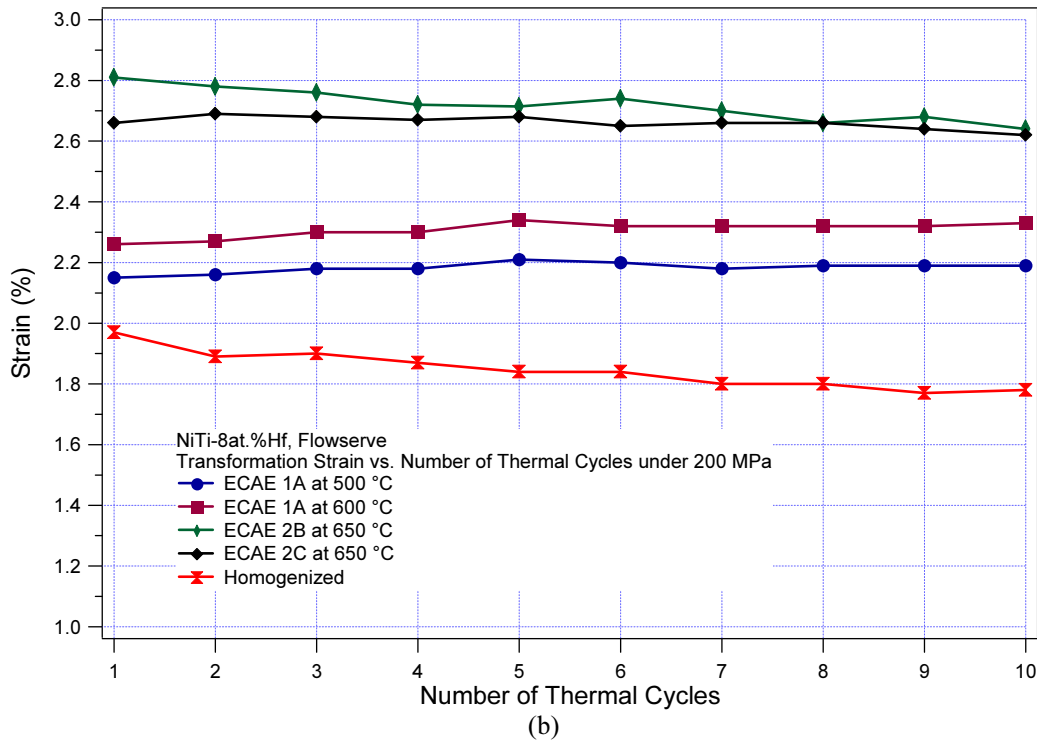


Figure 4.18. Continued. (b) 200 MPa.

Figure 4.18 shows the change in transformation strain as a function of number of thermal cycles under 100 and 200 MPa respectively. The homogenized sample has the lowest transformation strain, i.e. about 1.25% under 100 MPa and about 2.0% initially and decreasing to 1.8% with cycles under 200 MPa. The strain levels are higher in all the ECAE samples than those in the homogenized sample. The highest transformation strain was observed in ECAE 2B 650°C sample, which was initially 1.5% and increased to 2.0% after 6 cycles and stayed stable under 100 MPa. Under 200 MPa, the strain continuously decreased from 2.8% to 2.65% in 10 cycles. Other ECAE samples under 100 MPa demonstrated similar increasing strain behavior, but their strain levels are lower than that of the ECAE 2B 650°C sample. 1.45%, 1.6%, and 1.95% transformation strain levels are observed for ECAE 1A 500°C, ECAE 1A 600°C and ECAE 2C 650°C samples, respectively. Under 200 MPa, as opposed to homogenized and ECAE 2B 650°C samples, the other three ECAE samples did not experience any increase or decrease in transformation strains with cycling, i.e. a saturation occurred. The strain

levels are 2.2%, 2.3%, and 2.65% for ECAE 1A 500°C, ECAE 1A 600°C and ECAE 2C 650°C samples, respectively.

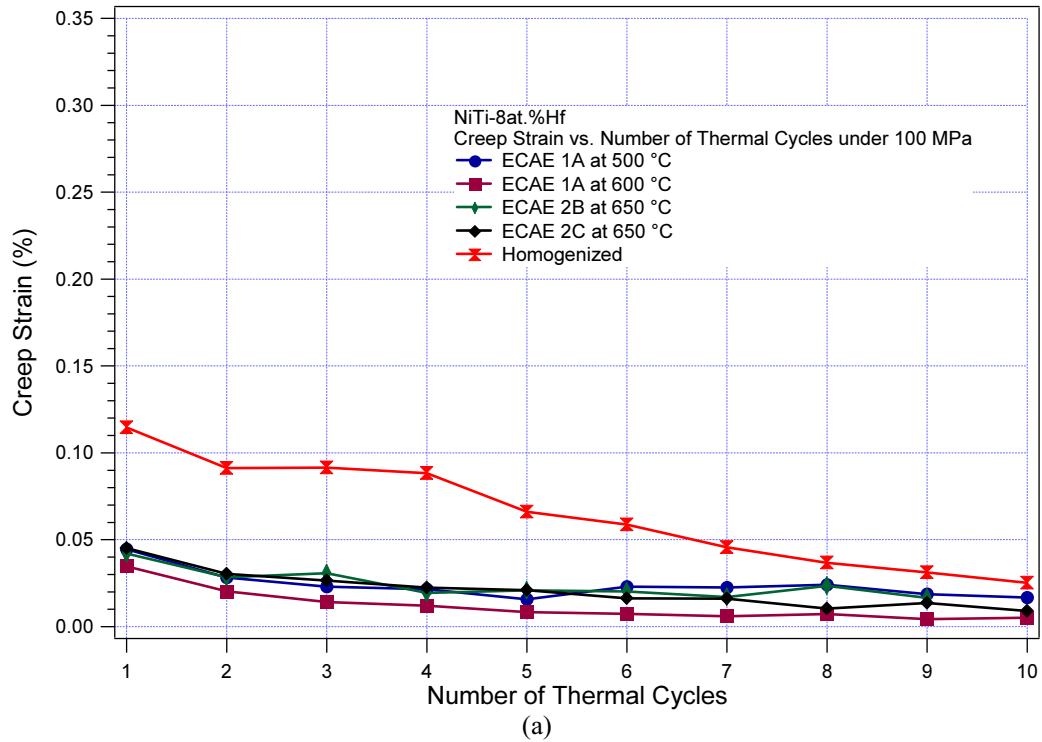


Figure 4.19. Creep strain (irrecoverable transformation strain) vs. number of thermal cycles of the homogenized and ECAE 49.8Ni-42.2Ti-8Hf flowserve material under (a) 100 MPa constant stress.

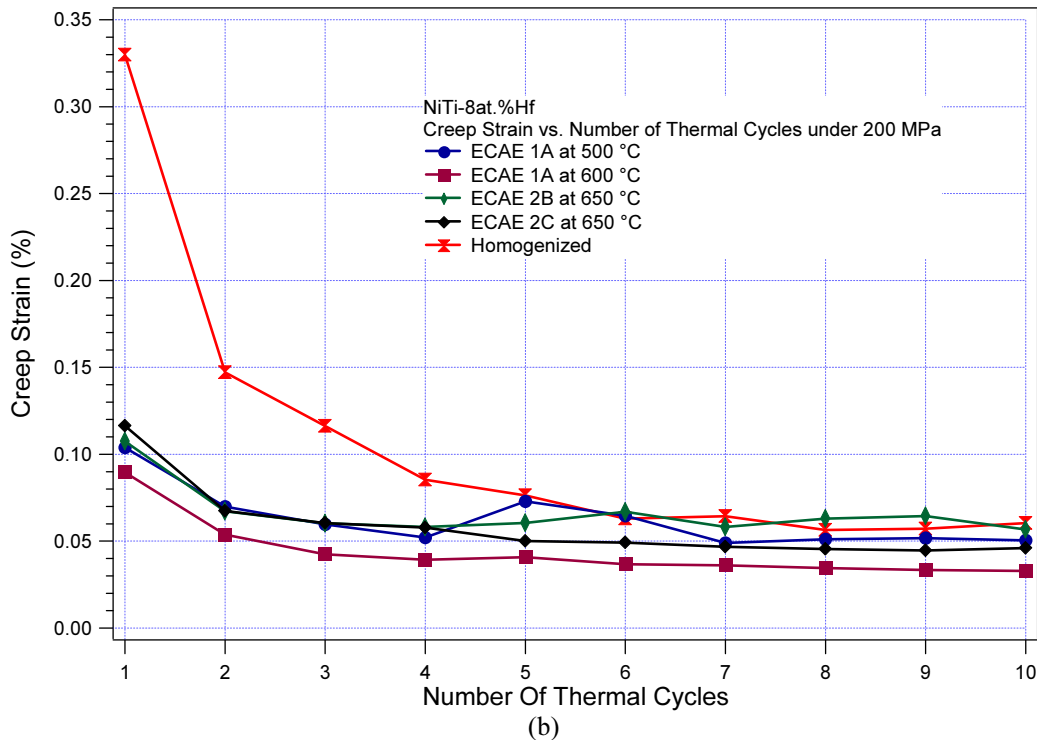


Figure 4.19. Continued. (b) 200 MPa.

Figures 4.19 displays the creep strains as a function of number of cycles for each case, and Figures 4.3.1-4.3.5 also include total creep strain levels. The total creep strain after 10 cycles under 100 MPa are 0.6% for homogenized sample, 0.17% for ECAE 1A 500 °C sample, 0.16% for ECAE 1A 600°C sample, 0.21% for ECAE 2C 650 °C sample and 0.22% for ECAE 2B 650°C sample. Under 200 MPa, they are 0.76% for homogenized sample, 0.46% for ECAE 1A 500°C sample, 0.38% for ECAE 1A 600°C sample, 0.48% for ECAE 2C 650°C sample and 0.50% for ECAE 2B 650°C sample.

Extruded samples show more stability than the homogenized sample. This can be attributed to the strengthening of the matrix, which indeed hinders slip deformation in martensite [11]. Since ECAE samples are stronger, the transformation is not totally accompanied by dislocation formation and the irrecoverable strain is less as compared to the weaker homogenized sample.

A significant drop in irrecoverable strain is observed after the first cycle, which is attributed to the so called “first cycle” effect. This effect again stems from the formation of localized lattice defects [8]. The martensitic transformation is always connected with

large amounts of shear strain and there by the formation of internal stresses is unavoidable. They are reduced by intrinsic defects due to lattice invariant deformation – variant boundaries, stacking faults and twins. All of these defects should annihilate during reverse transformation for a fully reverse transformation. Otherwise, they are accumulated during subsequent cycles as barriers to reverse transformation, and thus lead to irrecoverable strain. It is observed that this effect is maximum in the case of the homogenized material and is significantly lower in the case of the ECAE samples. The lowest irrecoverable strain levels are observed in the case of ECAE 1A 600°C samples and the highest in the case of ECAE 2B 650°C samples.

Please note that during strain measurements it is not clear yet how much experimental error is introduced, but we believe that some of the reported creep strain may come from experimental error. The main source of experimental error may be the way the extensometer is attached to the sample. The extensometer knife-edges sit on the flat surface of the sample and a stainless steel spring is used to hold the extensometer on the sample. Although springs with the same spring constant were used for all experiments as specified by MTS, we believe that there might sometimes be small slip during cycling.

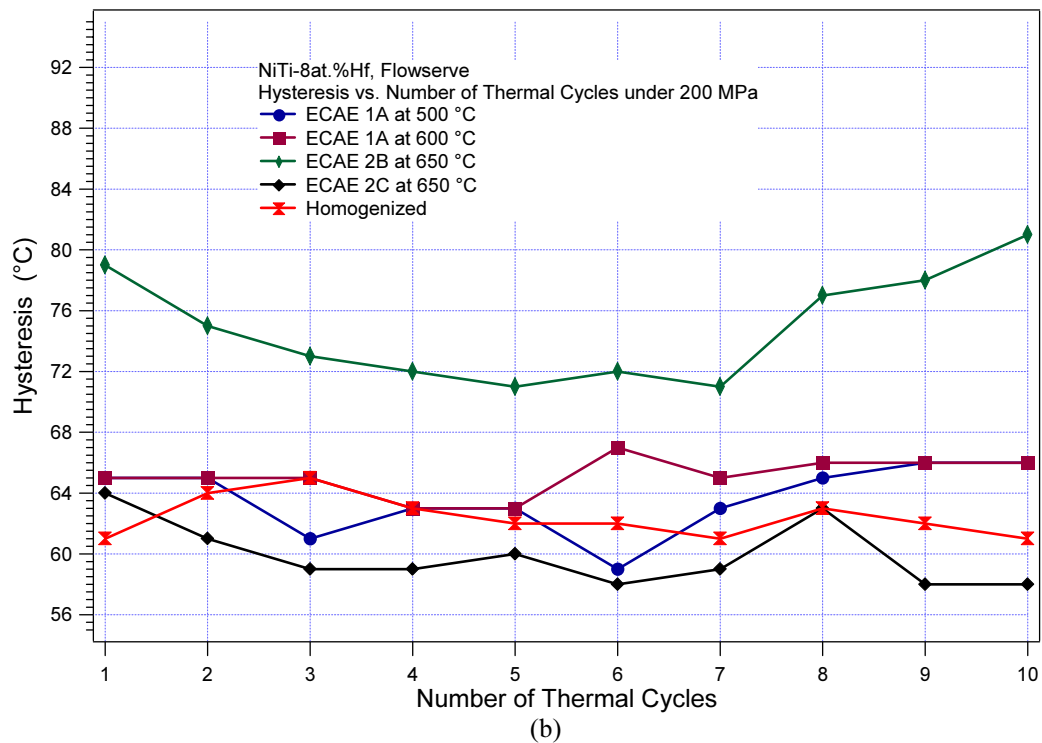
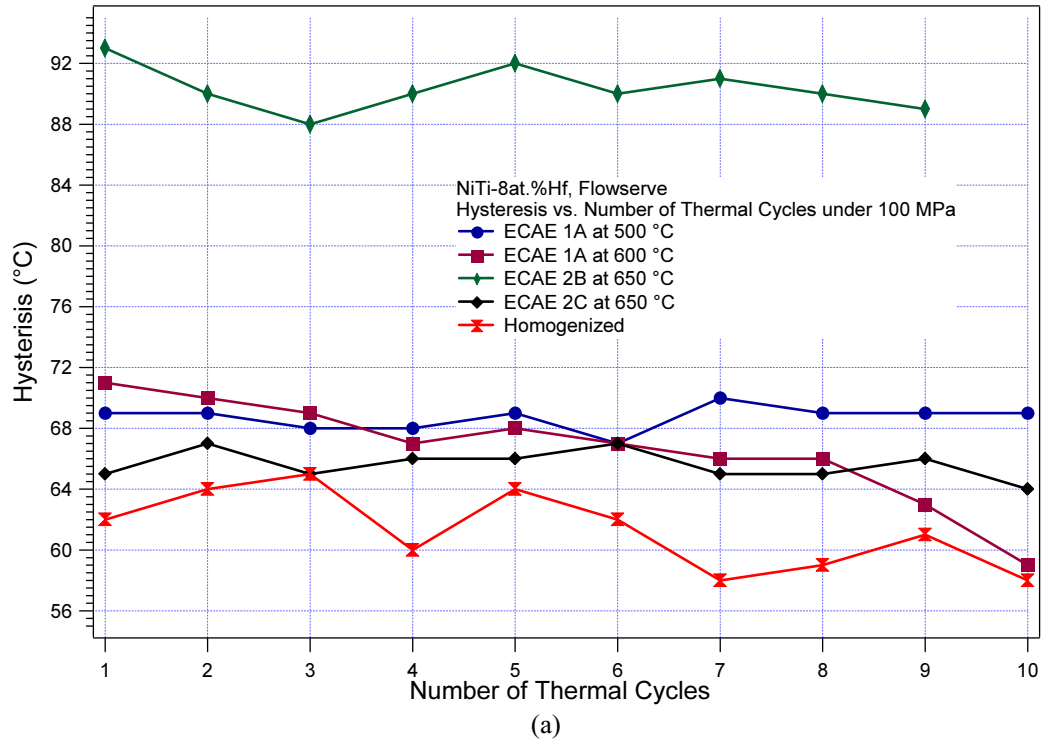


Figure 4.20. Hysteresis ($A_f - M_s$) vs. number of thermal cycles of the homogenized and ECAEd 49.8Ni-42.2Ti-8Hf flowserve material under (a) 100 MPa and (b) 200 MPa constant stress.

Figures 4.20 shows the change in hysteresis ($A_f - M_s$) as a function of temperature. The main observation in these plots is the difference in trend as a function of stress level in between the homogenized and the ECAE samples. A significant observation is that the hysteresis decreases with applied stress in the case of the ECAE samples although the opposite is expected. The decrease in thermal hysteresis as a function of applied stress is an unusual phenomenon because the hysteresis increases with increasing stress levels in conventional SMA's. Similar results were observed in the studies conducted by Hamilton *et al.* [23] on high Ni content alloys. This can be attributed to the increase in elastic strain energy stored during the forward transformation with increasing external stress. This could be because of the presence of coherent precipitates and/or the strengthened matrix, which makes dissipation low and the stored elastic strain energy assists the reverse transformation, which now requires only less chemical energy to complete the transformation because of the additional driving force from the stored strain energy. Another significant observation is that there is a drop in hysteresis with cycling. In conventional NiTi and Cu based alloys, when stress level increases, hysteresis also increases as observed in the homogenized case. The opposite behavior is evident only if coherent precipitates exist in NiTi alloys.

There are several factors that need to be considered in understanding the results on transformation strain levels, creep strain and hysteresis. Some of these factors are pre-deformation levels, texture, existence of precipitates, and grain size. Although it is difficult to draw conclusions without investigating all these effects, we will present some rationale that could explain these observations. When the materials are deformed by ECAE with only one or two passes, it is difficult to refine the grain size, but the forest dislocation density or density of vacancy-interstitial pairs, if recovery is involved, increases. Preliminary TEM results on two of the ECAE samples (1A 500°C and 2C 650°C) showed that dislocation density increased significantly after extrusion. This causes the strengthening of the material. Each ECAE sample has different levels of strengthening as shown by the different thermal cycling results. Increase in transformation strain levels is a consequence of the strength increase in the ECAE samples because the deformation structure formed during ECAE helps externally applied stress to bias the formation of single variant martensite. The transformation strain level

depends on the material's ability to form single variant martensite as opposed to self-accommodating transformation structure. For example under 100 MPa, probably the ECAE samples have higher volume fraction of single variant martensite than the homogenized sample, resulting in higher external strain levels. This can also be a consequence of the different textures, but our simulations demonstrated that texture evolution after only one or two passes is not significant to cause 40-50% change in transformation strains. The question of the increase in strain levels as a function of cycles under 100 MPa in the ECAE samples may be explained by the favorable storage of dislocations during cycling in the ECAE samples, which helps the externally applied stress to bias single martensite variant. However, this remains to be justified.

The decrease in hysteresis as a function of applied stress is an unusual phenomenon because hysteresis increases with increasing stress level in conventional shape memory materials. The conventional behavior is because of 1) more defect generation with increasing stress level, and 2) decreasing elastically stored energy and thus the need for additional thermal energy for recovery. However, if the material is strong, the defect generation during transformation is minimal, but increasing stress level increases the amount of single variant martensite with internal twins. This structure is more prone to storing higher elastic energy than self-accommodating martensite structure and thus the hysteresis decreases with increasing stress level. The significantly lower creep strains in ECAE samples can also be explained by the strengthening of the material.

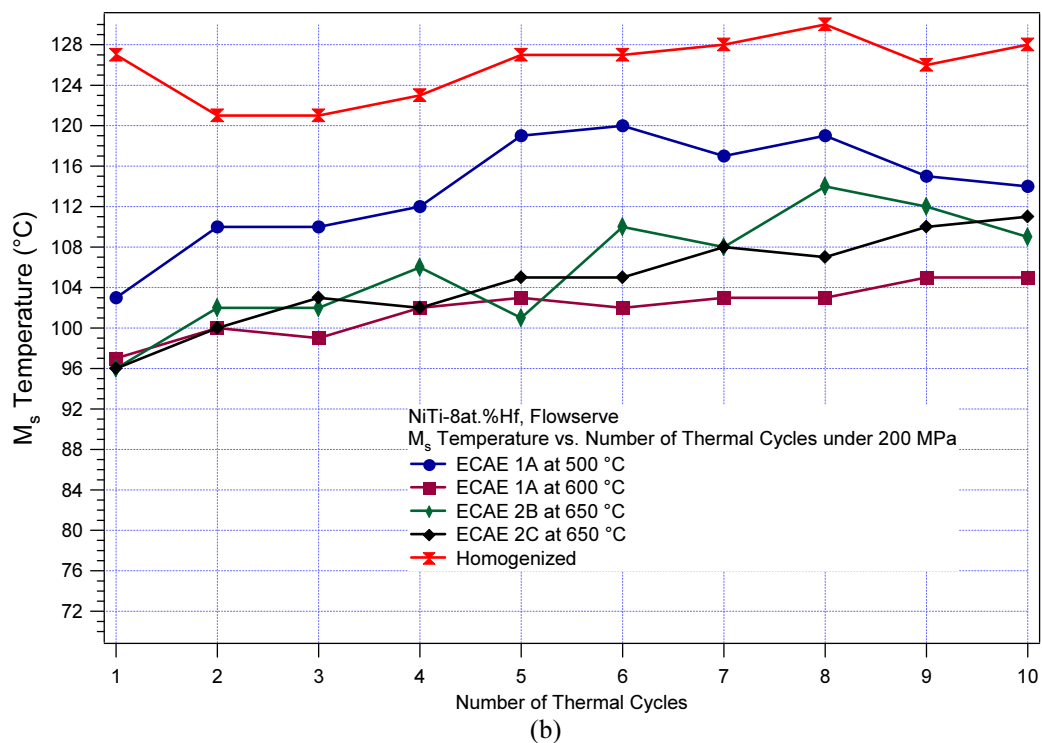
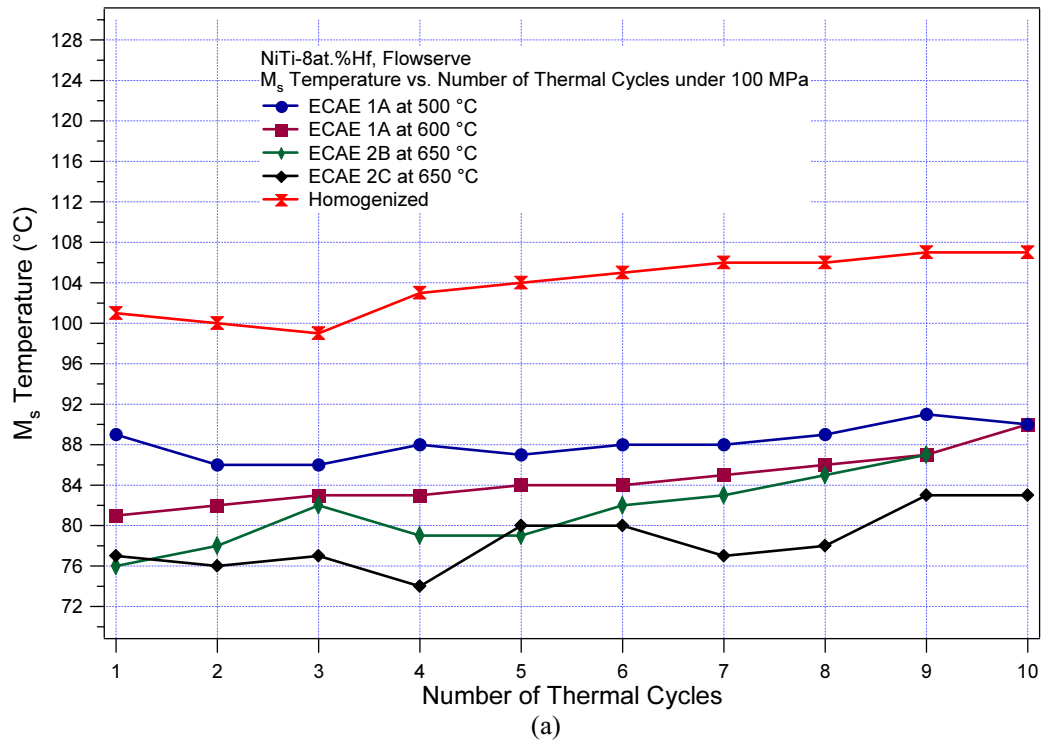


Figure 4.21. Change in M_s temperature vs. number of thermal cycles in the homogenized and ECAE 49.8Ni-42.2Ti-8Hf flowserve material under (a) 100 MPa and (b) 200 MPa constant stress.

Transformation temperatures of both the homogenized and the ECAE samples increase with increasing stress levels as shown in Figure 4.21. In all cases, M_s temperature increases with increasing number of cycles although the opposite is usually expected [16, 24, 25]. This increase in transformation temperatures was also observed during DSC cycling of other NiTiHf compositions [15]. This increase may be related to the argument that dislocations can be arranged in such a way that during martensitic transformation, they may lead building up a tensile internal stress that helps the externally applied stress to increase the M_s temperature further. Another possible explanation is the redistribution of existing defects (dislocations) and formation of new defects. The redistribution of existing defects as a result of phase transformation cycling under an external stress promotes the formation of preferred martensite variants in successive cycles, which in turn increases the transformation temperature [18].

Figure 4.22 shows the cyclic response for cast, HIP'ed and homogenized 49.8Ni-42.2Ti-8.0Hf from flowserve after two pass ECAE using Route C at 650°C and after annealing at 400°C for 15mins. The sample was cycled at 0 MPa load for 4 cycles and then 10 cycles each at 100 MPa and 200 MPa respectively. In Figure 4.3.10(a), we can see that there is no significant two-way shape memory effect. We can see an increase in transformation strain with increase in stress. At 100 MPa the transformation strain is 1.55% and at 200 MPa the transformation strain increased to 2.46%. When compared to the homogenized material and even with the ECAE 2C 650°C as extruded sample we can see a significant drop in the creep strain which is 0.05% for 100 MPa and 0.25% for 200 MPa. For the as processed sample the creep strains are of the order of 0.21% and 0.48% respectively which shows that annealing improves the stability of the material after ECAE. This can be attributed to reconfiguration in dislocation structure, recovery of forest dislocations that deteriorates the shape memory response and to further strengthening of the matrix due to vacancy-interstitial pair formation.

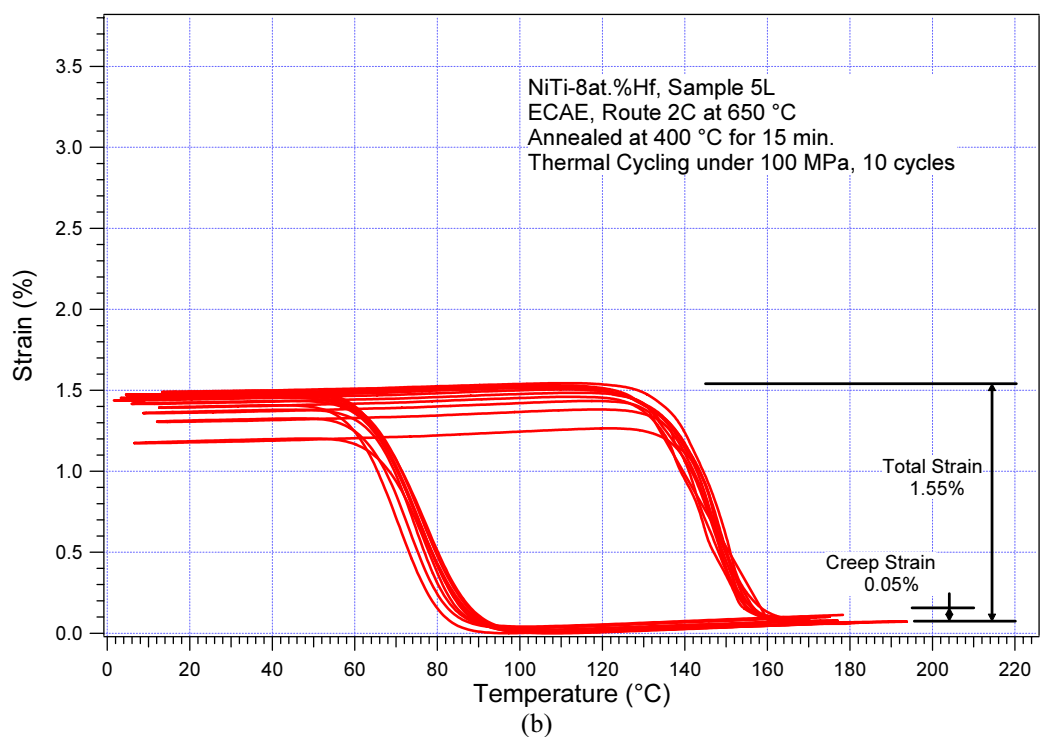
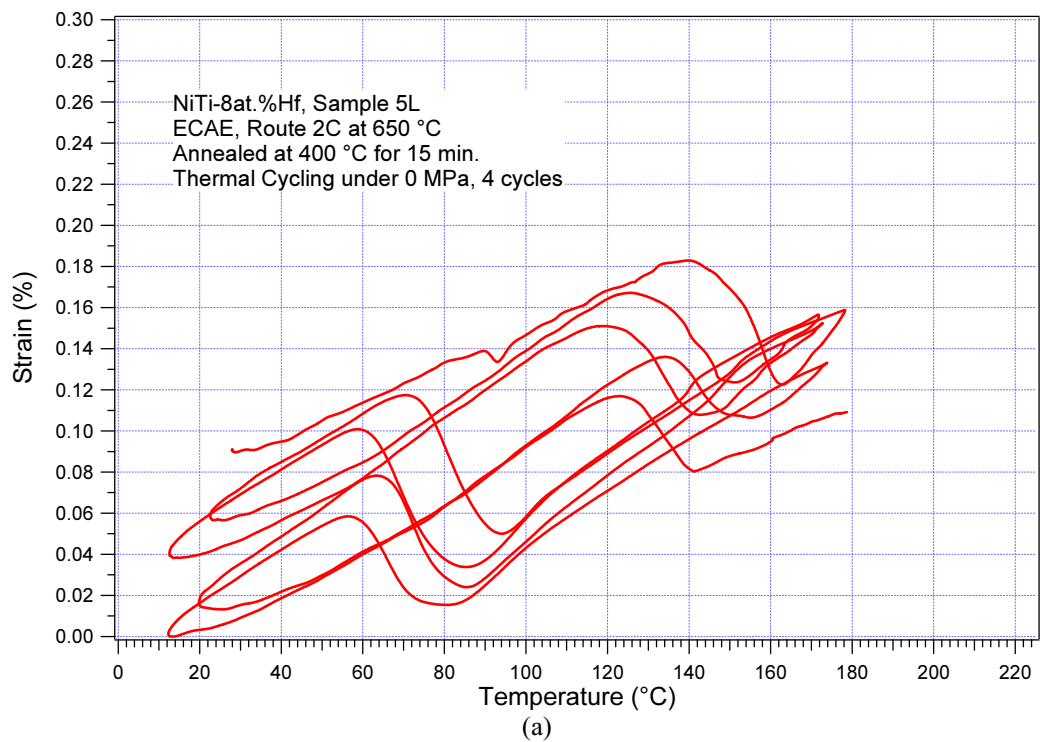


Figure 4.22. Transformation strain vs. temperature response of the ECAE 2C 650°C sample annealed at 400°C for 15 mins, during 4 thermal cycles under (a) 0 MPa and 10 thermal cycles under (b) 100 MPa.

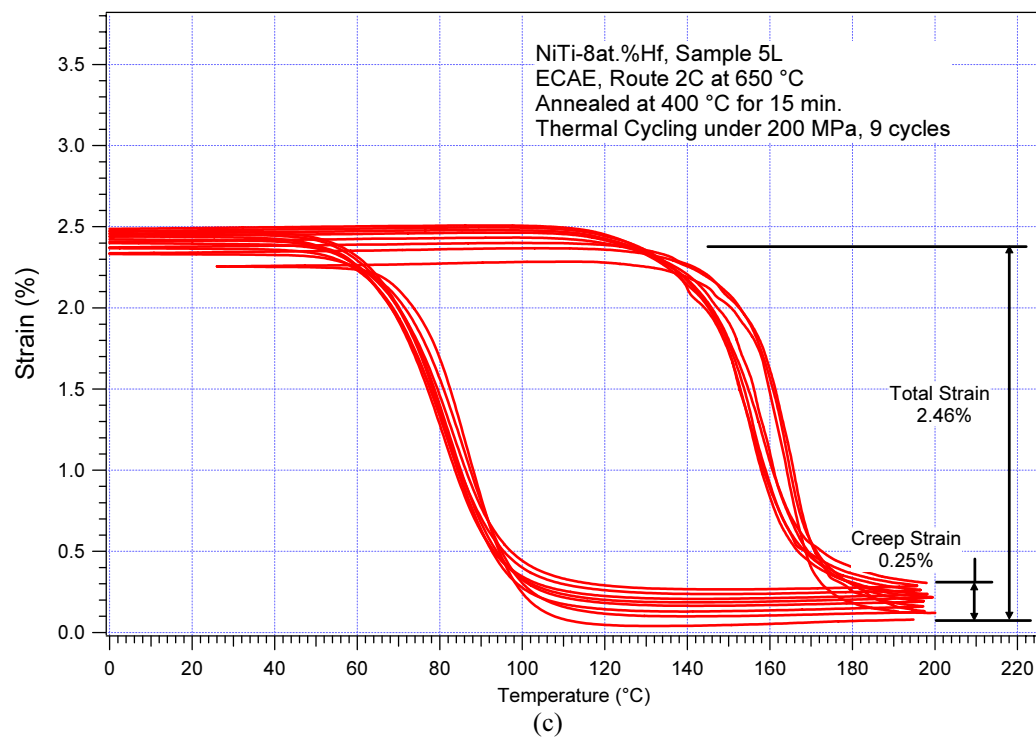


Figure 4.22. Continued. (c) 200 MPa.

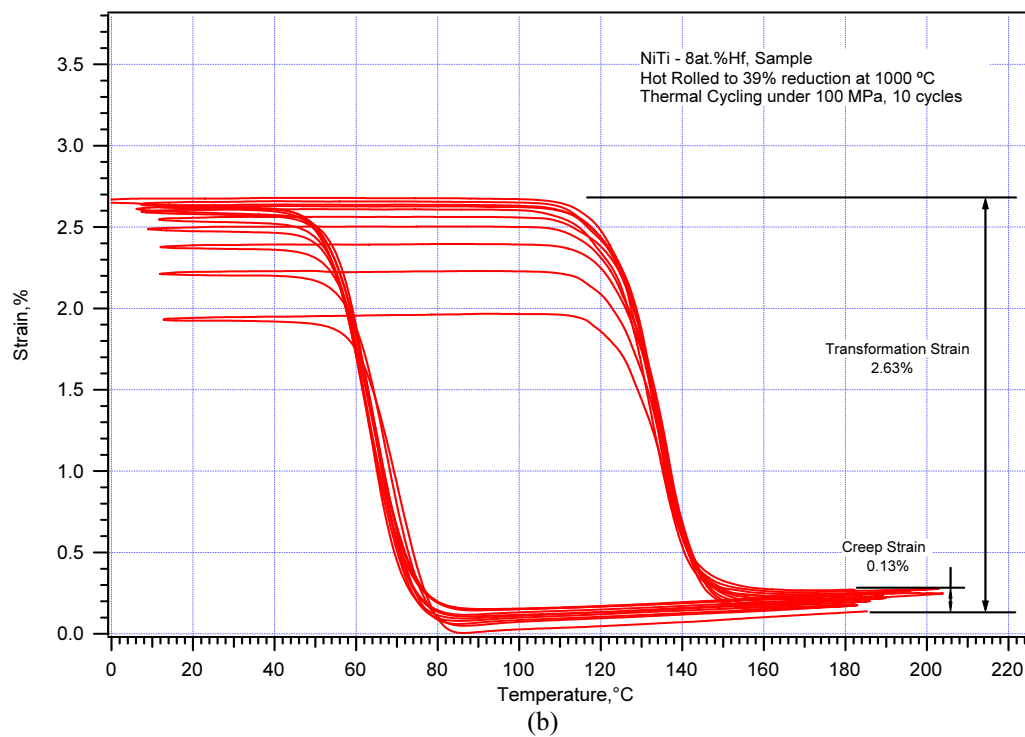
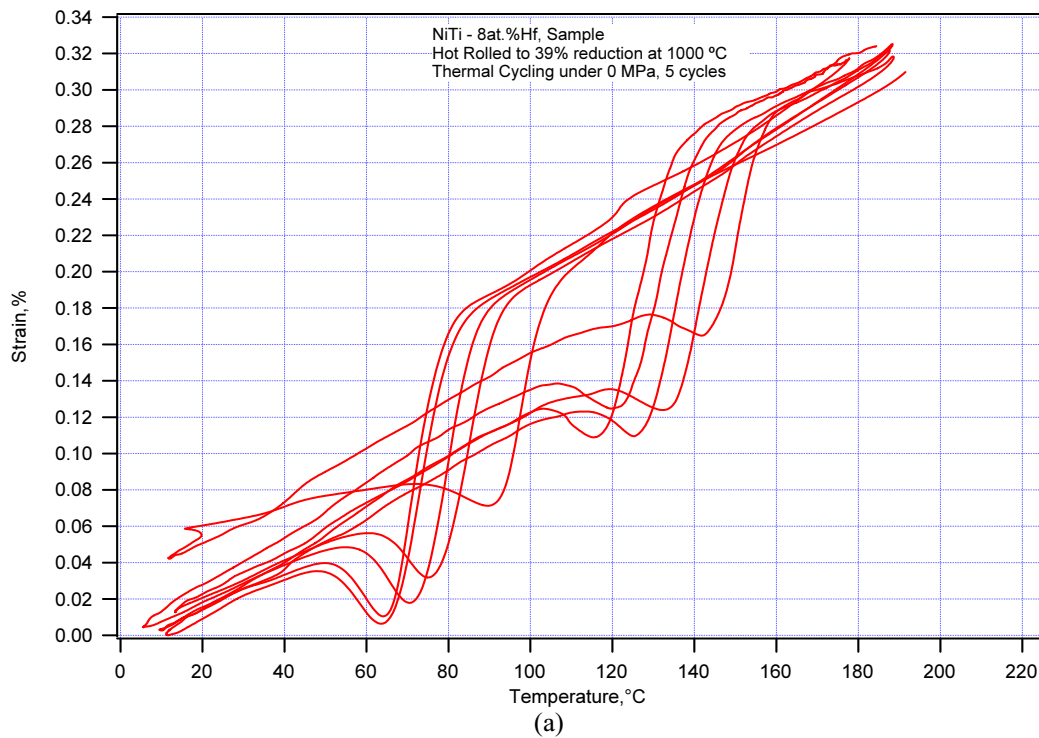


Figure 4.23. Transformation strain vs. temperature response of the hot-rolled sample during 4 thermal cycles under (a) 0 MPa and 10 thermal cycles under (b) 100 MPa.

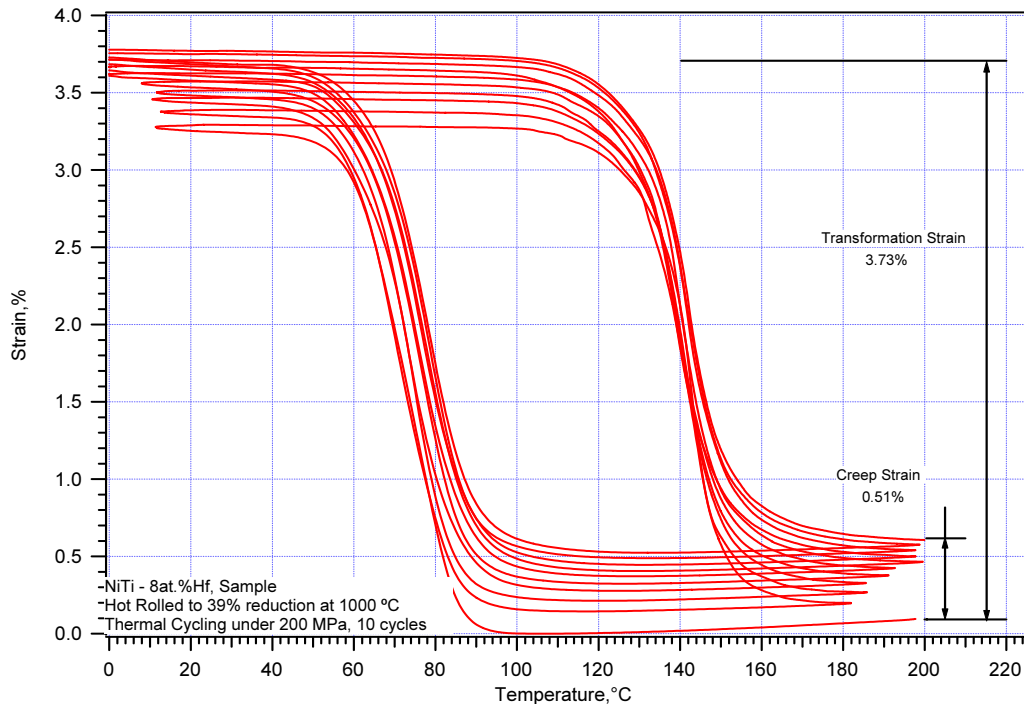


Figure 4.23. Continued. 10 cycles under (c) 200 MPa.

Figure 4.23 depicts the temperature vs transformation strain response of the hot-rolled sample. Here the highest transformation strain of 2.63% and a low irrecoverable strain of 0.13% is recorded at 100 MPa. When the load was increased to 200 MPa a significant increase in transformation strain, 3.73% and irrecoverable strain, 0.51% is observed. In case of thermal cycling at 200 MPa, a very small decrease in hysteresis with cycling is observed. Also the M_s Temperature increases with cycling and also a decrease in irrecoverable strain with cycles is observed as in the case of ECAE processed samples.

Figure 4.24 shows the cyclic response for cast, HIP'ed and homogenized 49.8Ni-42.2Ti-8.0Hf from flowserve after marforming to 10% reduction and annealing at 400°C for 15 mins. The sample was cycled at 0 MPa load for 4 cycles and then 10 cycles each at 100 MPa and 200 MPa respectively. In Figure 4.24(a) we can see that there is no significant two-way shape memory effect although it is larger than what was observed in all previous cases. We can see an increase in transformation strain with increase in stress. At 100 MPa the transformation strain is 1.13% and at 200 MPa the transformation strain

increased to 2.52%. When compared to the homogenized material we can see a significant drop in the creep strain which is 0.10% for 100 MPa and 0.32% for 200 MPa.

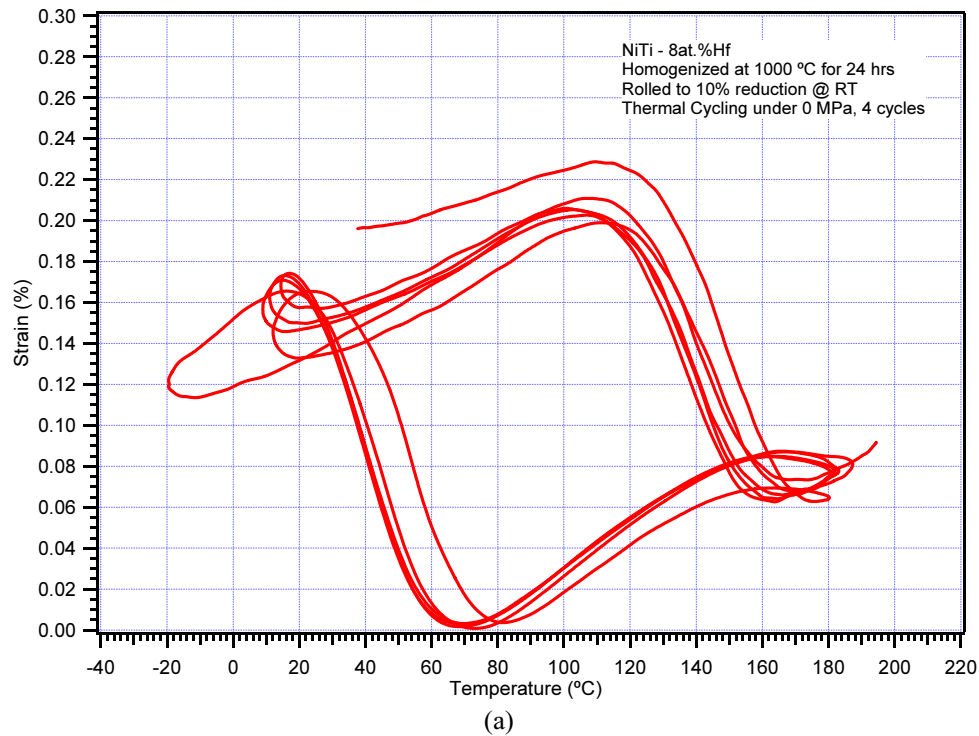


Figure 4.24. Transformation strain vs. temperature response of the 10% marformed sample during 4 thermal cycles under (a) 0 MPa.

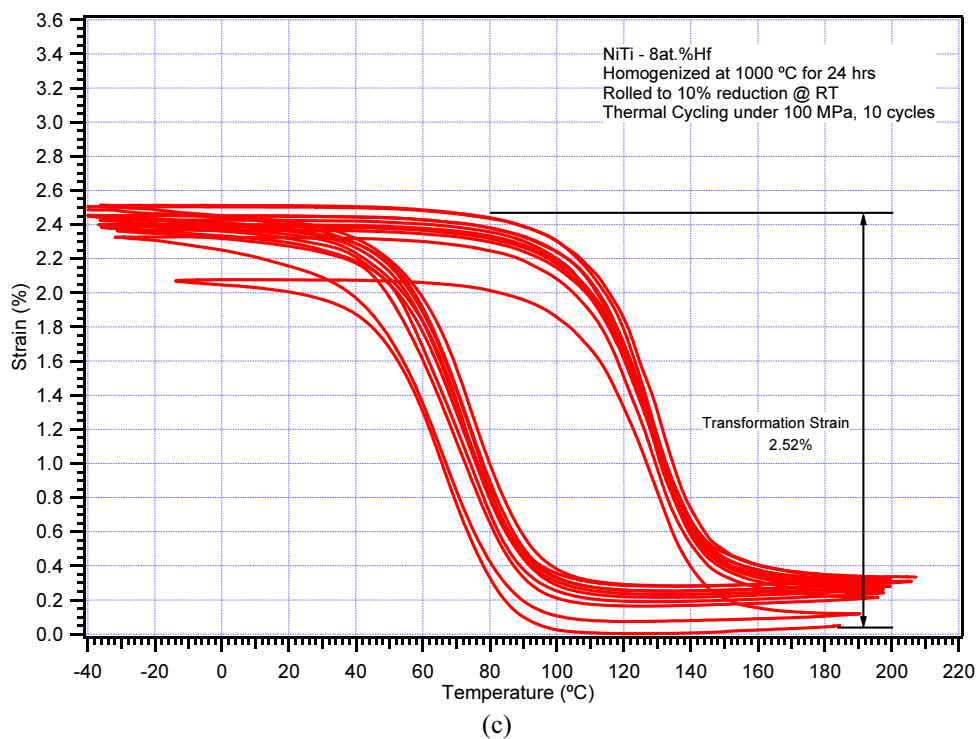
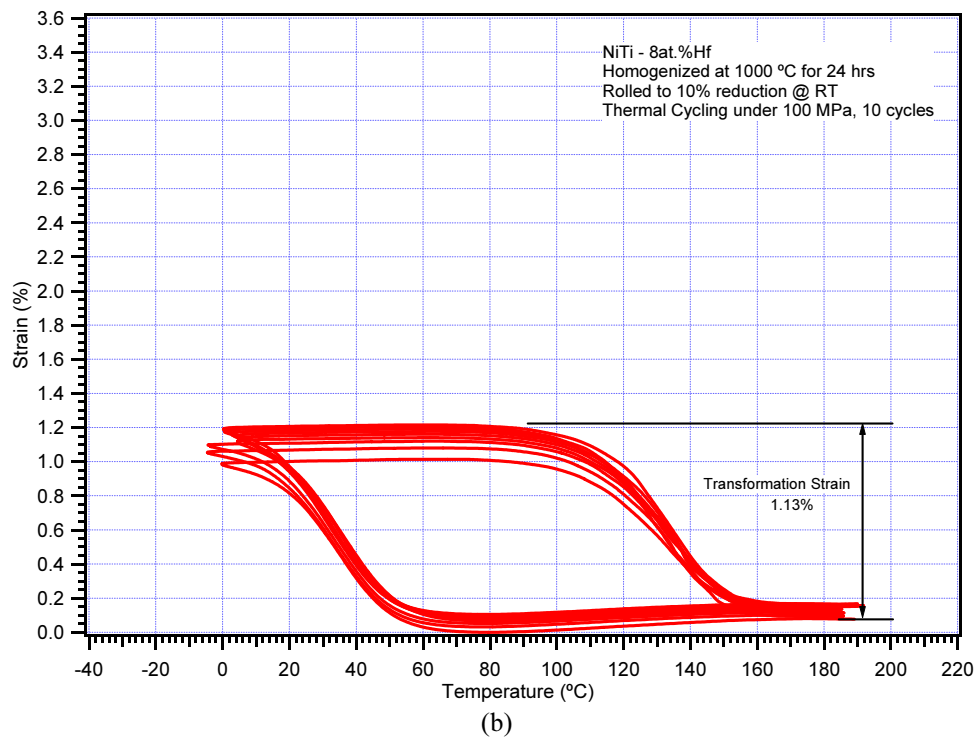


Figure 4.24. Continued. 10 thermal cycles under (b) 100 MPa. (c) 200 MPa.

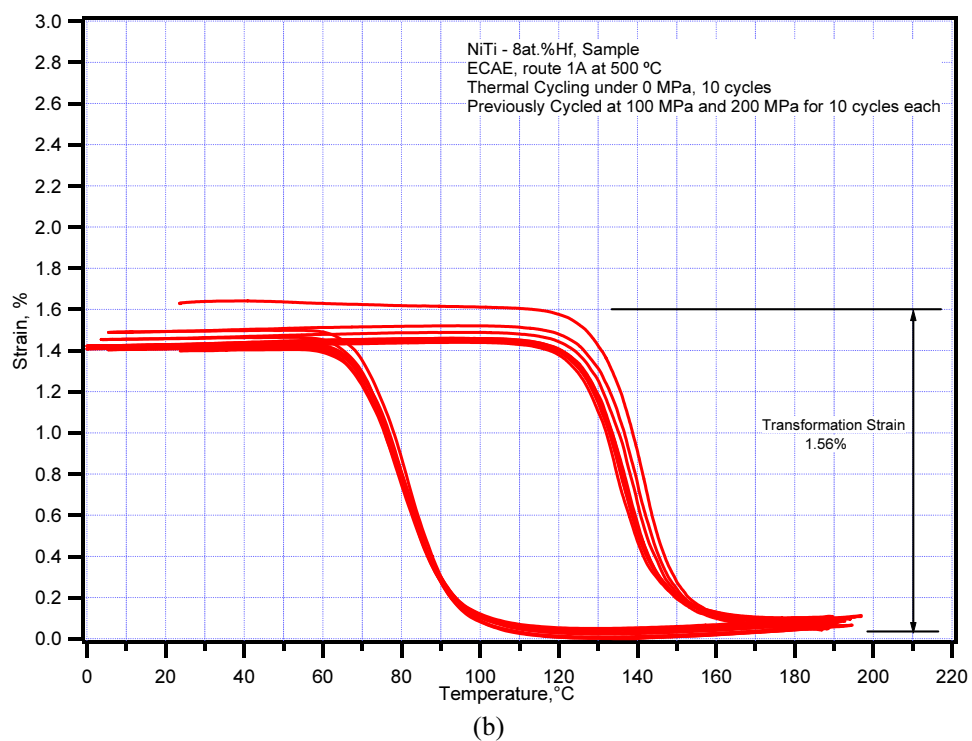
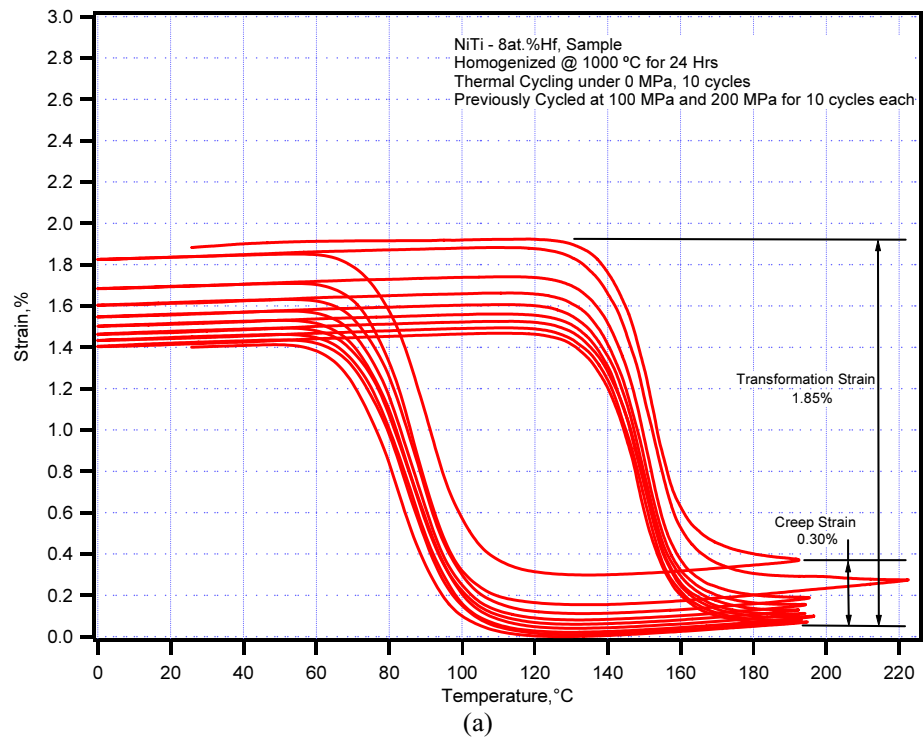


Figure 4.25. Two-way shape memory response of the samples after training under constant external stress of 100 MPa and 200 MPa. (a) Homogenized flowserve material, 49.8Ni-42.2Ti-8Hf, (b) homogenized flowserve material, 49.8Ni-42.2Ti-8Hf after one ECAE passes at 500 °C.

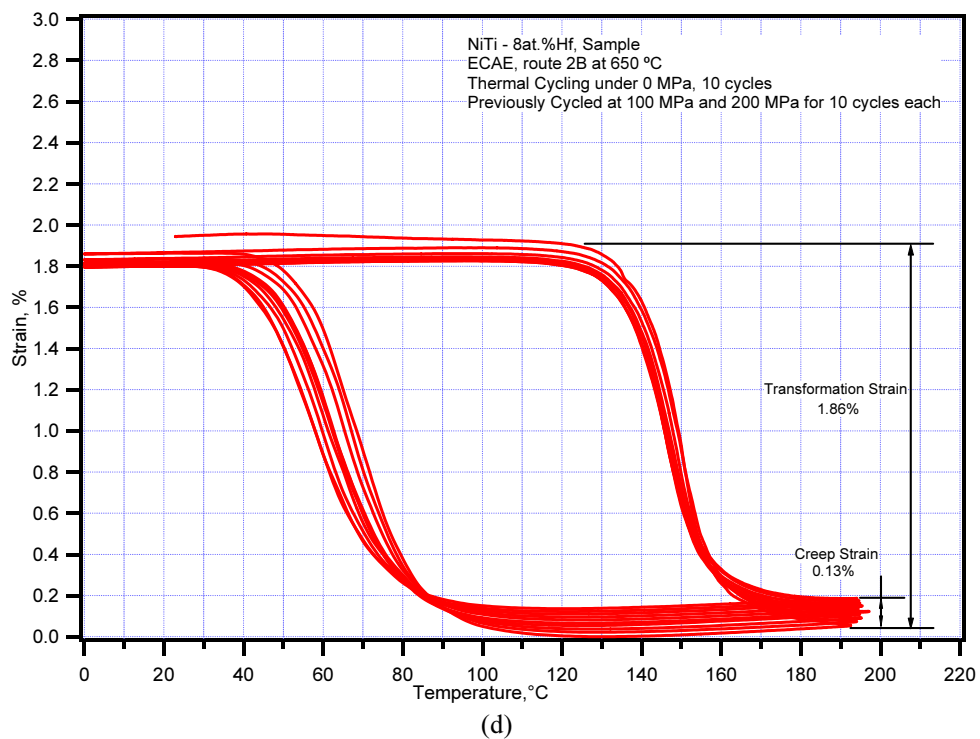
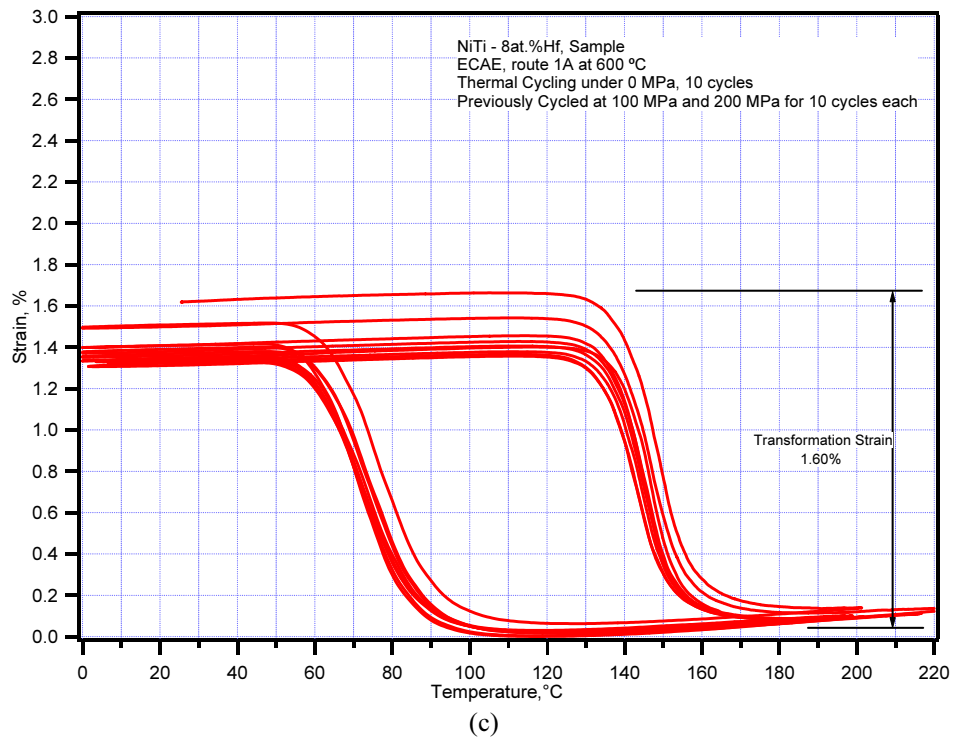


Figure 4.25. Continued. (c) homogenized flowserve material, 49.8Ni-42.2Ti-8Hf after one ECAE passes at 600°C, (d) homogenized flowserve material, 49.8Ni-42.2Ti-8Hf after two ECAE passes using Route B at 650°C.

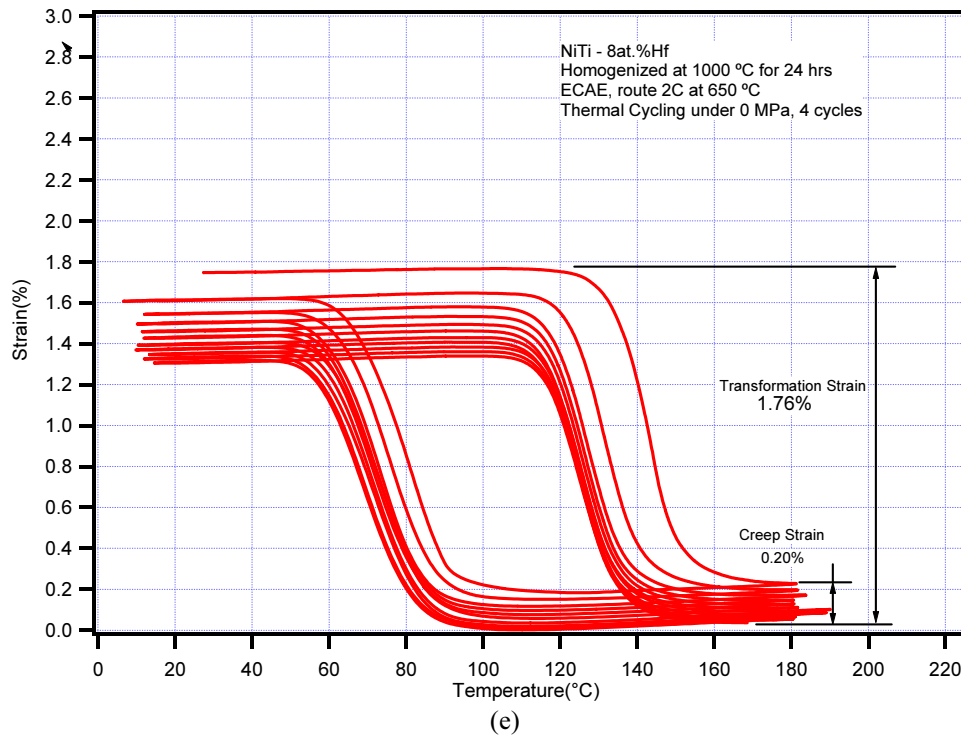


Figure 4.25. Continued. (e) homogenized flowserve material, 49.8Ni-42.2Ti-8Hf after two ECAE passes using Route C at 650°C.

Figure 4.25 depicts the two-way shape memory effect of the homogenized as well as ECAE processed samples after training. Subsequent to thermal cycling of the samples at 100 MPa and 200 MPa for 10 cycles each, the samples are unloaded to 0 MPa at austenitic stage and were again cycled at zero load for testing two-way shape memory effect. In Figure 4.25(a) we can see a significantly high amount of creep strain in the case of homogenized material which can be attributed to the softness of the matrix. This argument is strengthened by the results obtained from the ECAE samples, which show significantly lower amount of creep strain which shows stability of the material. This is in contrary to the very small two-way shape memory effect (TWSME) observed by *Meng et al* [26]. Previously the observed TWSME was less than 0.5% whereas we have observed TWSME higher than 1.5% which is stable. In previous results [26, 27] it was observed that TWSME in NiTiHf deteriorated with cycling. But in case of ECAE we can see a stable behavior with number of cycles. TWSME can be attributed to the creation of oriented stress fields due to martensitic deformation. During cycling at constant load training occurs and oriented stress fields are formed which increases gradually as a

function of number of cycles and thus the TWSME becomes stable. During thermal cycling, the dislocations introduced by the cycles interact with the oriented stress fields formed as a result of deformation to create a stable dislocation configuration which attributes to the stability of TWSME. This two-way shape memory effect can also be attributed to 1) the residual martensite variants in the parent phase after training [28] and also 2) because of the effect of the dislocations introduced by training [29].

All the above mentioned mechanical testing results are briefed in Table 4.1.

Table 4.1. Summary of the results from thermal cycling conducted under constant load.

Sample History	External Load – 100 MPa						External Load – 200 MPa						Two Way Shape Memory Effect (%)			
	M _t (°C)		Hysteresis (A _F M _t) °C		Strain (%)	Creep Strain(%)	M _t (°C)		Hysteresis (A _F M _t) °C		Strain (%)		Creep Strain(%)	Hysteresis (A _F M _t) °C		Transformation Strain (%)
	1st Cycle	10th Cycle	1st Cycle	10th Cycle	Last Cycle		1 st Cycle	10th Cycle	1 st Cycle	10th Cycle	Last Cycle		1st Cycle	10th Cycle		
Homogenized Sample 24hrs @ 1000 °C Material : HIPed flowserve	101	107	62	58	1.27	0.60	127	128	61	61	1.78	0.76	62	66	1.85	
ECAE 1A @ 500 °C Material : Homogenized flowserve	89	90	69	69	1.44	0.17	103	114	65	66	2.19	0.46	58	54	1.56	
ECAE 1A @ 600 °C Material : Homogenized flowserve	81	90	71	59	1.61	0.16	97	105	65	66	2.33	0.38	70	71	1.60	
ECAE 2B @ 650 °C Material : Homogenized flowserve	76	87	93	89	2.01	0.22	96	109	79	81	2.64	0.50	88	80	1.86	
ECAE 2C @ 650 °C Material : Homogenized flowserve	77	83	65	64	1.93	0.21	96	111	64	58	2.62	0.48	65	57	1.76	
ECAE 2C @ 650 °C Annealed for 15 mins @ 400 °C Material : Homogenized flowserve	92	95	74	77	1.52	0.05	104	121	73	77	2.23	0.25	—	—	—	
Hot Rolled Sample 40% Reduction @ 1000 °C Material : Homogenized AMES	82	81	72	74	2.52	0.13	91	104	73	77	3.20	0.51	—	—	—	
Marformed Sample 10% Reduction @ RT Annealed for 15 mins @ 400 °C Material : Homogenized flowserve	61	58	100	100	1.09	0.10	100	107	61	55	2.24	0.32	—	—	—	

CHAPTER V

CONCLUSIONS

In this study, a 49.8Ni-42.2Ti-8Hf (in at.%) shape memory alloy was severely deformed at high temperature varying from 500°C to 650°C using Equal Channel Angular Extrusion (ECAE) and at 1000°C by hot rolling.

- The stability of transformation temperature with thermal cycling was observed in ECAE samples, which was major problem in high temperature shape memory alloys. This can be attributed to the strengthening of matrix during the ECAE processing.
- A significant increase in recoverable strain level was observed in the ECAE processed sample using Route C after 2 passes at 650°C, showing the best transformation strain level (2% under 100MPa) when compared to the strain levels in case of homogenized samples (1.25% under 100MPa). This can be attributed to the oriented martensite formation and also the texture effects induced in the matrix during ECAE.
- Another significant observation is the decrease in the total irrecoverable strain in case of ECAE samples when compared with the high irrecoverable strain levels of homogenized sample.
- Decrease in thermal hysteresis with increase in external stress similar to that in the Nickel rich NiTi SMA's was another unusual observation in the case of the ECAE processed NiTiHf samples. The strengthening of the matrix during ECAE processing contributes to this observation.
- It is also observed that hot rolling gave the highest strain rates, when compared to all the different processing routes using ECAE. This may be because of the higher purity of the material obtained from AMES and presence of higher oxygen content in the material obtained from flowserve.
- Slight annealing treatment in 2C-650°C sample shows better stability.
- Two-way shape memory effect is observed after cycling which is highly stable in case of ECAE sample when compared to the homogenized material.
- Extrusions need to be conducted at lower temperatures for having finer precipitates evenly distributed along the matrix.

- The improved formability of NiTiHf alloy using ECAE shows the advantage of ECAE over conventional ausforming methods.

REFERENCES

1. Oulu University - <http://herkules.oulu.fi/isbn9514252217/html/x317.html>
[Accessed on 08-10-2004]
2. Funakubo H. Shape Memory Alloys, Amsterdam: Gordon & Breach Publishing Group 1987; p.1.
3. Liu Y, Liu Y, Humbeeck JV. Acta Mater 1999; 47: 199.
4. Shaw JA, Kyriakides SJ. Mech Phys Solids 1995; 43: 1243.
5. Lo YC, Wu SK, Wayman CM. Scripta Metall. 1990; 24: 1571.
6. Wu SK, Wayman CM. Metallography 1987; 20: 359.
7. Angst DR, Thoma PE, Kao MY. Journal de Physique IV 1995; 5.
8. Hornbogen E. Journal of Material Science 2004; 39: 946.
9. Hornbogen E, Mertinger V, Wurzel D. Scripta Mater 2001; 44: 171.
10. Hosogi M, Okabe N, Sakuma T, Okita K. Materials Science Forum 2002; 394: 257.
11. Goldberg D, Xu Y, Murakami Y, Morito S, Otsuka K. Scripta Metallurgica et Materialia 1994; 30(10): 1349.
12. Hurley J, Ortega AM, Lechniak J, Gall K, Maier HJ. Z. Metallkd. 2003; 94: 5.
13. Miyazaki S, Imai T, Igo Y, Otsuka K. Metall. Trans. A 1968; 17:115.
14. Xie Z, Liu Y, Humbeeck JV. Acta Mater 1998; 46: 1989.
15. Dalle F, Perrin E, Vermaut P, Masse M, Portier R. Acta Materialia 2002; 50: 3557.
16. Zhang C, Zee RH, Thoma PE, Boehm JJ. Mat. Res. Soc. Symp. Proc. 1998; 481: 237.
17. Meng XL, Cai W, Zheng YF, Tong YX, Zhao LC, Zhou LM. Materials Letters 2002; 55: 111.
18. Wang YQ, Zheng YF, Cai W, Zhao LC. Scr. Mater. 1999; 40: 1327.
19. Otsuka K, Oda K, Ueno Y, Piao M, Ueki T, Horikawa H. Scr. Metall. Mater 1993; 29: 1355.
20. Segal VM, Hartwig KT, Goforth RE. Mat. Sci Eng A 1997; 224: 107.
21. Segal VM, Goforth RE, Hartwig KT. Texas A&M University, U.S. Patent No. 5,400,633, 1995.
22. Mulder JH. Ph.D. Thesis, University of Twente, Netherlands 1995.
23. Hamilton RF, Sehitoglu H, Chumalyakov Y, Maier HJ. Acta Mater 2004; 52: 3383.

24. Golberg D, Xu Y, Murakami Y, Morito S, Otsuka K, Ueki T, Horikawa H. *Intermetallics* 1995; 3: 35.
25. Hornbogen E. *Acta. Met.* 1985; 33: 595.
26. Meng XL, Cai W, Zheng YF, Rao, Zhao LC. *Materials Letters* 2003; 57: 4206.
27. X. L. Meng, Y. F. Zheng, W. Cai YB, Zhao LC. *Journal of Alloys and Compounds*, 2004; 372: 180.
28. Perkins J. *Metall. Trans. A* 1984; 15a: 313.
29. Stalmans R, Van Humbeeck J, Delaey L. *Proceedings of the International Conference on Martensitic Transformations Monterey, California, 1992; ICOMAT-92: 1065.*

VITA

Anish Abraham Simon, son of Mr. Simon Abraham and Prof. Annie Simon and elder brother of Anjana Annie Simon and Anpu Mathew Simon, was born in Kerala, India in 1980. He graduated from Mar Athanasius College of Engineering, Kothamangalam under Mahatma Gandhi University, Department of Mechanical Engineering, in May 2001. In the Fall 2002, he enrolled in Texas A&M University to pursue a master's degree in the department of Mechanical Engineering. He completed his research and received a Master of Science degree majoring in mechanical engineering in December of 2004. Following graduation, Anish will seek a full-time job in the field of engineering. His permanent address is:

Poweth House

Karikulam P.O

Ranni

Kerala – 689682

India

Phone: 91-4735-226390

Email: anishsimon@gmail.com